MDH Pathogen Project Recharge Monitoring Study Final Report

03/2024

MDH Pathogen Project Recharge Monitoring Study Final Report

Minnesota Department of Health
Drinking Water Protection Section
PO Box 64975
St. Paul, MN 55164-0975
651-201-4700
health.drinkingwater@state.mn.us
www.health.state.mn.us

To obtain this information in a different format, call: 651-201-4700

Table of Contents

Introduction

For 12-months, beginning October 2020, intensive microbiological and chemical sampling was conducted at four public water supply sites to look for correlation between precipitation events and water quality degradation. The sites were selected based on results obtained from a previous sampling study conducted from 2014-2016 (Stokdyk, 2019), with additional consideration given to hydrogeologic setting and well owner interest. None of the wells has historically been considered at high risk based on sampling for traditional indicators such as total coliform or E. coli, but each showed susceptibility based on qPCR analysis for other microbial pathogens or indicators in the earlier study phase. The temporally dense, precipitation -event focus of this study contrasts with the 2014-2016 study, which was bi-monthly in nature and independent of proximity to precipitation events or seasonal considerations.

Site 1 is in northeastern Minnesota and is completed in a fractured crystalline bedrock aquifer common to this area (Figure 1). Site 2 is in north-central Minnesota in a geologically unprotected glacial sand and gravel aquifer. Site 3 is also in north-central Minnesota but represents a sand and gravel aquifer that is buried beneath finer-textured glacial sediments. Site 4 is in the southeastern Twin Cities Metropolitan Area and represents part of the Paleozoic bedrock aquifer system that is commonly used for water supply in that area. The well is finished in Cambrian sandstone of the Tunnel City Group and is overlain by permeable glacial sediments and both clastic and carbonate bedrock. Table 1 summarizes some of the pertinent hydrogeologic information about each site. Work at each site focused on a single well except for Site 3, where sampling was conducted on the blended water from two adjacent wells pumping from the same aquifer. This was done in accordance with the well owners' preference for operational efficiency.

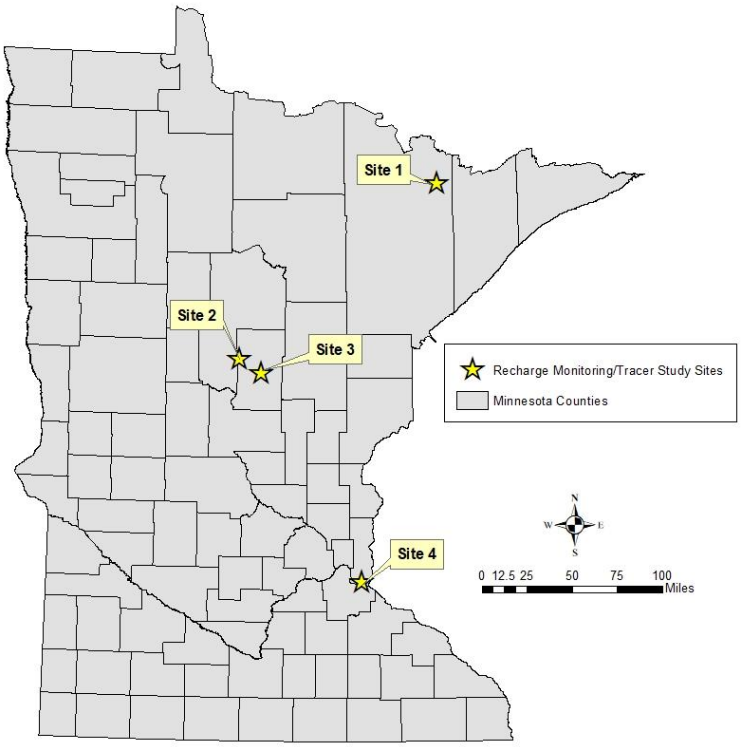

Figure 1: Location map of recharge study sites.

Table 1. Hydrogeologic information about well sites used in the recharge monitoring and dye trace studies. [1]Geologic sensitivity reflects the degree of geologic protection in the form of fine-grained materials such as clay or shale that overlie an aquifer (Geologic Sensitivity Project Working Group, 1991). High geologic sensitivities reflect an absence of overlying geologic protection.

Site	Aquifer	Geologic Sensitivity[1]	Well Depth (ft)	Casing Depth (ft)	Grout Type/ Depth (ft)	Static Water Level (ft)	Public Water Supply System Type	Average Daily Water Use (gallons)
1	Fractured Archean migmatite	High	262	29	Cement/29	19.6	Transient Noncommunity	376
2	Quaternary sand and gravel water table aquifer	High	107	99	Bentonite/30	52	Transient Noncommunity	5,800*
3	Quaternary sand and gravel buried aquifer	Moderate	68 78	53 48	Cement/30	35 35	Community	7,000
4	Cambrian sandstone of the Tunnel City Group	High	310	258	Cement/ 258	180	Nontransient Noncommunity	8,750*

*Indicates water use was not metered but estimated based on population serviced

Methods

The sampling plan centered on five to six precipitation or snowmelt events that occurred at each site and was developed based on statistical analysis of data from the 2014-2016 monitoring study. For example, Scher (2020) suggested that the likelihood of microbial detection in wells from that study phase was greatest within 14-days of 0.6 inches rainfall events, while Gretsch, et. al. (2018) suggested that human-specific viral detections were greatest within 24-hours of rainfall events with a median value of 0.06 inches from wells evaluated in a related study phase. Figure 2 shows the idealized sampling schedule for the project based on these considerations, as well as lab holding time requirements (96 hours) and shipping logistics. Sampling was triggered by a forecast rainfall event of 0.5 inches or greater within a rolling 10-day forecasting window using online sources such as Weather Underground and the National Weather Service.

The schedule included time-sequential collection using autosamplers (Owens et al., 2018) such that several samples were collected preceding the forecast rain event, leading to a period of high-intensity sampling accompanying and immediately following the event, followed by a tapered period of reduced sampling (Figure 2). In practice, this schedule was not always

followed due to unrealized or sudden-onset rainfall events that weren't successfully forecast within the 10-day preceding period.

Also, mechanical, and other logistical difficulties occasionally resulted in deviations from the idealized schedule. Precipitation events, defined as at least 12.7 mm of rainfall during the forecast window, spanned from 3-10 days, and associated sampling ranged from 20-30 days including pre, contemporaneous and post-event samples, with an average of 15 samples collected per event at each well. Altogether, 383 drinking water samples were collected during the study.

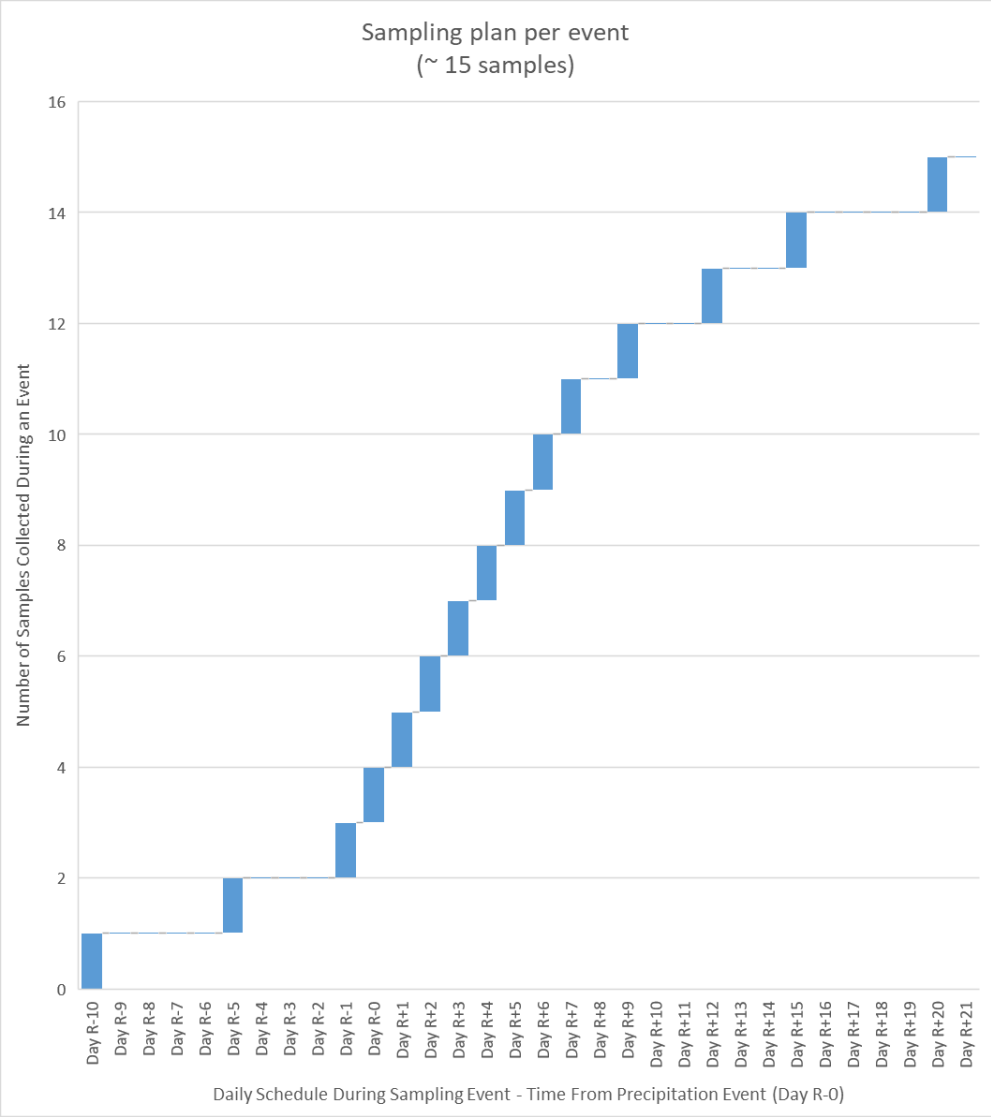

Figure 2. Recharge monitoring sampling plan.

Sampling was accomplished using enhanced versions of the automated samplers described in Owens et al. (2019). Enhancements included:

- The use of lower flow rate flowmeters to improve volume precision.

- The use of an additional flowmeter on the water quality sonde line to complete continuous real time mass flow verification.
- Additional flowmeter calibration steps to the datalogger program to document calibration measurements.
- The addition of quick disconnect fittings to reduce the potential for sample contamination during filter swaps.
- Use of a larger refrigerator to accommodate eight filters and the whole water sampling equipment.
- The addition of a peristaltic pump and valve to create the time-paced whole water sample.
- The use of an additional high precision diaphragm valve to the water quality line to control back pressure and flow rate through the system.
- The addition of video cameras to monitor equipment and check for leaks.
- The use of additional leak detectors inside and outside of sampler.
- The use of a faster CR1000X data logger.
- The use of a modified datalogger program to accommodate filter changes based on time vs flow volume, and add pre-storm, storm, and post storm sampling features.
- Used filter #8 to set flow rate and pressure for system.

The autosamplers were triggered remotely via cell phone based on weather forecasts. Samples were collected via in-line ultrafilters through which water flowed continuously for 24-hours during a given sample collection day, with variations due to mechanical or logistical issues. The target flow volume was 800 liters, but actual volumes ranged from 50 to 3,200 liters, with an average of 1,163 liters. Filters were changed out and shipped in batches, corresponding with lab hold time requirements. The ultrafilters were handled using sterile methods and shipped on ice by next day courier to the Laboratory for Infectious Disease and the Environment in Marshfield, Wisconsin. Samples were processed and analyzed by qPCR methods as described in Stokdyk et al., (2020). Table 2 summarizes the target organisms, which media they were detected in, and whether they are zoonotic or not.

*Table 2. Summary of target organisms in this study and media in which they were detected. *Indicates possible animal origin*

Organism	Detected in Drinking Water	Detected in Wastewater
Bacteroidales-like HumM2	Yes	Yes
*Campylobacter jejuni	No	No
Covid-19 2019-nCoV_N1	No	No
Covid-19 2019-nCoV_N2	No	No

Organism	Detected in Drinking Water	Detected in Wastewater
*Cryptosporidium	Yes	Yes
Enterohemorrhagic E. coli (eae gene)	No	No
*Giardia	Yes	No
Human adenovirus groups A-F	Yes	Yes
Human Bacteroides	Yes	Yes
Human enterovirus	No	Yes
Human polyomavirus	No	Yes
Norovirus genogroup 1	No	No
Norovirus genogroup 2	Yes	Yes
Pepper mild mottle virus	Yes	Yes
Rotavirus A (NSP3 protein)	No	Yes
Rotavirus A (VP1 gene)	No	Yes
Rotavirus C	No	No
*Salmonella (invA)	Yes	No
*Salmonella (ttr)	Yes	No
Shiga toxin 1-producing bacteria	No	No
Shiga toxin 2-producing bacteria	No	No

In addition to the microbial samples collected by ultrafilter method, the autosamplers were equipped to fill a one-liter bottle during the same 24-hour filling period as the first filter in each sampling event. These samples were also shipped to the lab for microbial analysis after pouring off a small volume for analysis of chemical and isotopic parameters. From this small volume of poured-off sample, analyses were conducted for chloride and bromide by the Public Health Laboratory at the Minnesota Department of Health and for the stable isotopes of water at the Environmental Isotope Lab at the University of Waterloo. The remainder of the 1-liter sample was analyzed for microbial DNA via QPCR, as was done for the ultrafilters, for temporal-averaging methods comparison purposes. Results from the 1-liter method are considered an active research area and are not incorporated in this report. Table 3 summarizes the water quality data that was analyzed for, including types of samples that were collected and their associated analytes.

Table 3. Summary of water quality data collected in this study by sample type. [1]Indicates parameters that showed poor analytical sensitivity and are not further analyzed in this report. [2]Indicates fluorescent dyes analyzed for at the two sites where dye trace studies were conducted. These sensors replaced bromide and chloride sensors at those sites.

Sample Type	Frequency	Analytes
Ultrafilter	One per each day of a sampling event	See microbial targets in Table 2.
1-liter bottle	One at the beginning of each sample event, then accompanying every filter change	Bromide, chloride, and the stable isotopes of water
Water quality Sonde	Continuous data logging throughout study	Temperature, specific conductance, pH, [1]turbidity, [1]fDOM, [1]optical brightener, [1]tryptophan, [1]bromide, [1]chloride, [2]eosin, [2]sulforhodamine

Each auto-sampler was paired with a nearby observation well completed in the same aquifer and in close proximity, as well as an associated weather station. These were equipped with logging and telemetry capabilities, for real-time analysis of precipitation and water level data collected at 15-minute intervals. Water quality field parameters were also collected continuously during the project via Eureka Manta +40 water quality sondes which were attached to the autosamplers and received continuous flow throughout the year-long monitoring study, recording data on 15-minute time intervals. Field parameters included water temperature, pH, specific conductance, turbidity, optical brighteners, fDOM, tryptophan, bromide, and chloride. At two of the study sites, bromide and chloride sensors were swapped out for dye sensors equipped to detect the fluorescent dyes used in the wastewater tracer studies, namely sulforhodamine and eosin.

Each autosampler was also paired with one or more on-site wastewater conveyance or disposal feature which was sampled once per precipitation event via a one-liter grab sample to evaluate correlation with microbial species observed in the well water. These consisted of gravity-drained septic systems at two of the sites, with a municipal sewer included at one of the sites and a sewage lift station at another. Finally, tracer studies were conducted at three of the four sites to evaluate possible contributions from nearby wastewater and stormwater infrastructure, and brine tests of the grouted annular space around the wells were conducted to look for evidence of possible fast-flow transport pathways for surface infiltration.

Quality Control/Quality Assurance

Quality control was addressed by adherence to the sample handling protocols described in the supporting materials of Owens et al., (2020). In addition, a single round of blank samples was collected at the outset of the study to assess the effectiveness of these sample handling techniques. All blanks returned non-detections, suggesting sample handling protocols were effective.

Data Analysis

Microbial detections were compared against precipitation and air temperature/snowpack data, in addition to water level hydrographs, to assess the temporal proximity of detections with groundwater recharge events. The lag times reported in this study represent the number of days that occurred between either at least 0.1 inch of precipitation, or the onset of above-freezing air temperatures while snowpack was present, and a microbial detection.

A quantitative microbial risk assessment (QMRA) was conducted for each site based on the observed pathogen detections using the methods described in Appendix A.

Description of Study Sites and Monitoring Results

Site 1 - Hydrogeology

Site 1 is in northeastern Minnesota along the shores of Burntside Lake, a 28.9 km^2 freshwater lake. The public water supplier serves a transient population that is seasonal in nature. Up to 350 people are served by several wells on the property. The surrounding land use is dominantly boreal forest except were developed to accommodate the facility's residents. The geology of the site is characterized by a thin, patchy cover of glacial sediments over Archean bedrock, which consists of alternating schist- and granite-rich migmatite (Figure 3). The granitic sequences belong to the Lac Le Croix granite (MGS 2019, personal communication). Most bedrock structures (geologic contacts, faults, and foliation) are steeply dipping and trend to the east-northeast (40-90 degrees), roughly parallel the North Arm of Burntside Lake, whose location is fault-controlled (Sims and Mudrey, 1978). The terrain is hummocky, reflecting the irregular bedrock surface.

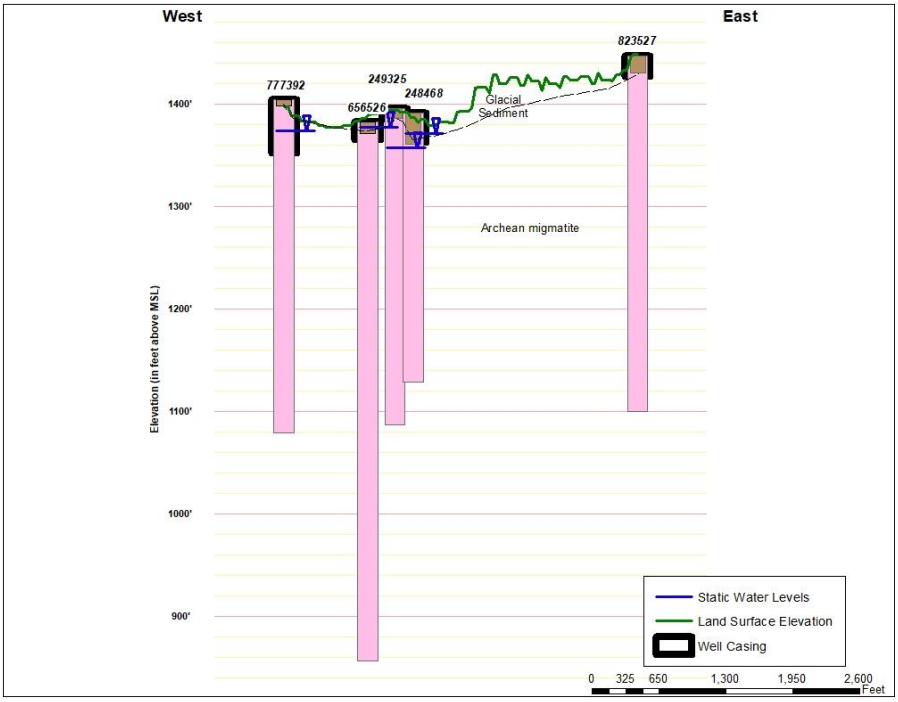

Figure 3. Geologic cross-section through Site 1, looking north. The study well is labeled 248468.

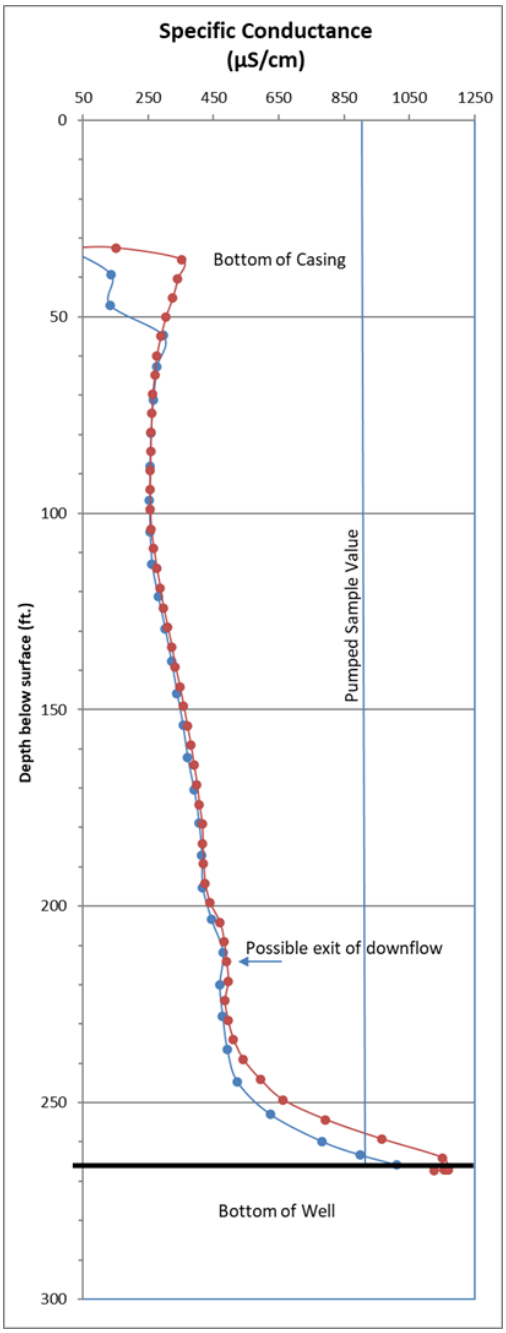

Figure 4. Specific conductance log of water column at Site 1 well.

The well selected for this study was not sampled previously by qPCR methods, instead it replaced another nearby well that was included in the earlier study, and which had been subsequently taken off-line by the well owner. A downhole video, geophysical and geochemical inspection of these two wells and a third well in the vicinity revealed a consistent pattern of small diameter, high-angle fractures common to the upper 150-190 feet below the bedrock surface and diminishing with depth. The geochemical signatures across wells were also consistent and show two dominant water quality regimes. The shallow regime extends from the top of the water column to depths of approximately 200-feet and consists of water with low conductance and short residence times based on responses to snow melt events (Barry and Green, 2019). The deep regime was observed at depths below 200-250 feet and consists of water with elevated specific conductance (Figure 4), primarily from chloride and bromide, and very low chloride/bromide ratios. These data suggest long residence times and may reflect a component of Canadian Shield brines (Davis et al., 1998). Natural downward hydraulic gradients and well pumping mixes these two regimes, so that water samples collected from the pumping wells is a mix whose proportions are thought to be dependent on well usage and seasonal recharge patterns (Minnesota Department of Health, 2020). At this well, the deep regime is thought to contribute from approximately 30-60% of the flow to the well based on analysis of specific conductance characteristics between the two regimes and pumped samples from the well, with the percentage decreasing during periods of greatest well use and during influx of recent recharge from precipitation and snowmelt events. Well logging showed that intra-borehole flow was relatively stagnant, with a possible exit point of weakly downflowing water at approximately 215 feet. Logging of other nearby wells showed a similar absence of vigorous flow conditions, with modest evidence of downward flow observed in the shallow borehole segments and slight upward flow observed at greater depths in one of the wells (Minnesota Department of Health, 2020). The pump depth for this well is 240-feet, which facilitates direct capture of deep regime water.

Depth to water at this site is within 40-feet of the land surface and is closely tied to the nearby lake level. Groundwater flow patterns are not well known, but limited water level and isotopic data suggest that Burntside Lake is the dominant local discharge area, with flow directed towards it from surrounding areas. Localized flow patterns may exist that are based on topography and/or preferential flow along northeast-trending geologic structures. The 10-year time of travel capture zone for this well is shown in Figure 5 and was determined using a modified calculated radius approach (Minnesota Department of Health, 2011), assuming flow is dominated by this northeast structural grain. This capture zone may significantly underestimate actual distances depending on fracture conductivity and connectivity, and the northerly flow direction may be underrepresented. Aquifer porosity was estimated to range from 1-10% based on visual observation of borehole walls and bulk hydraulic conductivity was estimated at 8 ft/d based on analysis of specific capacity data from an adjacent well included in the previous phase of the study.

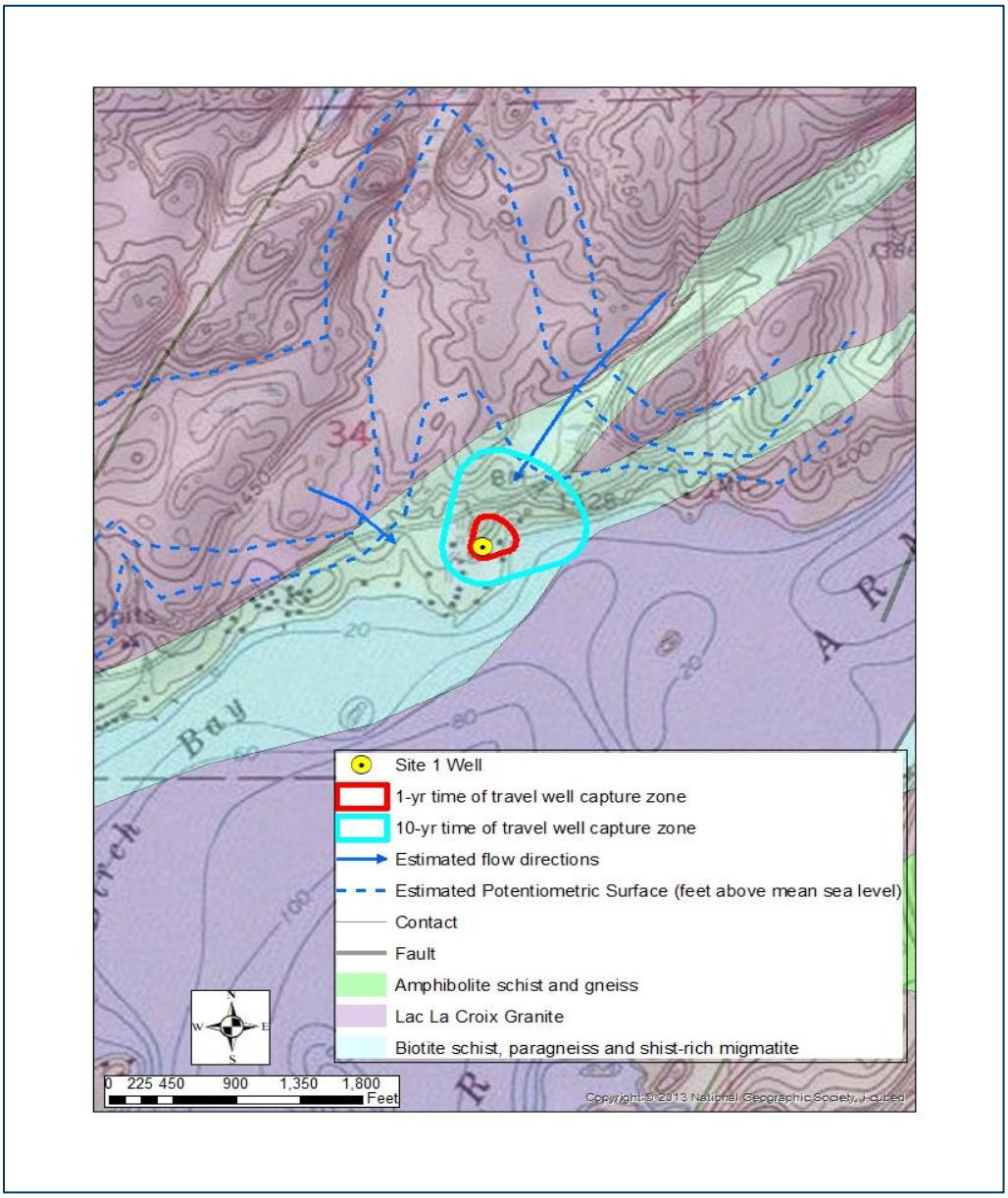

Figure 4. Site 1 hydrogeology.

Site 1 - Potential Contaminant Sources

An inventory of potential contaminant sources located within 200-feet of the public supply wells at this facility show an array of potential pathogen sources near the well included in the study (Figure 6). Possible sources of septic waste include pit toilets, septic tanks, drainfields, sewage lift stations and sewer lines. The nearest of these sources are buried sewer lines located 55 and 70 feet from the well and a pit toilet 78 feet away. A sewage lift station located 180 feet from the well was sampled once during each precipitation event to compare the microbial suite present there with that observed in the well water.

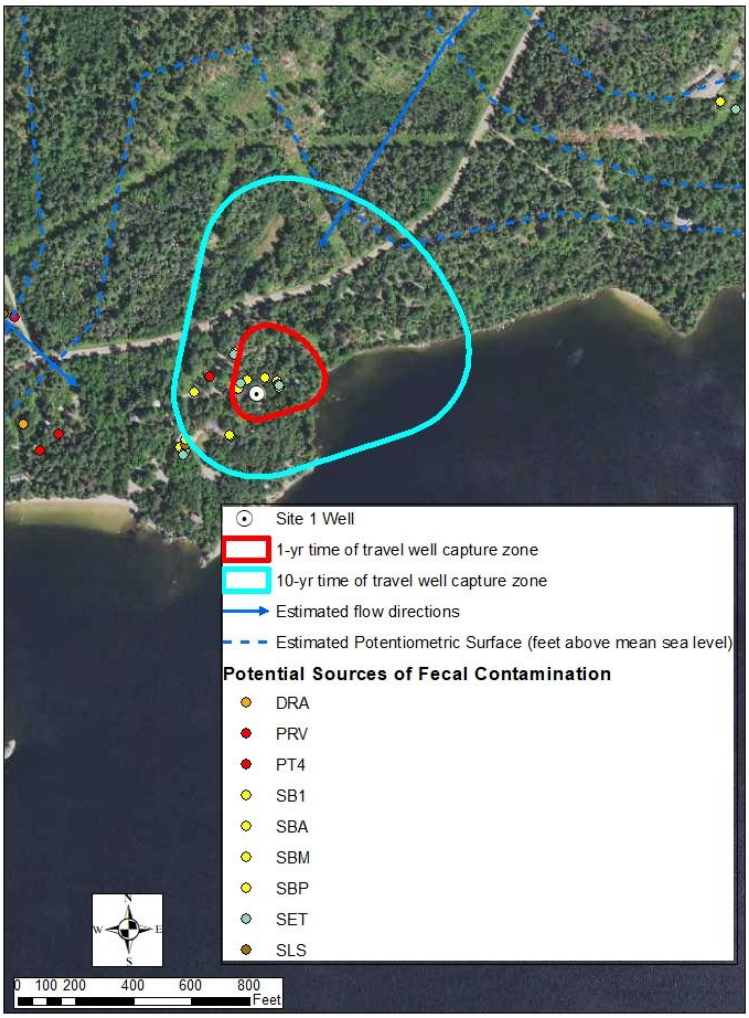

Figure 5. Potential sources of fecal contamination in the capture areas for the well at Site 1.

Site 1 - Monitoring Setup

The monitoring setup at this site matched that described in the Methods section, with these additional details added for clarity:

- The autosampler at this site was attached to an untreated water tap in a cabin that was fed from the study well; the water system used a series of two hydropneumatics bladder tanks with individual capacities of 20 gallons. Flow through this setup was continuous throughout the duration of the study except for a few short periods of power loss related to electrical storms.
- The observation well for this site was completed in the same aquifer as the study well and located 250 feet away.
- The wastewater sampling site at this facility consisted of a sewage lift station located 180 feet from the well and was sampled once during each sampling event.

Site 1 – Comparisons with water use and precipitation regimes from preceding water years and study periods

The months during which sampling occurred during this study were classified as wet, other than the single shortened sampling that occurred during the dry summer of 2021 (WETS, Minnesota DNR, 2022). The preceding months were evenly split between dry and wet, with a single normal month. For comparison, the preceding sampling months in the 2014-2016 study included three dry periods and two each of normal and wet.

Water use from the study well was considered normal compared to historical patterns, despite the COVID pandemic. However, the well that was used for this study differed from that used from the 2014-2016 monitoring period.

Site 1 – Description of Sampling Events

Five sampling events took place at Site 1 during this study (Table 4, Figures 7-9). Events 1 and 2 captured a series of late fall rains that followed a dry summer and early fall. These were essentially continuous, spanning October 6-November 29, 2020, with a one-week period (November 2-November 9) separating them. Total rainfall during this period equaled 4.7 inches and resulted in a water level rise of 4.31 feet in the observation well. Event 3 ran from March 3-March 30, 2021 and captured the onset of early spring warmth accompanied by the complete loss of approximately 12-inches of snowpack and accompanied by rain totaling 1.62 inches. A water level rise of 3.91 feet was observed during this period, starting on March 9. This rise was noted during a time when at least partial frozen ground conditions were suggested by standard indicators, such as the presence of lake ice and frozen soil beneath area highways, revealing the shortcomings of those indicators and/or the importance of recharge via macropore flow in partially frozen ground (Mohammed et al., 2019). Event 4 ran from May 17-June 11, 2021 and captured late spring/early summer rain totaling 1.33 inches. Water level observations during this and subsequent monitoring periods were confounded by pumping of the observation well for irrigation purposes. Event 5 ran from August 25-October 5, 2021 and captured 6.95 inches of late summer-fall rains that followed a significant drought. Again, water level observations were confounded by irrigation pumping.

*Table 4. Summary of sampling events at Site 1. Microbial abbreviations are as follows: HB = Human Bacteroides, B-like Hum = Bacteroidales-like HumM2, PMMV = Pepper Mild Mottle Virus, Noro = Norovirus, Sal= Salmonella. *Source is MDNR Climatology (2022)*

Event	Dates	Type	Cumulative Precipitation During Event (in)	Water Level Change from Baseline During Event (ft)	*Precipitation History from Sampled/Prior Month	Number/% of Samples Positive for Any Microbial Parameter	Lag Time in Days Between Precipitation and Microbial Detections (Shortest/Longest/Avg)	Microbes Detected (pathogens in red)	Maximum Concentration (gc/l)
1	10/6-11/2 2020	Fall Rain After Dry Summer	3.58	+2.92	Wet/Dry	2 (13%)	4/13/8.5	HB, Sal, PMMV	1.92
2	11/9-11/29 2020	Continued Fall Rain	1.11	+1.77	Wet/Normal	4 (33%)	0/4/2.5	HB, Sal, Noro	34.04
3	3/3-3/30 2021	Spring Thaw, Snowmelt and Rainfall	1.70 and melting of ~ 12-inches of snow pack	+3.9	Wet/Dry	8 (57%)	0/6/2.6	HB, B-like Hum, Sal	1.12
4	5/17-6/11 2021	Late Spring/Early Summer Rain	1.33	Not Known	Dry/Wet	5 (42%)	0/23/7	HB, B-like Hum	2.96
5	8/25-10/5 2021	Late Summer/Fall Rain After Dry Summer	6.95	Not Known	Wet/Dry	4 (13%)	0/3/1	HB, Noro, PMMV	2.02

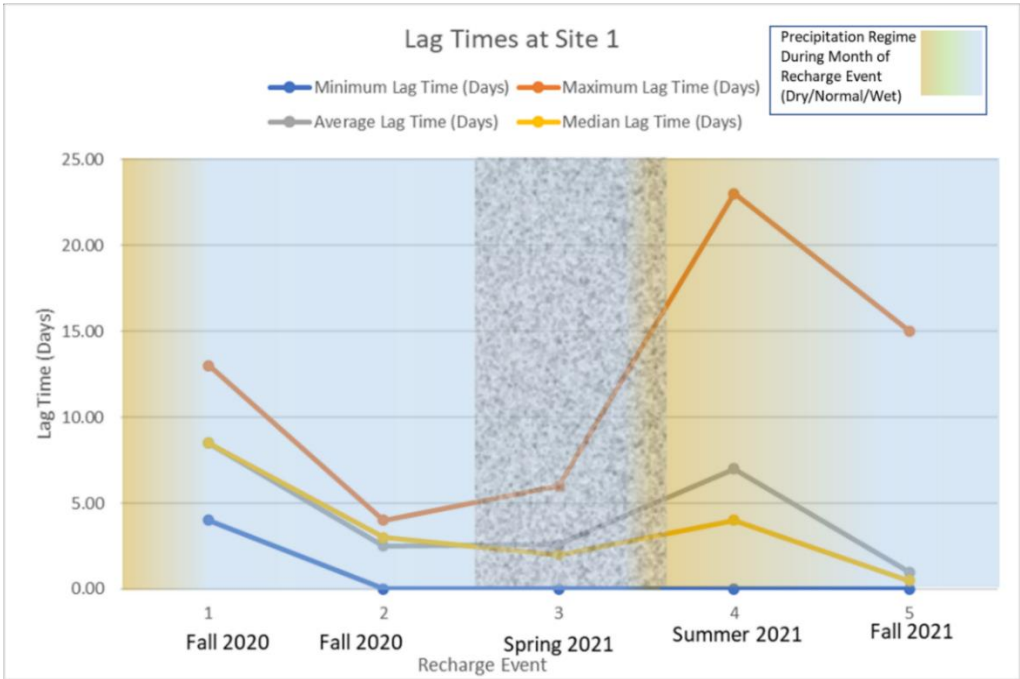

Figure 6. Summary of lag times observed at Site 1. Stippling indicates period of possible frozen ground conditions based on indicators such as lake ice and frost depth beneath area highways. Precipitation regimes from MDNR Climatology (2022).

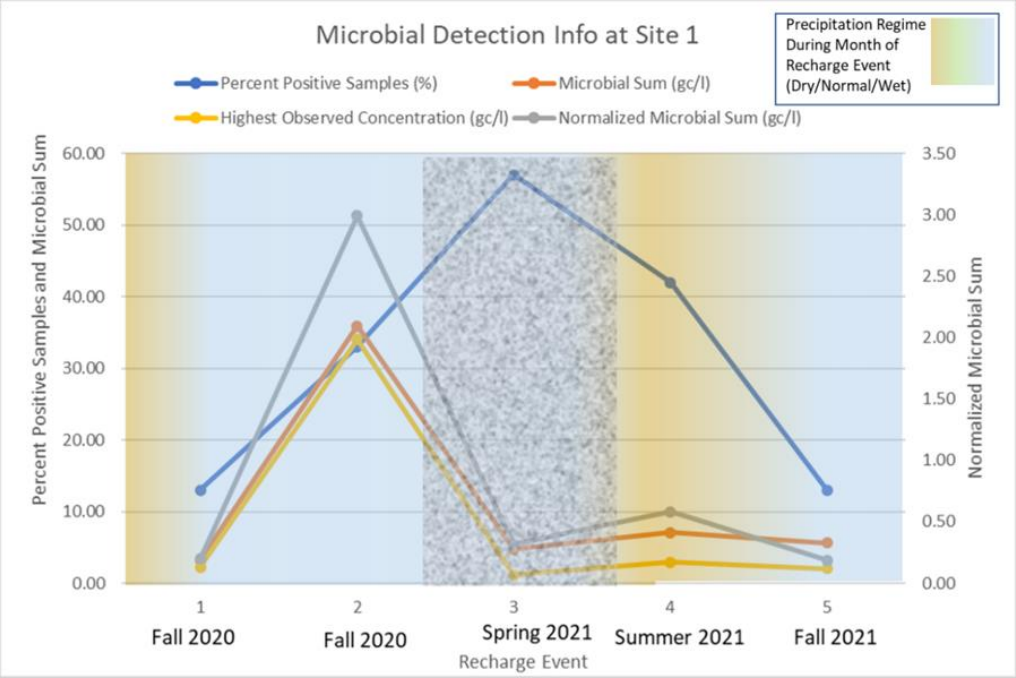

Figure 7. Summary of microbial detections at Site 1. Stippled pattern indicates period of possible frozen ground conditions based on indicators such as lake ice and frost depth beneath area highways. Precipitation regimes from MDNR Climatology (2022).

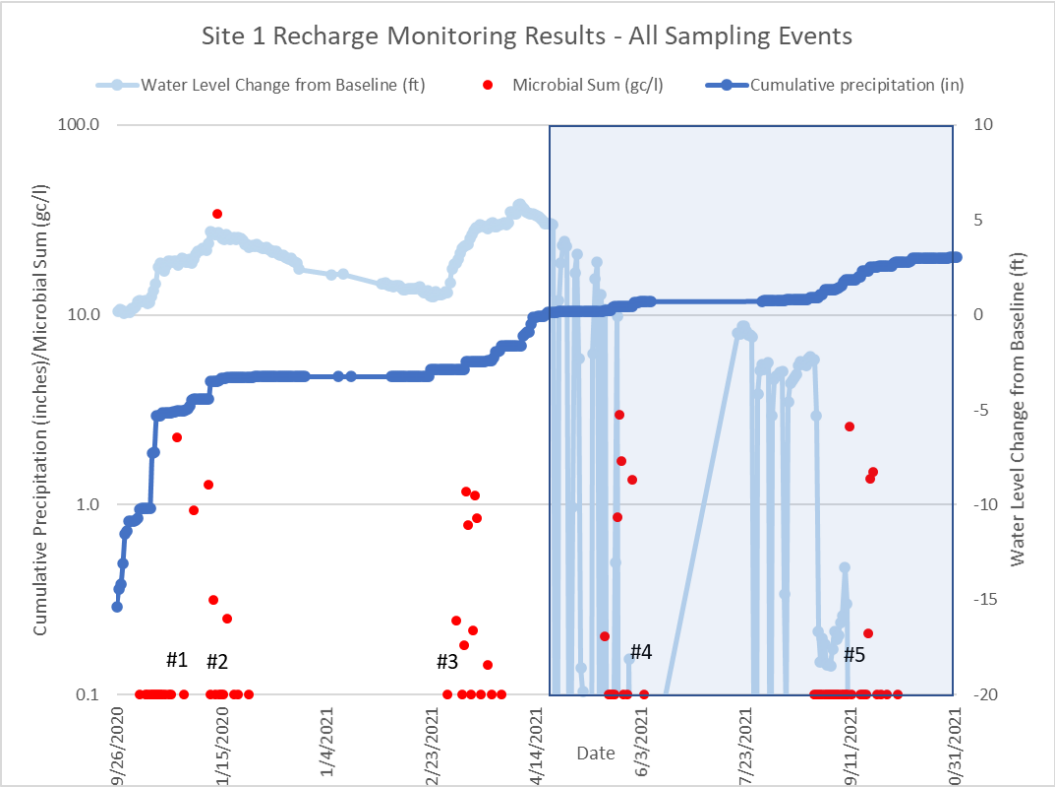

Figure 8. Sampling events at Site 1. Microbial non-detections were converted to values of 0.1 gc/l for plotting on log scale. Blue box shows period of irrigation pumping at observation well.

Site 1 - Monitoring Results

Microbial results

Of the 89 samples taken from this well, 25 (28%) showed some level of microbial detection. Most were very low concentrations (<1 gc/l), and most were from non-pathogenic indicator organisms (Human *Bacteroides* and *Bacteroidales*-like HumM2). For comparison with the 2015-2016 study on a nearby well, all six of those samples were positive, again mostly for the *Bacteroides* indicator parameters, and the highest concentration observed from those samples was approximately ten times higher than the highest observed at Well 3 during this phase of the study. There were a few norovirus and *Salmonella* detections observed at the current study well, with the norovirus detection on November 13, 2020, representing the highest concentration observed from this well at 32 gc/l. Those pathogens were not detected during the 2014-2016 sampling, but cryptosporidium, another pathogen, was detected at the well that was used in the previous study but not at Well 3. These differences may be attributed to the wetter precipitation regime during the 2014-2016 monitoring phase, or to differences in contaminant sources and flowpaths around the two respective wells.

Microbial detections from Site 1 showed relatively long lag times initially following a dry late summer period but decreased through the late fall of 2020 and spring of 2021 as wet conditions prevailed. Lag times rose again during the drought summer of 2021 before dropping with the return of wet conditions in the fall of 2021 (Figure 7). For example, the initial detections noted

from the October 2020 sampling event followed 13-days after the onset of that 2-inch rainfall (Figure 10), resulting in a median lag time of 8.5 days for this initial event, whereas median lag times for all subsequent events were four days or less. Same-day detections were observed in all but the first sampling event, and maximum lag times of 13 days or more were observed in both early fall events in addition to the summer drought period. The first microbial detection observed in the final monitoring event occurred 15-days after the first rainfall event of greater than 0.5 inches following the summer/fall drought, a lag time like that observed at the outset of the study, although the median lag time for this event was the lowest of the group.

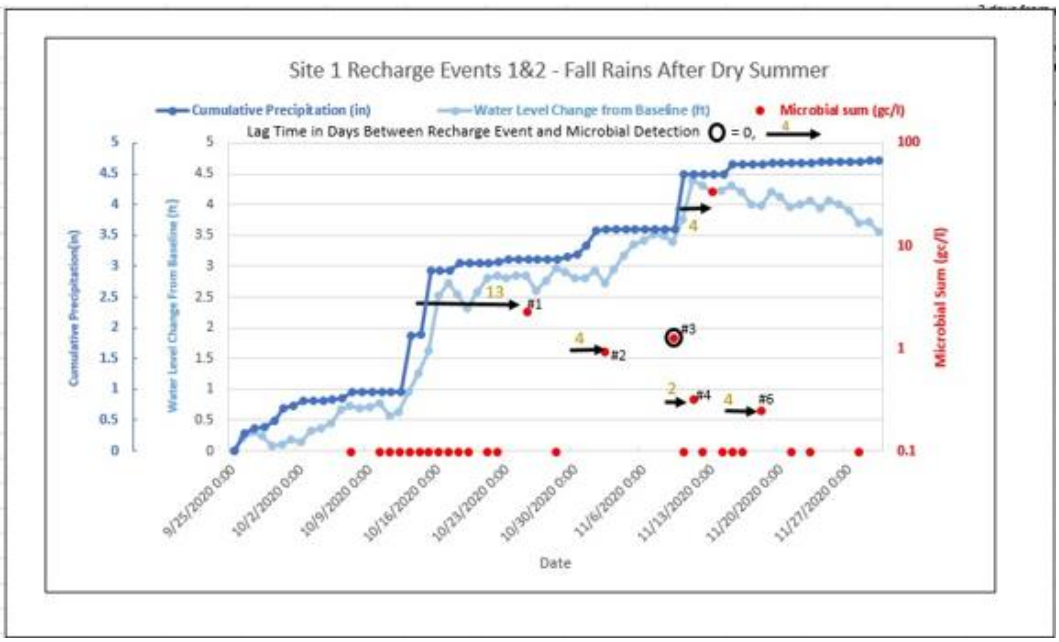

Figure 9. Microbial detections compared to cumulative precipitation and water level changes during Sampling Events 1 and 2. Microbial non-detections were converted to values of 0.1 for plotting in log space.

The long lag times observed both early and late in this study may relate to moisture conditions. The initial fall 2020 sampling event followed a drier than normal 30-day period, and the sampling that occurred in the summer of 2021 was during a significant drought (MDNR Climatology, 2022). The onset of fall rains in 2020 and 2021 may have triggered appreciable movement of wetting fronts in the vadose zone needed for the delivery of microbes to the water table following dry summer and early fall periods. The onset of wet weather beginning on October 12, 2020, resulted in an addition of 4 inches of rainfall over the period October 12-November 10, with a resulting 3.7-foot rise in water level at the observation well. Relatively small rainfall amounts following this initial wetting period appeared to result in low-level microbial detections, with rainfall totals as small as 0.1 inches graphically correlating with positive values. Shorter lag times may reflect more saturated conditions in the vadose zone allowing for more rapid transit of microbes. The occasional long lag time detection observed during sampling events otherwise characterized by short lag time intervals may relate to groundwater flow paths that vary with aquifer water level and/or varying contributions from

the two water quality horizons noted in this aquifer system, including the possibility of varying proportions of conduit versus matrix storage and transport.

Microbial detections were noted within two days of the onset of spring thaw, which was marked by the start of above-freezing air temperatures combined with intermittent rainfall on a dwindling snowpack (Figure 11). Complete loss of snowpack, that had totaled approximately 12-inches prior to the onset of warm weather in early-mid March, occurred during the period March 3-19, 2021, and was coincident with the onset of rainfall totaling 0.5 inches on March 11. This combination of factors resulted in an increase in water level of nearly 3.6 feet in the observation well over the period March 9-25. Sampling during this event showed the highest percentage of microbial detections of any event monitored for this study, with 8 of 14 samples (57%) testing positive (Figure 8). In contrast, sampling events 1 and 5, which occurred during the driest portions of the study, showed the lowest percentage of positive samples (15% and 13%, respectively). Microbial sums peaked in the second sampling event, largely driven by a single high-concentration detection of norovirus (Figure 8).

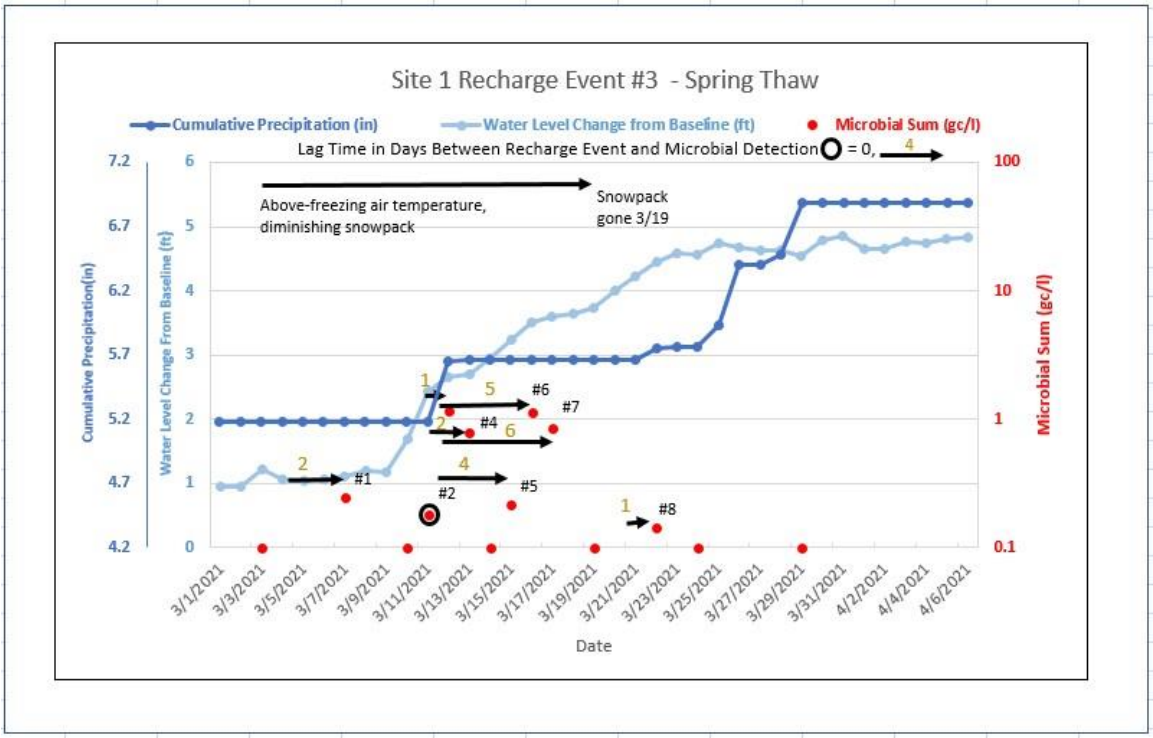

Figure 10. Precipitation monitoring during spring thaw at Site 1.

Data Logger results - Water level and chemical responses to precipitation

Water level hydrographs showed a rapid response to precipitation events at this site. For example, a 2-inch precipitation event near the beginning of the monitoring study in mid-October 2021 resulted in a water level rise of just over 2-feet during a 5-day period (Figure 9). Similar flashy response was noted through the first three monitoring events. Water level responses at the observation well were confounded later in the monitoring study due to occasional pumping of this well to meet irrigation watering needs during the 2021 drought.

Specific conductance values at the start of the monitoring study were relatively high, averaging 700 µS/cm or greater until November 1, 2020, after which daily average values never exceeded that threshold and often were well below it (Figure 12). These initial high values appear to be related to relatively large contributions from the high conductance pool of water noted in the bottom 30-50 feet of this well (as described above) during drier conditions. That is, the shallow flow horizon, which extends to a depth of nearly 200 feet based on specific conductance readings, showed an average value of 359 µS/cm when the well water column was logged in 2019. In contrast, the bottom 30 feet of the well averaged 1069 µS/cm. The values recorded in the 650-700 µS/cm range, common to about 2/3 of this monitoring study, equate to approximately 51-58% contribution from the deep flow horizon based on mass balance mixing analysis, whereas this horizon must have accounted for less than 30% of the total mix during the periods of low specific conductance that were common in spring and summer of 2021 (values in the 450-500 µS/cm range). This decrease in relative contribution of the deep flow horizon of approximately 20-30% by volume may reflect the shallow component of fast-recharging surface infiltration that diluted this signal, and which may account for some of the observed microbial detections. When looked at in greater detail, many of the days with microbial detections noted at this study side were preceded by higher daily specific conductance average values, especially during the spring, reinforcing the notion of short-duration contributions from more dilute recharge at the time the sample was collected. Examples from the May 20-26, 2021, period suggest these contributions may constitute up to 10% by volume of the well water column at times, but at other times may be negligible with no significant impact on daily average specific conductance. These observations are like those of Barry and Green (2019) based on the flashy chemical and isotopic responses to snowmelt at the observation well. In fact, the final sampling event at this site resulted in a nearly identical dilution trend as observed during the initial event and may represent a typical pattern for this site. Also, the wide coefficients of variance noted during the period of irrigation use at the observation well in the summer of 2021 may represent enhanced mixing of the shallow and deep-water quality horizons due to relatively larger water level fluctuations in the aquifer.

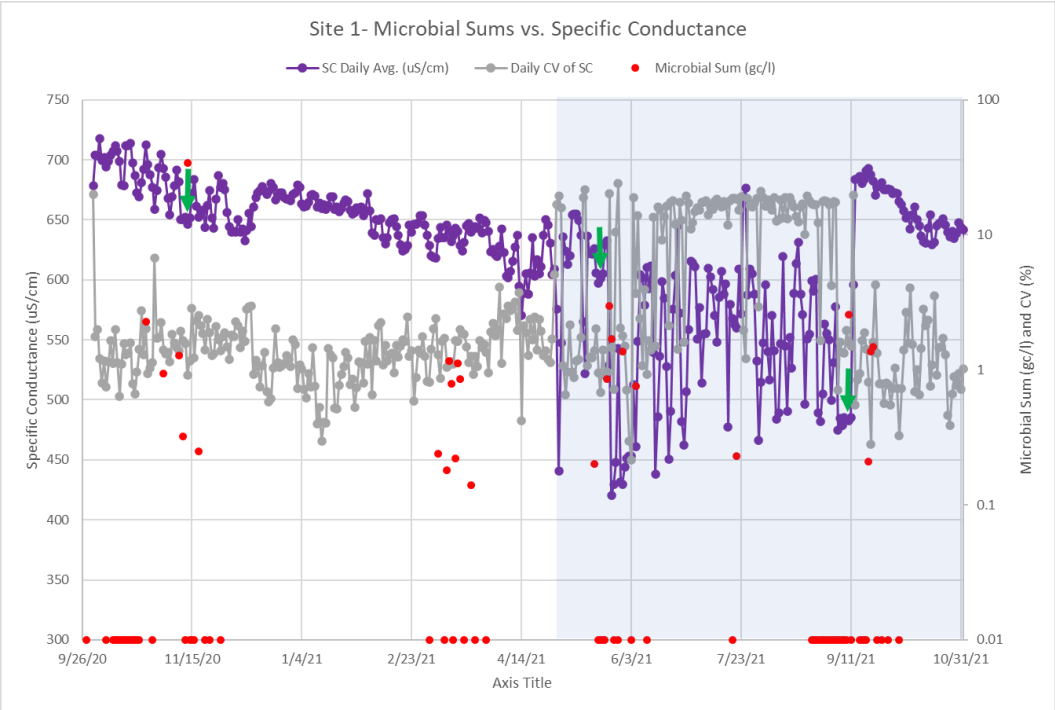

Figure 11. Specific conductance daily average values and coefficients of variance (CV) during the monitoring study compared with microbial detections. Blue box shows period of irrigation pumping at observation well. Green arrows show decreases in specific conductance associated with highest concentration microbial detections.

Water temperature varied significantly between the two measuring points at this site (Figure 13). Measurements at a depth of 66.8 feet in the observation well were relatively flat throughout, showing a slight decrease beginning on April 30, 2021, roughly coincident with the onset of irrigation pumping at this well and accompanied by relatively high daily variability, and a notable rise in the late fall towards the end of the monitoring period. In contrast, the sonde linked to the sampled well recorded large temperature swings and trends not seen in the observation well data, such as the large rise in temperature during the summer of 2021. The most likely explanation for this difference is the effect of ambient air temperature on the sonde data, especially when flow through the monitoring cell was relatively slow. Alternatively, or in addition, water temperature dynamics at the well that was used in the study may differ from those at the observation well. Average daily water temperatures as recorded by the sonde for each day with a negative microbial result were 1°C cooler than those days on which a microbe was detected, suggesting a similar mixing mechanism with recharge water as described for specific conductance.

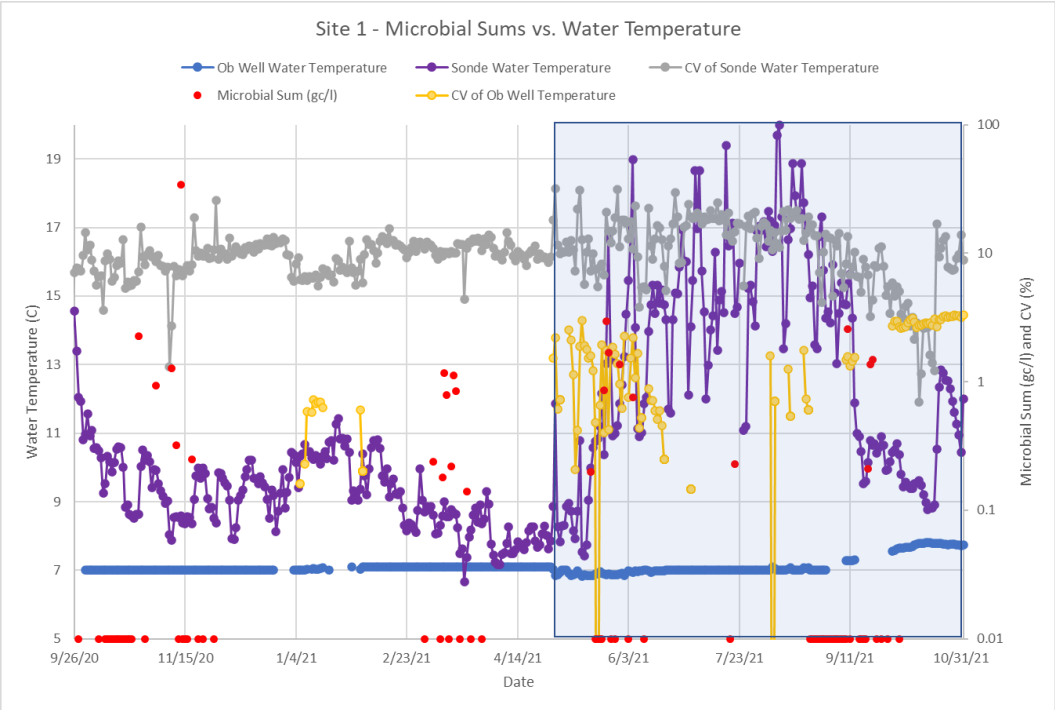

Figure 12. Water temperature variations during the monitoring study at Site 1 as measured at the onsite water quality sonde and observation well. Blue box represents period of irrigation pumping at the observation well during the drought of 2021.

Values of pH were relatively high during the earliest phases of the monitoring study, generally remaining above 7.7 until the spring snowmelt (Figure 14). This phase initiated a decline in pH values that continued throughout the remainder of the study, with final values typically in the 7.4 range. These observations are not as compelling as the specific conductance and temperature data but may still reflect on the relative importance of the deep water quality horizon initially in the study which apparently decreased with time due to dilution from recharge. Although pH was not measured in the borehole logging studies conducted at this site, Canadian Shield brines have showed relatively high pH water at depth, with values in the 8-9 range being typical (Gascoyne, 1996). The most recent reference for the pH of rainwater in this region showed an average value of 5.8 in 2020, so would be consistent as a relatively low pH source that may mix with the higher pH water native to the deeper portions of the fractured rock flow system (National Atmospheric Deposition Program, 2022).

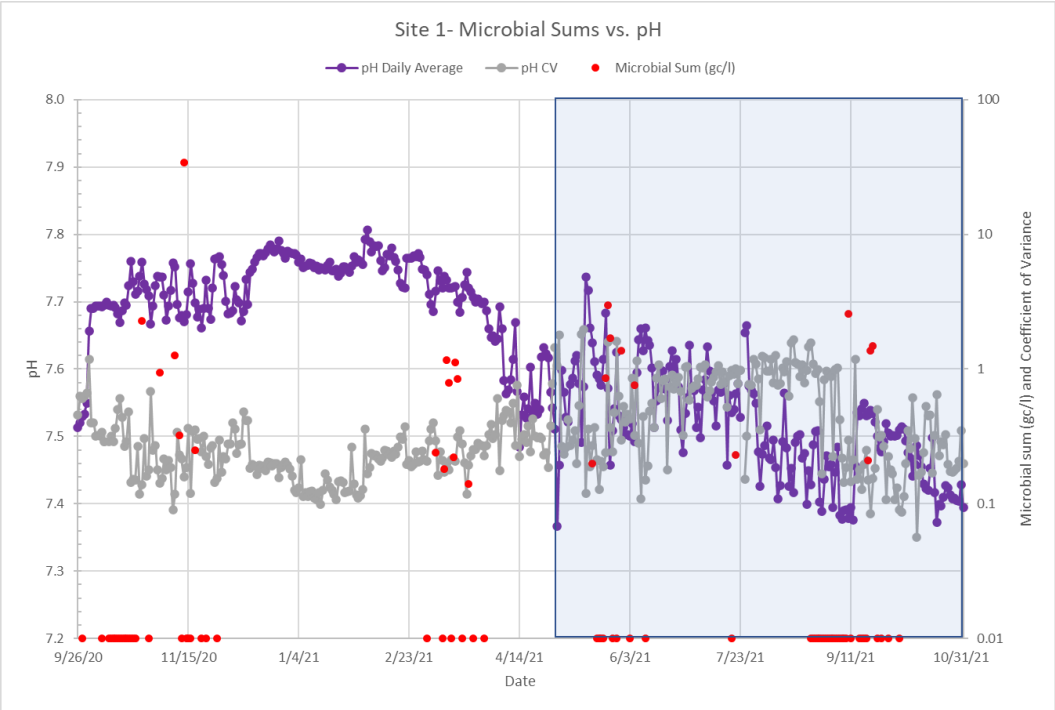

Figure 13. Observations of pH at Site 1. Blue box represents period of irrigation pumping at observation well.

Aside from the observations about specific conductance, temperature and pH noted above, the other data from the water quality sondes yielded significant noise and lack of sensitivity to other parameters being monitored. As a result, they are not discussed further in this report.

Chemical and isotopic results

All but one of the chloride and bromide results from the whole water samples showed clustering outside of the field for dilute groundwater (Figure 15). These samples do not fall on any of the established mixing lines for chloride sources, but is like that for seawater; moreover, the observed average chloride/bromide ratios of approximately 100 are in the range observed for Canadian Shield brines which may have an ancient seawater source (Bottomley, 1996). This is consistent with the observations about specific conductance noted above, which show the influence of the deep flow horizon on well water chemistry, even at relatively small percentages by volume. It's unclear why the single sample with very low chloride and chloride/bromide is so different from the others and may represent a slug of low chloride recharge delivered via the fracture system but, alternatively, may represent a spurious and incorrect result. If a valid result, it suggests potential for short-term events characterized by dilute groundwater to dominate over the more typical brine influence. It is worth noting that the wastewater samples from this site were nearly identical to the drinking water samples in terms of their chloride and bromide signatures. This suggests relatively little waste-derived chloride was mixing with well water before flowing to the sewage lift station during the study, thereby retaining the well water signature. Aside from the outlier value noted above, chloride values ranged from 30.6 to 96.9 (Figure 16), with higher values likely reflecting relatively large contributions from the deep flow horizon, as seen with the specific conductance data set

(Figures 4, 12) and the chloride/bromide ratio (Figure 18). Sampling periods, especially those of the late summer and fall, showed the same decreasing trends observed in specific conductance. In contrast, the spring sampling period was represented by relatively constant to slightly rising values.

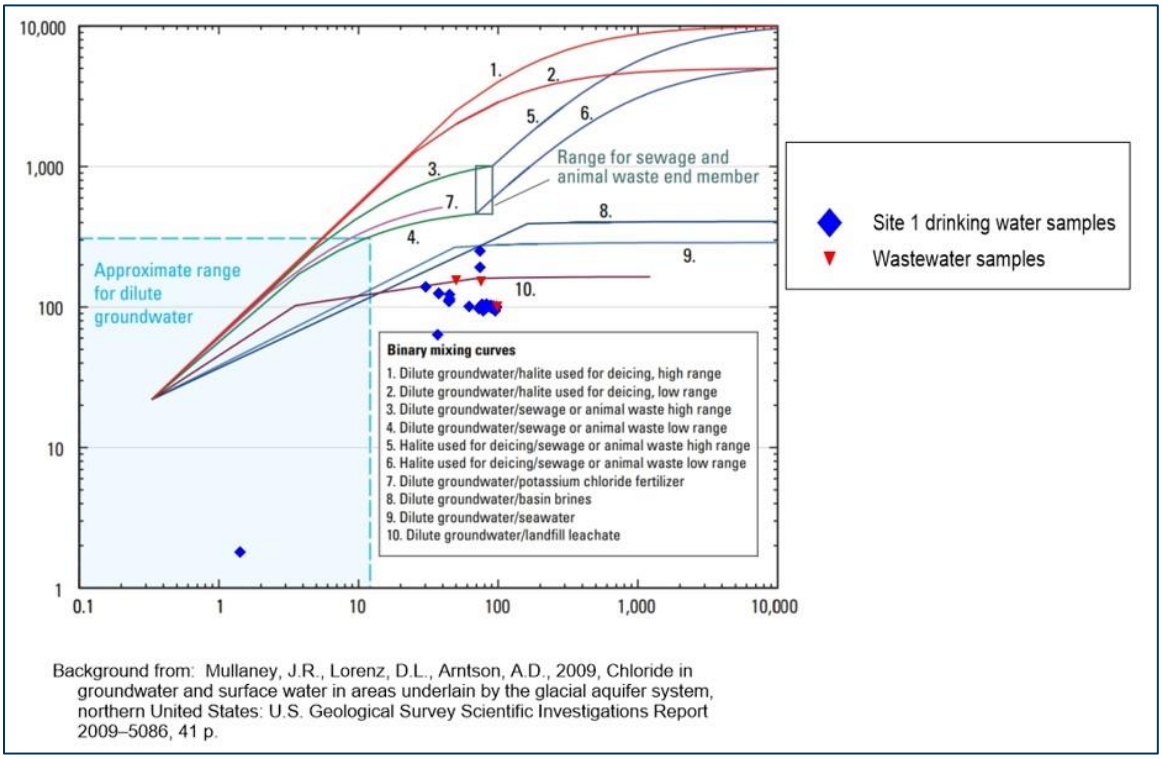

Figure 14. Chloride vs. chloride/bromide results for Site 1 compared to the fields shown in Mullaney et al., 2009.

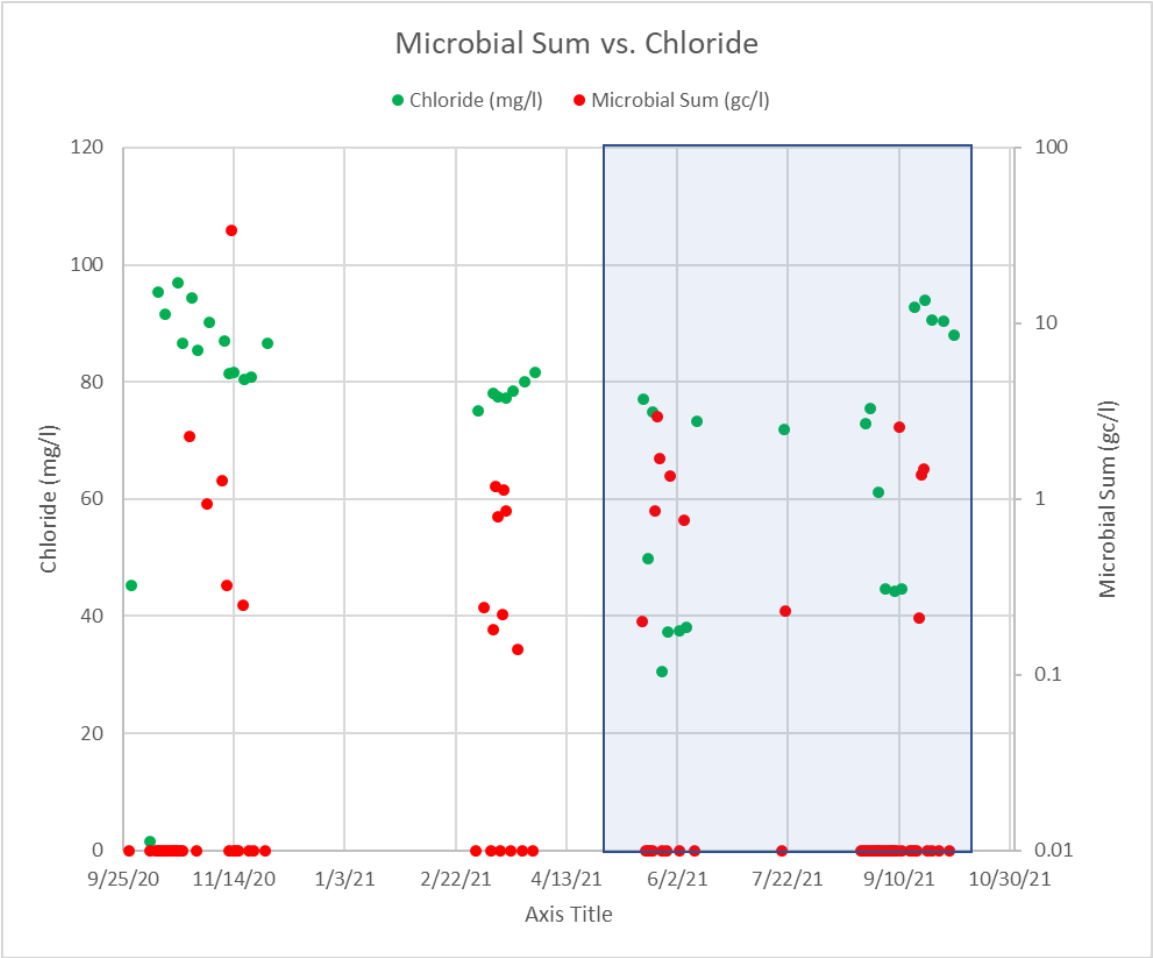

Figure 15. Chloride values versus microbial sums at Site 1. Microbial non-detects were converted to values of 0.01 for plotting on log scale. Blue box represents period of irrigation pumping at observation well.

Direct comparison of chloride and microbial results is not possible because chloride samples were collected concurrently in a location in the water system different than that used for microbial sampling; although this precludes a full characterization of their relationship, a high-level view suggests microbial detections are most closely related to relatively low or decreasing chloride value trends. This same relationship was noted in the discussion of specific conductance and invokes a small proportion of fast-moving recharge to dilute the salinity in this well and likely deliver a microbial load. These results are echoed by the bromide data, which show a similar trend of relatively high values during dry stretches characterized by relatively few or delayed microbial detections, with lower values observed during periods of spring rain and during the large swings in water level associated with irrigation pumping, accompanied by more frequent microbial detections (Figure 17). Bromide is naturally elevated in Canadian Shield brines (Bottomley, 1996), like chloride, so it is expected that they would share a similar pattern.

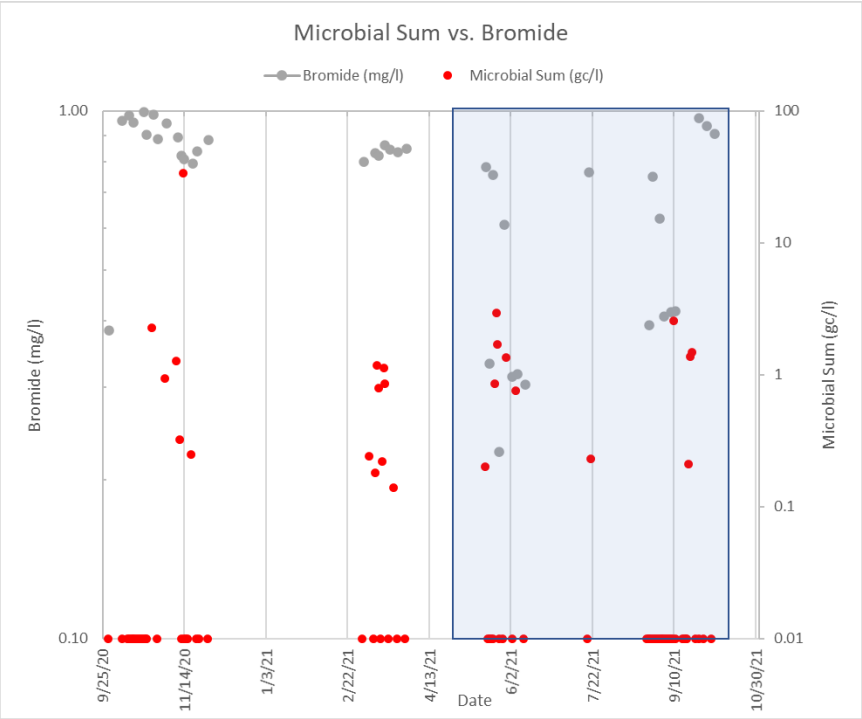

Figure 16. Bromide versus microbial sum in whole water samples from Site 1. Microbial non-detections were converted to values of 0.1 for plotting on log scale. Blue box represents period of irrigation pumping at observation well.

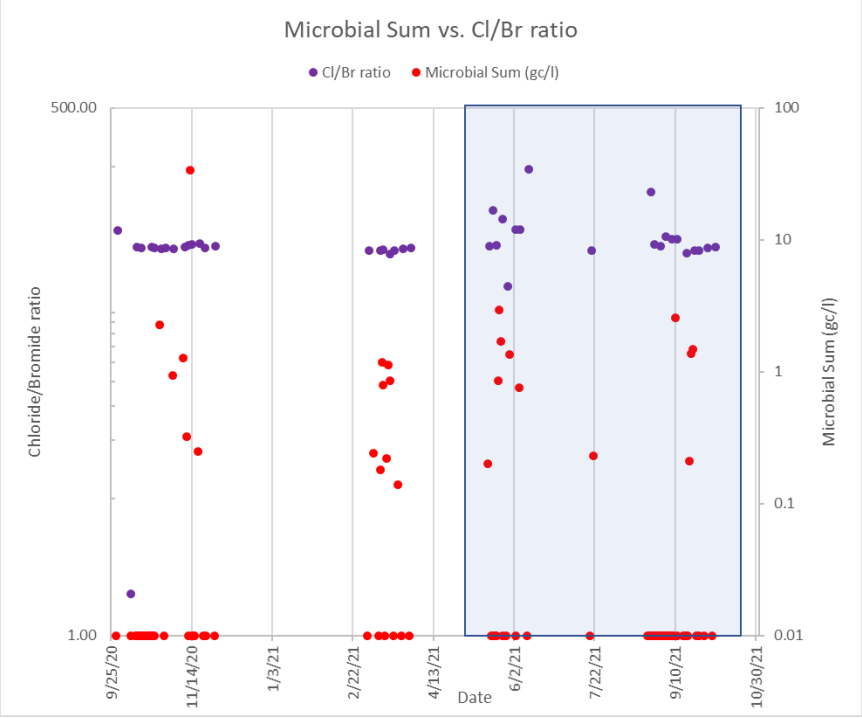

Figure 17. Chloride/bromide ratios over time compared with microbial sums. Blue box represents period of irrigation pumping at observation well.

The stable isotopes of water all plotted essentially on the meteoric water line (MWL) of Landon et al. (2000), indicating no significant capture of evaporated surface water. This confirms the position of the nearby lake as a discharge feature that was not contributing to the well water.

The variation in oxygen-18 and deuterium observed during the study showed that less negative (isotopically heavy) values were generally related to increased periods of microbial detection, but the differences were not great (Figure 19). Samples that were within one day of a microbial detection averaged –11.98 per mil for oxygen-18, while those within one day of non-detect samples averaged –12.07 per mil. Also, the lack of exactly coincident samples for both the water isotopes and microbes limits this analysis, as noted above for the chloride and bromide assessments. We speculate that the well water results are consistent with being impacted by recharge events or pumping which results in mixing between deep and near-surface flow zones. Heavier (less negative) water isotopes in the shallow system are consistent with the pattern observed from depth-discrete samples taken from a nearby well that showed isotopically heavier water towards the top of the water column (Minnesota Department of Health, 2020).

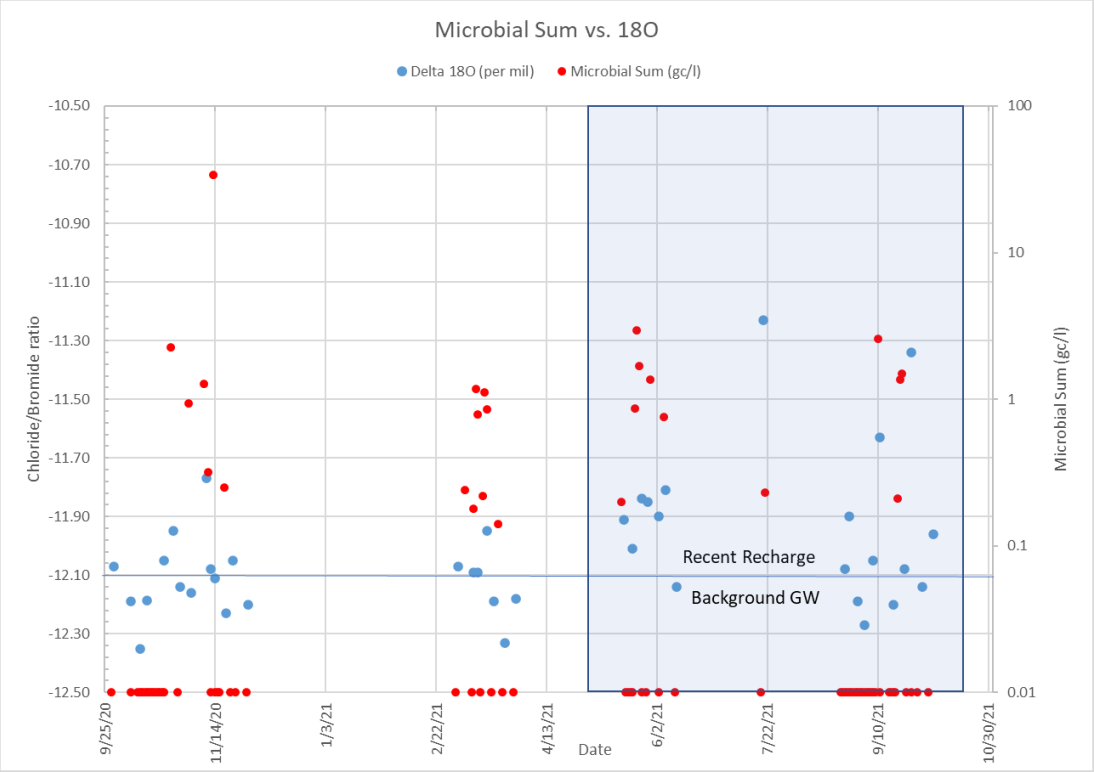

Figure 18. Comparison between oxgen-18 values and microbial detections. Microbial non-detections were converted to values of 0.01 for plotting purposes. Blue box shows when observation well was used for irrigation. Blue line represents possible boundary separating results dominated by the deep-water quality horizon (Background GW) and those reflecting pulses of recent recharge.

Comparison with wastewater samples

A relatively high-level norovirus detection in drinking water during Event 2 followed a norovirus detection from the sewage lift station by approximately 3-weeks (Figure 20). Norovirus was found in the septic waste in most samples, but only seen this one time at the well. Pepper mild

mottle virus and Human *Bacteroides* were consistently found in the septic waste and occasionally in close time frames with the drinking water detections (within one-week). *Salmonella* was only found in a drinking water sample, never in the septic waste, whereas rotavirus, human polyomavirus, adenovirus, and *Cryptosporidium* were only found in the septic waste. Although not a definitive characterization, the relations noted above suggest that the sewage lift station may be a contamination source for nearby wells; Borchardt et al. (2004) noted highest pathogen occurrence near a lift station. However, it is not possible to separate the risk posed by this feature from any related sewer connections that might be leaky. Also, the lack of a one-for-one correlation in time with all microbial organisms suggests that any connection between these wastewater components and the well may be relatively indirect and subject to significant time lag.

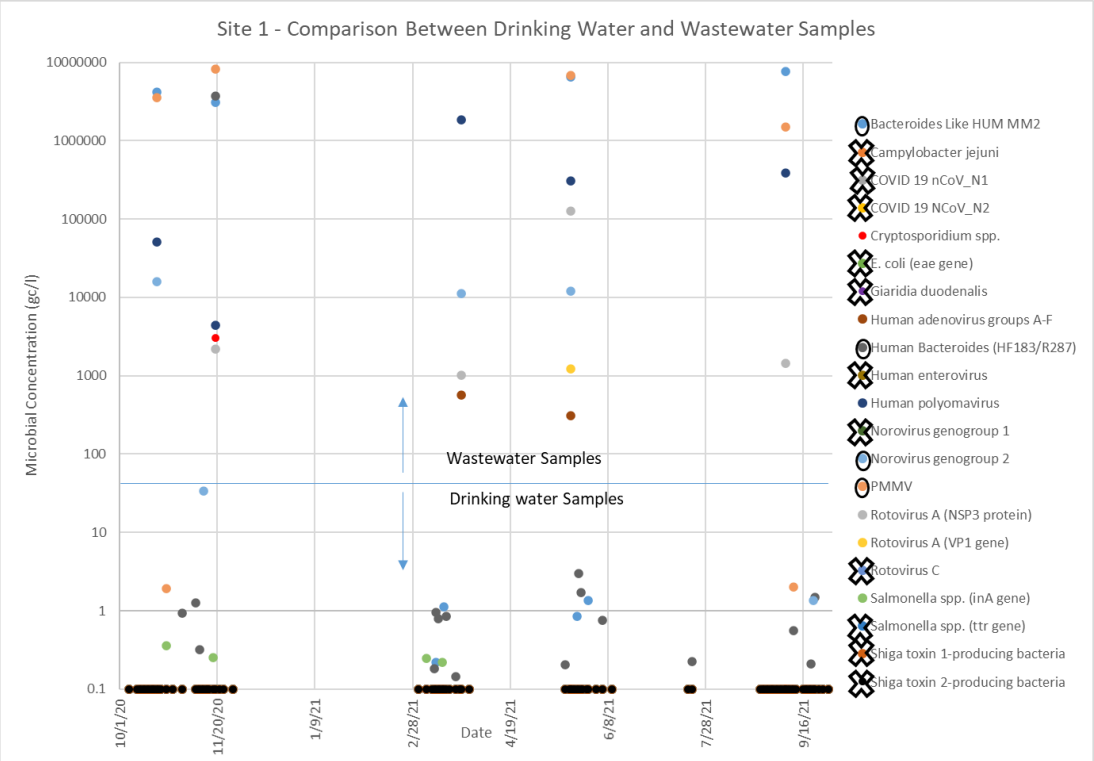

Figure 19. Comparison between drinking water and wastewater microbial results. Results below detection were converted to 0.1 for plotting purposes. Circled organisms were detected in both the drinking water and wastewater. Organisms with an "X" were not detected in either source. The remaining organisms were detected in only drinking water or wastewater, not both.

Site 1 - Groundwater age dating

Samples were collected for SF6, dissolved gas and tritium analysis on October 20, 2021, and analyzed at the University of Utah Department of Geology and Geophysics Dissolved Gas lab. The results showed contamination with excess terrigenic helium, which indicates that at least some component of the well water was of very great age. However, the presence of tritium at 3 tritium units (TU) and the flashy response to recharge noted in the hydrograph and microbial and chemical results at this site suggests that this well water is a mixture of very old and young water. Assuming that the deep flow horizon is represented by water with no detectable tritium,

as suggested by the presence of terrigenic helium, and that the shallow horizon is represented by approximately 7 TU (MDNR, personal communication, and MDH well logging study, 2019), then the deep flow horizon represented approximately 55% of the well water volume at the time of sampling, consistent with estimates provided by specific conductance values generally for this well. As noted previously in the discussion of specific conductance, temperature and pH, this percentage likely varies with recharge events, during which the young water component in the well may increase relative to the old water component by up to 10-20% by volume. Lag time analysis suggests that this young water fraction recharges the aquifer on time frames of hours to days.

Site 1 - Tracer Studies

Dye trace investigations were launched at varying times throughout the project, with differing objectives (Barry, 2022c). Eosin was introduced in a urinal at a cabin near the well sampled for the 2014-2016 study (Well 7) on March 6, 2019. This trace was intended to look for connections between the wastewater conveyance piping leading from this cabin to the community drainfield, or the drainfield itself, and Well 7. Fluorescein, also known as uranine, and sulforhodamine B were introduced on September 3, 2021, the former into a floor drain of a lodge building near Well 7 to assess its possible connection via wastewater piping, and the latter was introduced in a pit toilet thought to be possibly connected to the well sampled during the precipitation monitoring phase of the project (Well 3). Figure 21 shows the location of dye deployment sites with respect to wells that were monitored.

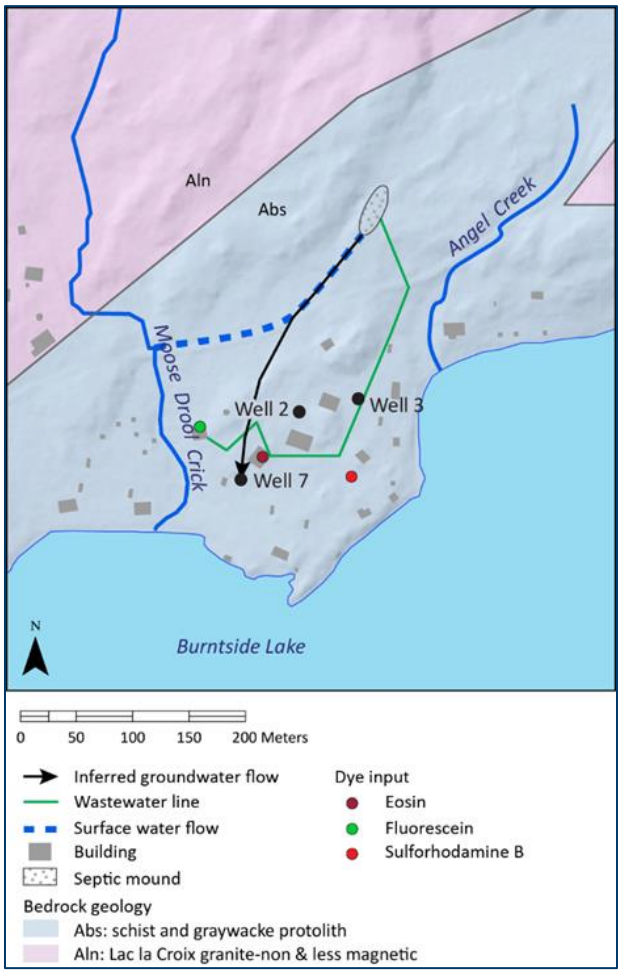

Figure 20. Bedrock geology, dye input locations, and inferred groundwater flow of eosin dye (Barry, 2022c).

Results from the first tracer study showed a connection between the community drainfield and both surface water features and Well 7. Dye initially arrived at Moose Drool Crick April 3 – April 10, 2021, via a seep from the drainfield. Initial dye detections at the well occurred on September 7-13, 2021, with the first strong detections noted during the period November 5 – December 1, 2021. Changes to the discharge piping from Well 7 that occurred early in the study and unbeknownst to the study team resulted in uncertainty about whether dye arrived sooner than September 7, 2021. If not, the 31-month lag time between dye release in the wastewater system and arrival at Well 7 suggests a tortuous groundwater flowpath via relatively low-conductivity fractures and involving interaction with surface water features. Retardation based on interaction between fractures and the rock matrix cannot be ruled out.

As of December 2022, the second and third dye traces did not show detections at the wells that were monitored, although eosin was observed at a surface water monitoring point (Moose Drool Crick near its mouth at Burntside Lake). In addition, rising groundwater levels associated with above-normal precipitation in the spring of 2022 resulted in the observation of sulforhodamine B in water ponded at the land surface outside the pit toilet where it had been deployed, pointing to this feature as a potential threat to groundwater quality under some conditions.

The absence of dye detections from these last two tracer tests may indicate that the wastewater components that were dosed were not sources of microbial contamination at the study wells. Alternatively, if the long lag time noted between the eosin dye deployment and its arrival at Well 7 is characteristic of shallow groundwater flow at this site, it's possible that these dyes may still be enroute. If multi-year lag times are characteristic for groundwater movement between possible pathogen sources and study wells, it raises the question of the viability of the microbial genetic material detected in both this and the 2014-2016 study. Or this observation may simply reflect that other possible pathogen sources, perhaps more directly connected to the wells, are present and were not dye traced. Included may be the septic lift station that was sampled as part of the recharge monitoring project, or its sewage conveyance connections.

Additional observations involving measurements of specific conductance, water isotopes and fluorescein at the surface water features and wells involved in the dye trace studies confirm short times of travel between recharge events and the shallow bedrock aquifer (Barry, 2022c). These estimates range from hours to a few days, consistent with those observed in the microbial data generated here. Taken together with the dye trace observations noted above, these data support a conceptual model of fast vertical movement of water and contaminants from the land surface to the shallow groundwater system, followed by relatively slow lateral movement. In such settings, the risk posed by short-lived contaminants, such as pathogens, is dominated by proximity between pathogen sources and wells.

Site 1 - Annular space test

The competency of the grout seal in the annular space between the well casing and borehole wall was tested at Well 3 and Well 7 using a brine solution deployed at the surface and specific conductance measurements conducted in the well water, after methods described in Walsh (2018). The brine consisted of a 1% NaCl solution with an average specific conductance of 16,000 µS/cm. Approximately 180 gallons were deployed at Well 3 on November 5, 2021, and approximately 60 gallons was used at Well 7 between September 22-September 24, 2021 (Barry, 2022c). It was calculated that if 50% of this solution were to permeate the grout seal and make it to the well bore, it should raise the specific conductance of the well water to at least 1000 µS/cm. Specific conductance was measured at 15-minute intervals at the raw water tap used for the microbial sampling, and follow-up samples for bromide and chloride were taken to look for the presence of a brine signature. Specific conductance measurements continued for at least five months following the end of brine deployment. No rise in specific conductance beyond the range observed during the study was noted, suggesting that rapid movement of surface water along the annular space of the well was not a likely pathway for the microbial detections observed in this study.

Site 1 - QMRA

Quantitative microbial risk assessment (QMRA) was used to estimate daily risk based on pathogen detections at each site. The QMRA methodology is described in Appendix A. For this QMRA, risk is calculated as the estimated risk of infection from one day drinking water with the pathogens detected in a given sample. A risk estimate, such as .001, could be viewed as 1/1,000 people who drink the water will get an infection, or an individual has a 1/1,000 chance of

getting infected on the given day. An acceptable risk benchmark commonly applied to drinking water is .0001. It should be noted that not all infections lead to illness.

The most concerning detections of genetic material at Site 1 were the two norovirus detections, one on November 13, 2020, with a concentration of 34.04 gc/L, and one on September 21, 2021, with a concentration of 1.37 gc/L. The maximum estimated daily risk was 0.51 for the November 13, 2020, norovirus detection. It should be noted that any detection leads to an estimated risk above the commonly applied acceptable risk benchmark, and that the highest estimate indicates five out of ten people drinking the water could become infected.

There were pathogen detections in six out of the 89 samples at Site 1. Given that the public population served by Site 1 is transient (e.g., they are at the facility for approximately one week per year), most people are likely to be served water that is free of pathogens. However, treatment or use of an alternate source that is free of pathogens would be necessary to ensure full public health protection.

Detections of human fecal indicator bacteria were more frequent than pathogens, and were at very low levels, supportive of small volumes of contaminated water entering the well.

For a norovirus detection to occur in a well at this site, there presumably needs to be someone at the site that is shedding the virus into the wastewater (or possibly onto the ground), making it hard to predict when norovirus risk will occur. Norovirus is easily spread person-to-person and from surfaces, and those transmission pathways are likely to impact risk in addition to any risk from drinking water.

Site 1 - Conclusions

The well at Site 1 showed microbial detections that appreciably lagged precipitation events following the dry fall of 2020, but which became more coincident in time in subsequent events once wetter antecedent precipitation conditions occurred. Average lag times reduced from nearly 9 days initially to 2-4 days post-precipitation, with several same-day detections noted. The greatest frequency of microbial detections and the shortest lag times were observed with the onset of spring thaw through to early summer 2021, prior to the onset of very dry conditions. Accompanying these detections, especially those of higher concentrations, were short-term changes in specific conductance, chloride, bromide, and the stable isotopes of water that may be coincident with short-term pulses of young recharge resulting in changes to the proportions of deep and shallow groundwater present in the water column. Mass-balance analysis suggests that these doses of young water likely add around 10-20% of the well water column by volume.

The source(s) of the microbial detections observed in this study are not known with confidence. Several potential fecal sources exist within the well capture zones (Figure 4) including the sewage lift station, related sewer piping and several pit toilets and a community drainfield. Sampling of the sewage lift station showed some coincidence with microbial detections observed in the drinking water, but the correspondence was not consistent and often lagged in time. Confounding our understanding between the connection between this feature and the drinking water results is that it failed to develop a unique chemical signature for chloride and bromide, suggesting relatively little sewage contribution to the overall flow through the system.

It is possible that the lift station or associated sewer lines leak and intermittently provide a pathogen source to the drinking water, but this was not proven definitively.

All told, these results fit a conceptual model of small volumes of fast-moving recharge driven by intermittent rainfall or snowmelt events mixing with a reservoir of older, relatively unimpacted groundwater in the aquifer tapped by this well. The exact pathways traveled by these pulses of young recharge are unknown, but the absence of any obvious problems with well construction or the grout seal at this well suggests they are not specifically well-related and may be naturally occurring within the fractured-rock groundwater system. Preferential flow conduits may include bedrock fractures and other high-conductivity pathways such as gravel lags in the glacial drift. The dye trace studies described above support this conceptual model and add the apparent disconnect between the short vertical times of travel between the land surface and shallow aquifer system and relatively long lateral travel times within that system. These studies also pointed out the connection between a community drainfield at this site and at least one well. Relocation or mitigation of this drainfield would likely benefit groundwater quality at the site, although it's unclear if the benefits would extend to all wells in the vicinity due to uncertain connectivity and flowpaths. The absence of dye detections at the well that was used for sampling suggests it is not impacted by the fecal sources where dye was deployed, although it's unclear if those dyes are enroute and may arrive eventually, or if other possible sources exist in the vicinity where dyes were not deployed. The sewage lift station that was sampled for this project may be such a feature, or the wastewater conveyances that flow to and from it. In the absence of a "smoking gun" for the source of microbes observed at this well, it is not clear that new well construction or reconstruction would provide significant benefit, unless a new well could be placed upgradient of any potential fecal sources or constructed in such a way as to isolate the deep flow horizon from the shallow one. However, such construction could create logistical difficulties for siting and piping, and possible inadequate yield or water quality

Site 2 - Hydrogeology

Site 2 is in north-central Minnesota, approximately twelve miles from the Mississippi River which is the dominant discharge feature in the area. Groundwater from a 4-inch well supplies a restaurant that serves a transient population of approximately 50 persons per day. Prior to the onset of the study, the facility had also included a day care that served approximately 60 children. The surrounding land use is a mix of developed land, deciduous forest, and grassland/pasture.

The surficial geology of the site is characterized by approximately 110-feet of unconsolidated Pleistocene sediment of the St. Croix phase of the Rainy Lobe, consisting primarily of coarse-grained glaciofluvial material (Figures 22 and 23, Setterholm, 2004). The total thickness of glacial sediment in the area ranges up to approximately 200-250 feet which rests on Precambrian crystalline bedrock (Setterholm, 2004).

Depth to water is approximately 50-feet below the land surface at the well site and groundwater flow directions are variable, with several flow divides noted based on water levels from nearby wells. However, a westerly flow direction seems dominant in the vicinity of the facility's well (Figure 22), and vertical hydraulic gradients appear to be relatively low and slightly upward in the general area, reflecting the abundant lakes and wetlands that represent localized

discharge zones. Capture zones of one and ten-years were generated using a stochastic modeling method called Oneka (Figures 22 and 24).

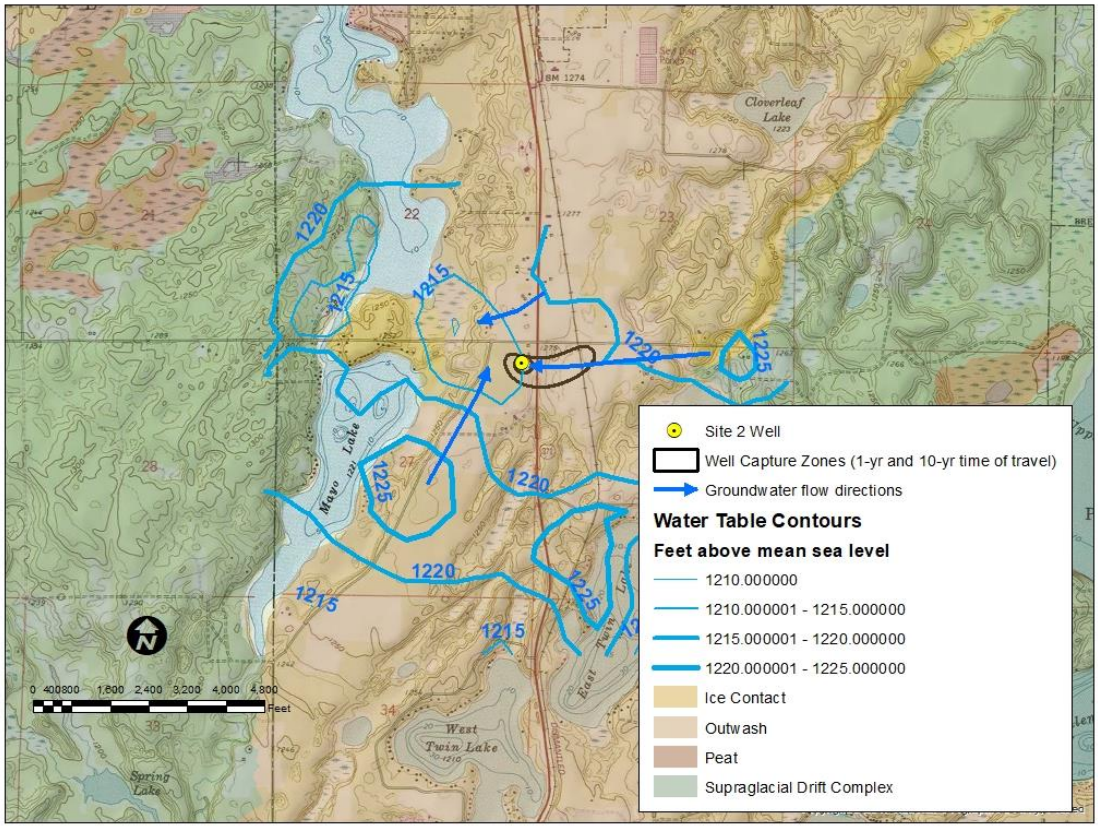

Figure 21. Site 2 hydrogeologic setting.

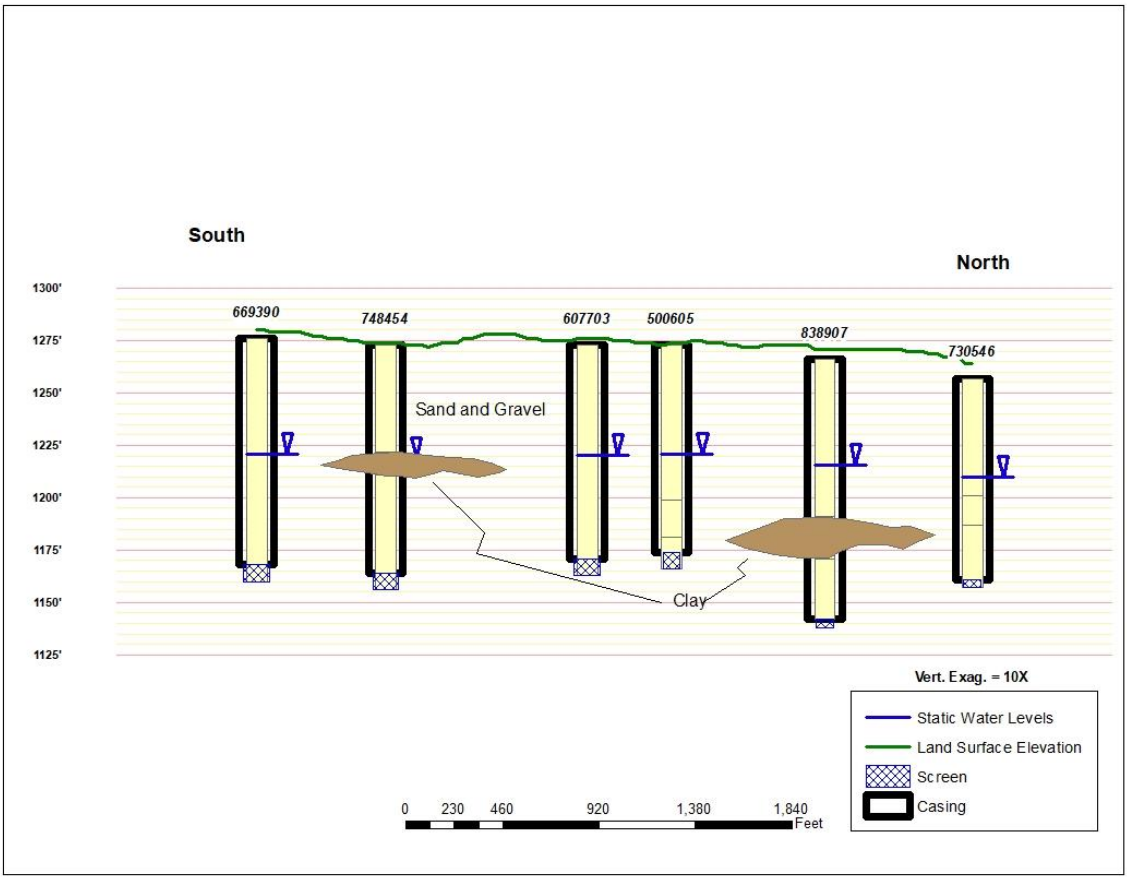

Figure 22. Geologic cross-section through Site 2, looking west. The well sampled for the study is labeled 500605.

Site 2 - Potential Contaminant Sources

An inventory of potential contaminant sources located within 200-feet of the public supply well at this facility shows several possible sources of microbial contamination within the one-year time of travel capture zone for the well (Figure 24). These include two septic systems and associated drainfields and sewer lines connected to the facility. Prior to the study, both septic systems were active, but the southern system underwent a significant decrease in loading due to the day care moving away from the facility. The change from day care to a private residence resulted in some continued loading later in the study, but much reduced from pre-study loads for that portion of the septic system. In addition, pressure-testing studies at both systems revealed damaged sewer lines exiting the building and leaking to groundwater, at one location only approximately 20-feet from the well. Both were repaired prior to the recharge monitoring study but represented significant contamination sources for some time before their repair.

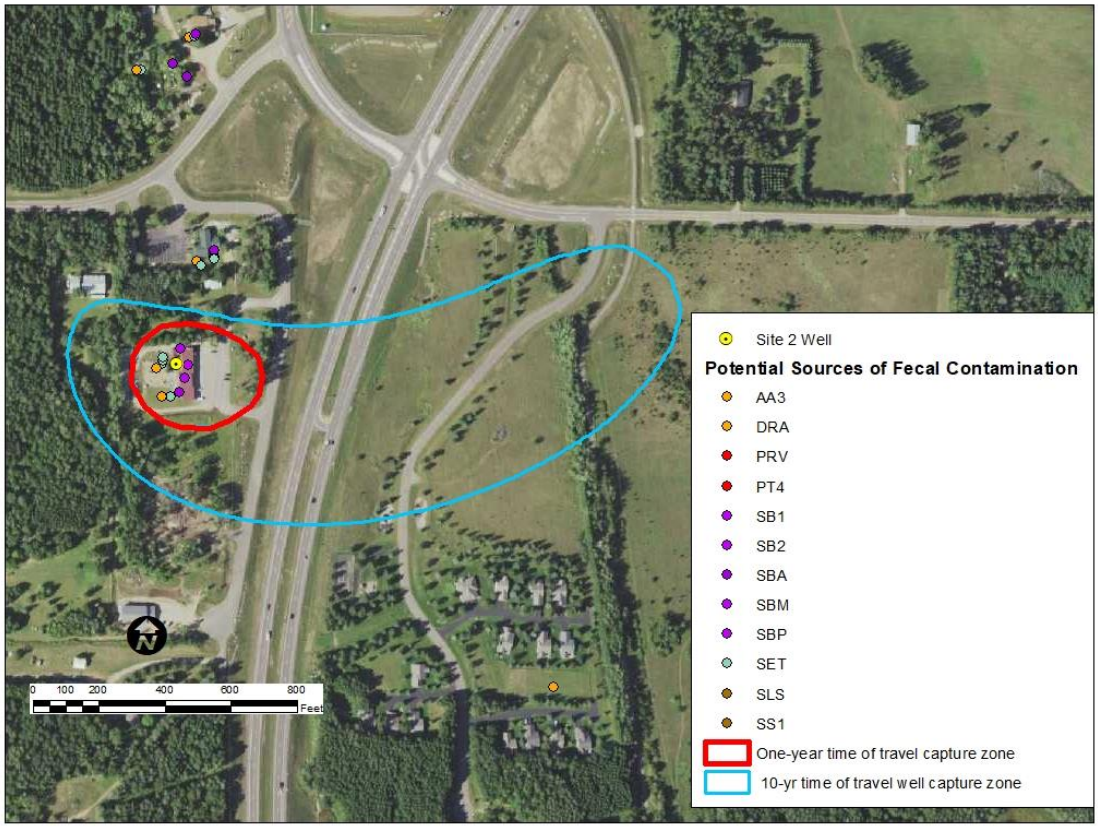

Figure 23. Location of possible pathogen sources with respect to Site 2 well and capture zones.

Site 2 - Monitoring Setup

The monitoring setup at this site matched the general description noted under the discussion of study design, with these additional details specific to Site 2:

- The autosampler at this site was attached to an untreated water tap from the study well downstream from a single hydropneumatic bladder tank with a 33-gallon capacity. Flow through this setup was continuous throughout the duration of the study except for a few brief maintenance periods.
- The official observation well for this site was completed in the same aquifer as the study well and located approximately 6-miles to the southeast. An additional observation well was later constructed on-site, but its record does not span the entire study period so is only used for reference.
- The wastewater sampling at this facility included two sets of septic systems consisting of a series of tanks in sequence that discharged to separate drainfields, with septic tanks located approximately 46 and 100 feet from the well and the drainfields located further away at 64 and 108 feet. Only a single wastewater sample was collected from each septic system during the final precipitation event monitored at Site 2 due to access issues during earlier sampling events. The sample from the northern septic system came from the first and

smallest septic tank in the system, which may not represent the time-integrated composition of the microbial load seen by the groundwater system due to the short residence time within the tank. The sample from the southern septic system was from a larger tank.

Site 2 – Comparisons with water use and precipitation regimes from preceding water years and study periods

The months during which sampling occurred during this study were classified as wet, other than the single shortened sampling event that occurred during the dry summer of 2021 (WETS, Minnesota DNR, 2022). The preceding months were evenly split between dry and wet, with a single normal month. For comparison, the preceding sampling months in the 2014-2016 study were evenly split between wet, normal, and dry.

Water use from the study well was probably lower than historical averages due to the loss of the day care previously served by the well, however water use is not metered so this reduction cannot be quantified accurately. Based simply on estimates of population served by the restaurant and day care, the relocation of the day care may have resulted in an approximate 50% reduction in water use when compared with the 2014-2016 monitoring period.

Site 2 – Description of Sampling Events

Five full and two partial precipitation events were monitored at Site 2 during this study (Figures 25-27 and Table 5). Events 1 and 2 captured a series of late fall rains that followed a normal late summer period in terms of rainfall. These two events were essentially continuous, spanning October 8-November 30, 2020, with a one-week period (November 2-November 8) separating them. Total rainfall during this period equaled approximately 2.8 inches and resulted in short-lived water level rises of only a few hundredths of foot on an otherwise falling hydrograph, reflective of the relatively dry antecedent conditions. Events 3 and 4 also ran together and spanned from March 1-April 25, 2021. These events captured the onset of early spring warmth accompanied by the complete loss of approximately 7-inches of snowpack and accompanied by rain totaling 3.7 inches. A water level rise of 0.7 feet was observed during the period encompassed by Events 3 and 4, where a continuously rising hydrograph trend started the first week of March. This rise was noted during a time when at least partial frozen ground conditions were suggested by standard indicators, such as the presence of lake ice and frozen soil beneath area highways, revealing the shortcomings of those indicators and/or the importance of recharge via macropore flow in partially frozen ground (Mohammed et al., 2019). Event 5a ran from May 17-May 21, 2021 and was aborted because the forecast rainfall amount did not occur. A water level decline of 0.03 feet accompanied this period. Event 5b ran from July 5-July 29, 2021. It anticipated a rainfall event on July 7 which did produce 0.88 inches of rainfall, but this sampling event was terminated in favor of another more significant-rainfall event. The water level continued to drop during this period by a few hundredths of a foot, reflecting the drought conditions that were firmly established. The final sampling event (5c) spanned August 18-September 20, 2021 and captured 7.65 inches of late summer-fall rains that followed the significant drought. This rainfall stopped the steady hydrograph decline, resulting in an

overall increase in water level of 0.04 feet, with occasional rises of 0.2 feet noted during this period.

Table 5. Summary of precipitation events monitored at Site 2.

Event	Date	Type	Cumulative Precipitation During Event (in)	Net Water Level Change from Baseline During Event (ft)	Precipitation History from Current/Prior Month	Number/% of Samples Positive for Any Microbial Parameter	Lag Time in Days Between Precipitation and Microbial Detections (Shortest/Longest /Avg)	Microbes Detected (pathogens in red)	Maximum Concentration (gc/l)
1	10/8-11/2 2020	Fall Rain	1.49	-0.05	Normal/Dry	12 (80%)	0/6/1.6	HB, PMMV, Giardia	2.35
2	11/9-11/30 2020	Fall Rain	1.38	0	Wet/Normal	10 (83%)	0/7/2.3	HB, Giardia	18.16
3	3/4-4/6 2021	Spring Thaw, Snowmelt and Rainfall	1.4 on top of melting of approximately 6-inches of snowpack	+0.26	Wet/Dry	19 (95%)	0/8/1.6	HB, B-like Hum, Giardia, Salmonella	1.01
4	4/7-4/25 2021	Spring Rain	2.8	+0.38	Wet/Wet	13 (100%)	0/6/2	HB, PMMV, Giardia	2.99
5a	5/17-5/21 2021	Late Spring/Early Summer Rain	0.01	-0.03	Dry/Wet	3 (100%)	3/5/4	HB, Giardia	2.07
5b	7/5-7/29 2021	Summer Rain	2.24	-0.21	Wet/Dry	2 (67%)	7/8/7.5	Giardia	1.0
6	8/18-9/20 2021	Late Summer/ Early Fall Rain	7.65	+0.04 overall, with rises up to 0.2	Wet/Dry Normal/Wet	17 (74%)	0/9/1.7	HB, B-like Hum, PMMV, Giardia	1.7

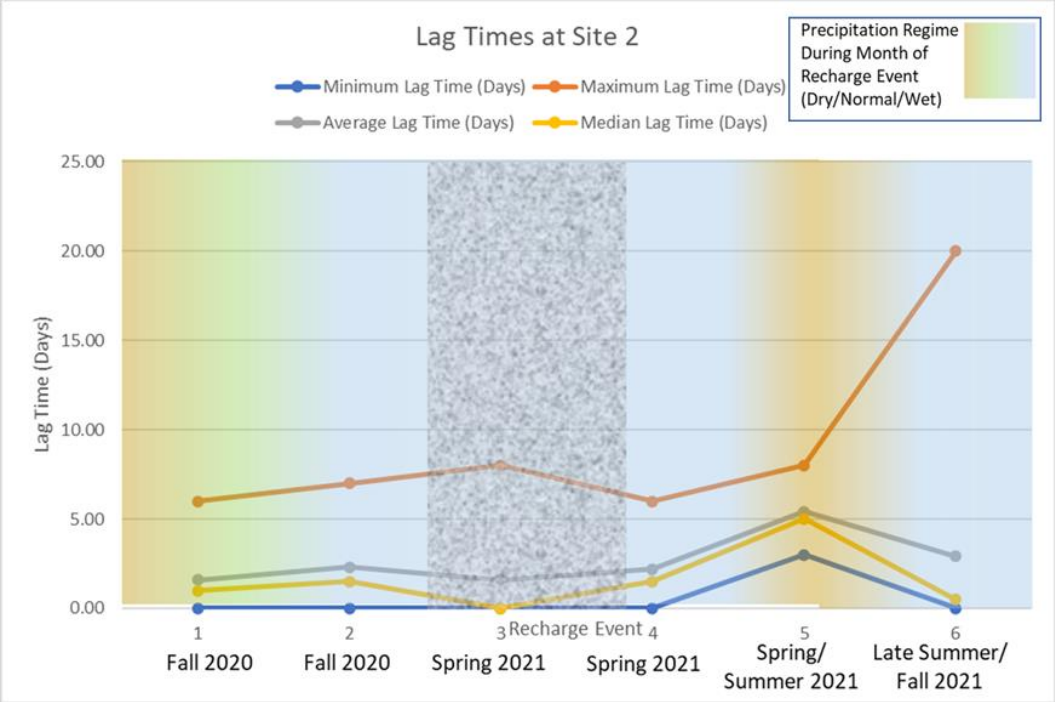

Figure 24. Summary of lag time information for Site 2. Stippled pattern indicates period of possible frozen ground conditions based on indicators such as lake ice and frost depth beneath area highways. Precipitation regimes from MDNR Climatology (2022).

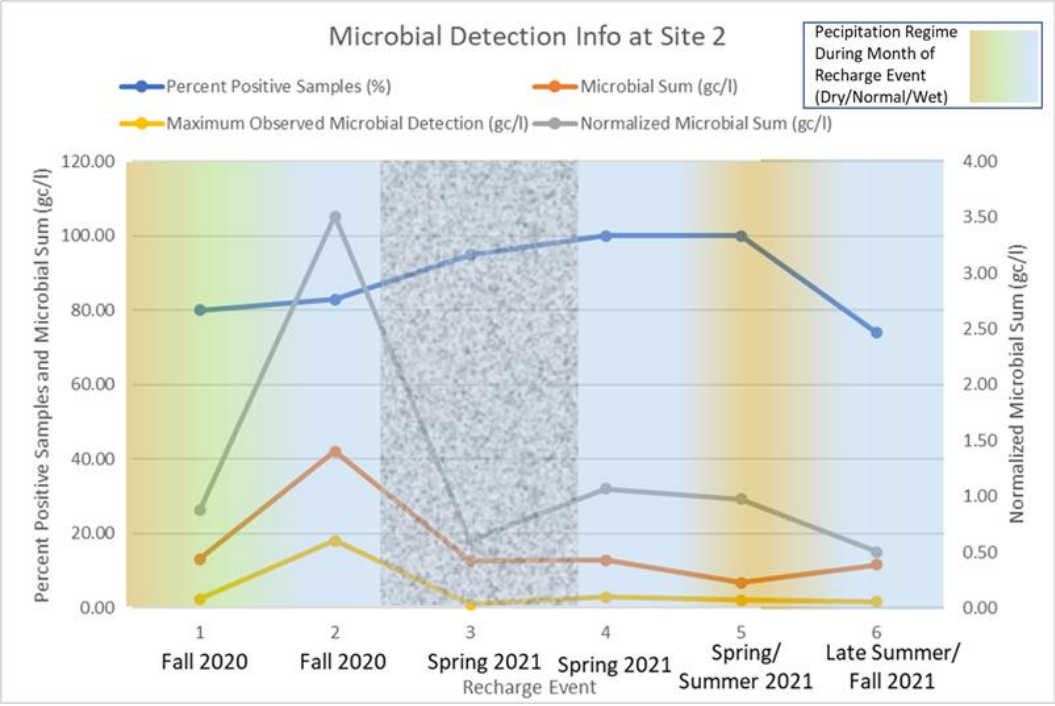

Figure 25. Summary of microbial detections at Site 2. Stippled pattern indicates period of possible frozen ground conditions based on indicators such as lake ice and frost depth beneath area highways. Precipitation regimes from MDNR Climatology (2022).

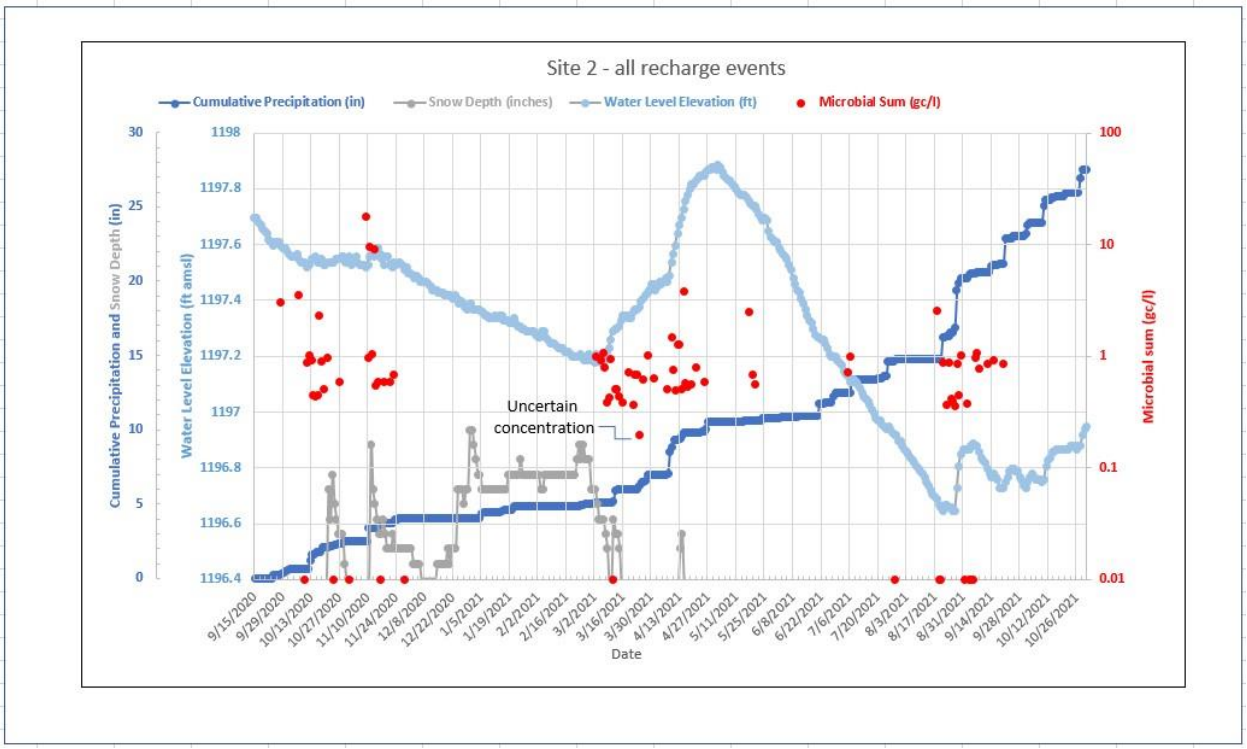

Figure 26. Precipitation monitoring events at Site 2. Microbial non-detections were converted to values of 0.01 gc/l for plotting on log scale. Point labeled "uncertain concentration" lacked sample volume information so could not be quantified and is shown here as a minimum estimated value for plotting.

Site 2 - Monitoring Results

Microbial results

Of the 93 samples taken from this well, 77 (83%) showed some level of microbial detection which represented 97 positive results for unique microbiological targets (16 samples were positive for more than one target organism). *Giardia* was detected in every positive sample, occasionally joined by an indicator organism (Human *Bacteroides*, *Bacteroidales*-like HumM2 or pepper mild mottle virus). *Salmonella* and adenovirus were the only other pathogens detected and were only detected a single time. Concentrations were generally low, with many results around 1 gc/l or less. A notable exception was a *Giardia* detection of 18.2 gc/l on November 6, 2020.

In the 2014-2016 study at Site 2, eight of 12 samples were positive (67%), again with most of the detections coming from *Giardia*. The highest concentration observed from those samples, a rotavirus detection at 228 gc/l, was approximately ten times greater than the highest microbial level measured during this most recent study. Moreover, rotavirus was detected during 2014-2016 but not in this current study, whereas adenovirus was detected in this study but not during 2014-2016. *Giardia* concentrations from that monitoring phase averaged 3.3 gc/l, approximately three times that seen in the more recent monitoring study (0.88 gc/l).

Of the 12 sampling episodes in 2014-2016, the sampling month's precipitation regime was wet compared to historical standards in six, whereas four were dry and two normal. During this current study phase, four of the seven monitoring events were preceded by dry conditions, with only two considered wet and one normal. Despite these differences in antecedent precipitation regimes, overall detection frequencies were similar between the two study phases. This may relate to the presence of an appreciably thick unsaturated zone at this site. At approximately 50-feet, this package of dry sand and gravel may retain, delay, and perhaps reduce predation of microbes, such as *Giardia*. It is conceivable that the day care facility (which ceased operation immediately before the start of this study) was a source of *Giardia* that is still moving through the unsaturated zone. The decrease in average *Giardia* concentrations between the two study phases noted above may reflect degrading of this source. Alternatively, the reduction may simply reflect the difference in a current *Giardia* source, the number of samples, sampling frequency or other factors such as well use and precipitation regimes.

The lag times between the onset of precipitation events and microbial detections at Site 2 were relatively consistent throughout the study, with median values of just under two days, although there were many incidences of detections coincident with the onset of rainfall or snowmelt (Table 5, Figures 25, 29 and 30). This two-day average lag time was also observed for water level responses between the two observation wells for this site, suggesting that this time period reflects a representative transit time through the vadose zone here (Figure 28). Longer lag times were observed during and immediately following the drought that persisted through the summer of 2021, which is expected as the ability of the unsaturated zone to transport water and pathogens is a function of the unsaturated zone moisture content. The onset of significant late summer/early fall rains that ended that drought again reduced median lag times to those more typical of earlier in the study when wetter regimes were in place, although the highest maximum lag time of the study (20 days) followed the return to wet conditions (Figure 25). The percent of samples with detections also showed correlation with antecedent wetness, with highest percentages occurring in the spring of 2021 prior to the onset of drought conditions (Figure 26). Although lag times between precipitation events and microbial occurrence generally decreased after drought conditions broke in the late summer and early fall of 2021, the frequency of microbial detections reached its lowest level. Microbial sums peaked in the second precipitation event during late fall of 2020, largely driven by a single detection of *Giardia* at relatively high concentration (Figure 26). Figures 29 and 30 show microbial detections compared against cumulative precipitation and water level hydrographs from the observation well for fall 2020 and spring 2021 for comparison.

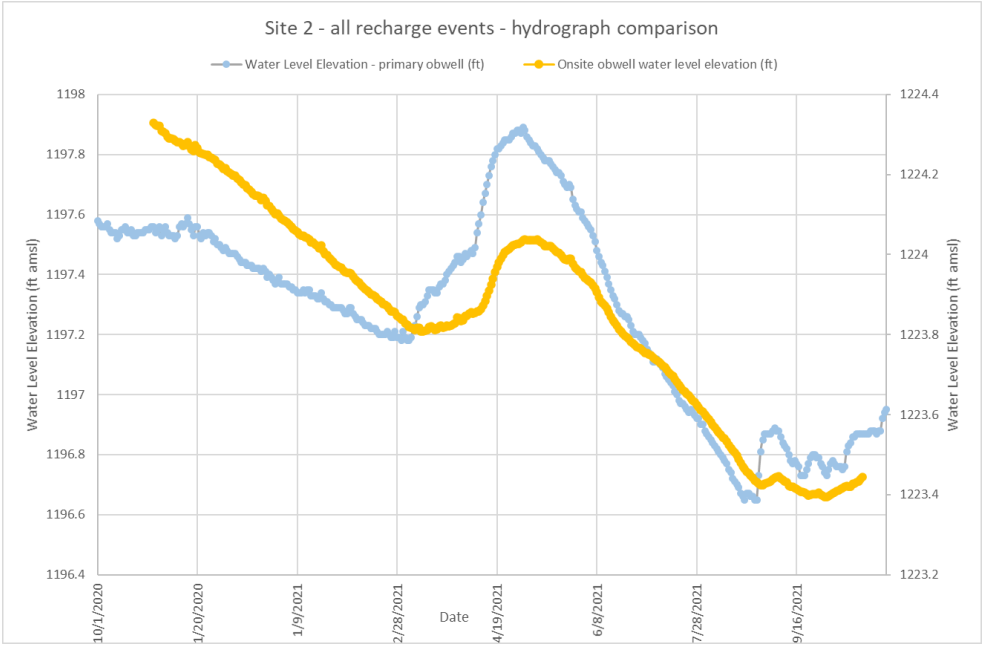

Figure 28. Comparison between hydrographs for the observation wells for Site 2, showing the average two-day lag time for the on-site well compared with the official observation well with much shallower depth to water (~11 ft. vs 50 feet).

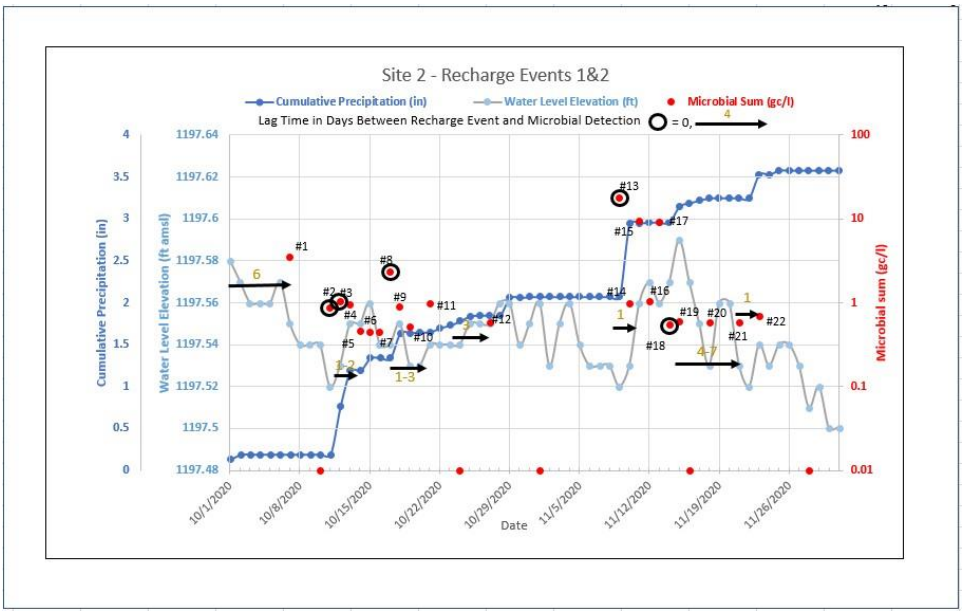

Figure 29. Microbial detections compared to cumulative precipitation and water level changes during Precipitation Events 1 and 2. Microbial non-detections were converted to values of 0.01 for plotting in log space.

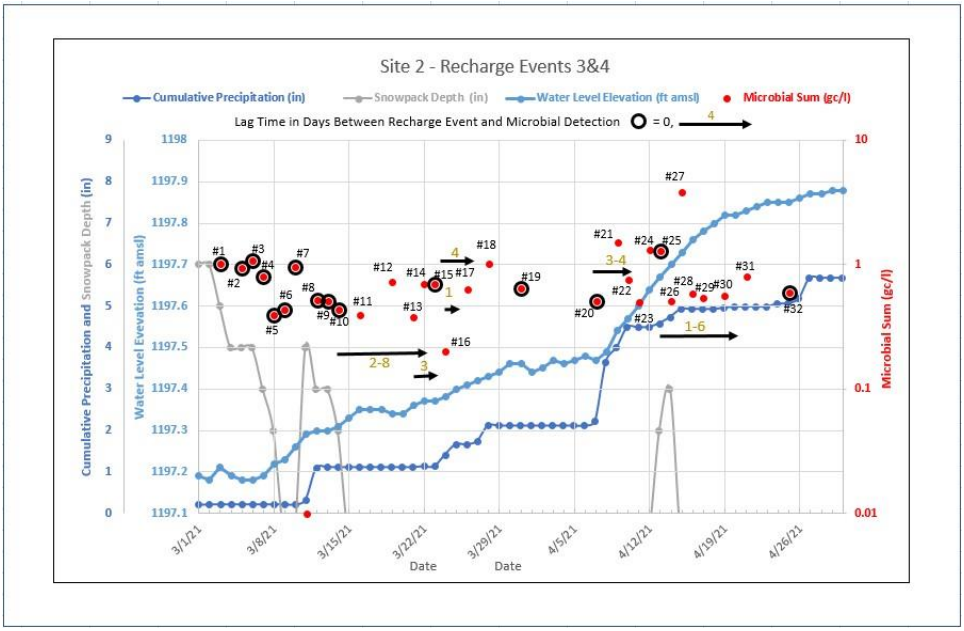

Figure 30. Precipitation monitoring during spring thaw at Site 2.

Data Logger Results - Water level and chemical responses to precipitation

Water level hydrographs were collected at an initial "primary" observation well and a later onsite observation well monitored when it became available (Figure 28). Both observation wells showed rapid responses to precipitation and snowmelt, with rises often noted within a few days of an event, but commonly these were relatively small rises on otherwise falling trends (Figures 27 and 28). Only the spring thaw and late summer/early fall rainfall resulted in rising hydrographs. The response of the on-site observation well was more muted, and it lagged the other observation well by two-days on average (Figure 28). These differences can be attributed to the depth to water at these sites, which was approximately 11-feet at the primary observation well and approximately 50 feet at the on-site well. The observed response between the two sites is consistent with the relation of unsaturated-zone thickness reported by Bradbury et al. (2008).

- Specific conductance values varied from approximately 389-423 µS/cm over the study period (Figure 31). Maximum daily coefficients of variance (CV) barely exceeded 1% and the average value was only 0.13%, likely reflecting the enhanced mixing of recharge events resulting from the 50-foot-thick unsaturated zone (Bradbury et al., 2008). Falling and rising trends observed in the data seemed to correlate with precipitation events, with falling trends apparently reflecting the addition of slightly lower conductance recharge and rising trends representing the return to higher values during drier stretches. Microbial detection frequency seems correlated with the falling trends and may reflect the importance of recharge events on driving microbes to the water table and well intake after the initial pulse of the event has arrived. These recharge pulses likely represent a very small proportion of the overall well water volume. For example, the addition of only 10% by volume of relatively low conductance recharge (assuming a specific conductance of 200 µS/cm) could reduce the average well water value of 409

µS/cm to the minimum observed value of 389 µS/cm. Such small volumetric contributions are supported by other chemical and isotopic data generated by this study."

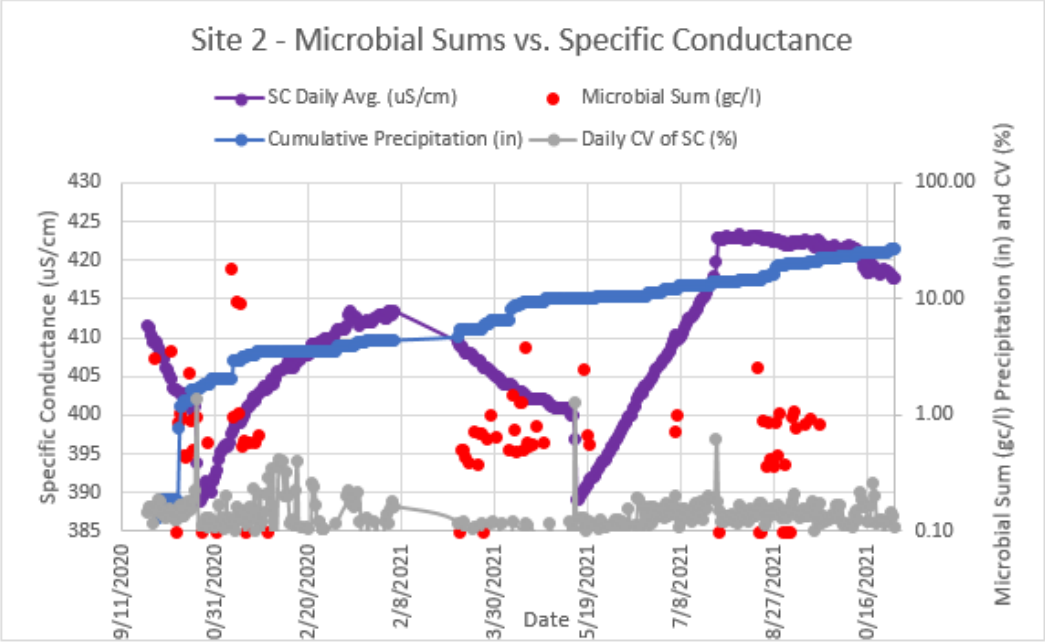

Figure 31. Specific conductance daily average values and variability (CV) during the monitoring study compared with microbial detections and cumulative precipitation.

Water temperature was relatively variable when measured at the sonde, with an average CV of 3% and the maximum daily values approaching 10% (Figure 32). However, measurements taken at the observation well at a depth of 16.6 feet show much less variability, averaging less than 0.1%, although capturing the same general trends. This suggests that the sonde data was impacted by ambient air temperature due to low flow rates through the cell. The initial declining trend observed in the fall of 2020 from both data sets may reflect the addition of fresh recharge, as suggested by the specific conductance data. The general rising trend noted in the latter half of the study appears related to warming recharge, with the additional warming at the sonde related to ambient air. No obvious correlation between water temperature and microbial detection or concentration was noted, although the greatest detection frequency, observed in spring 2021, corresponded with the bottoming of the water temperature trend.

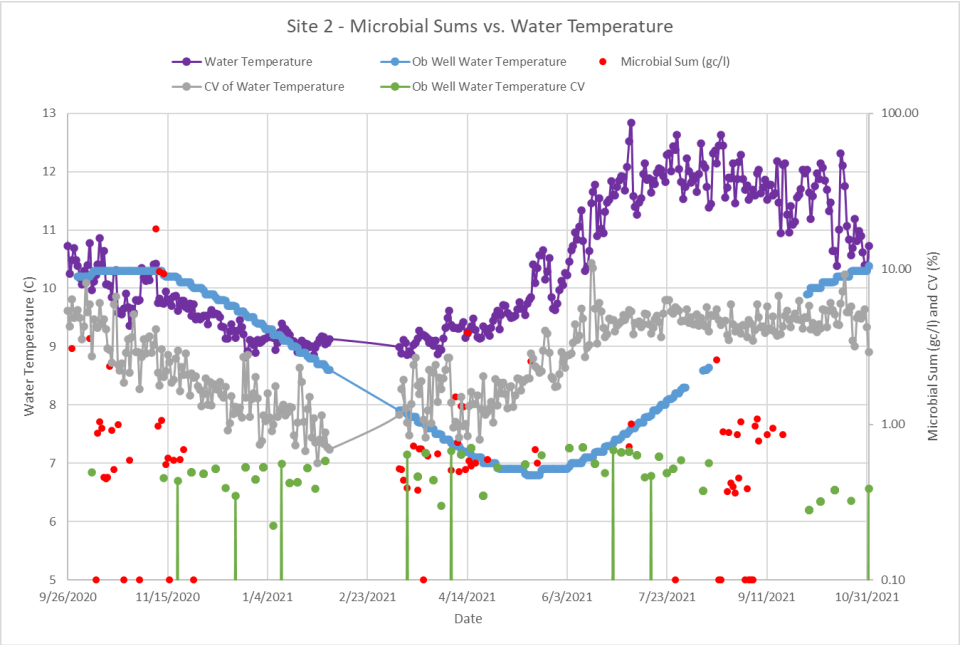

Figure 32. Water temperature variations during the monitoring study at Site 2 as measured at the onsite water quality sonde and observation well.

Well water pH was relatively constrained during the study, varying only between approximately 7.6 and 7.8 (daily CVs averaged 0.25%). There was no clear relationship observed between pH of the well water and microbial occurrence, although several of the higher concentration detections were coincident with small local minima (Figure 33).

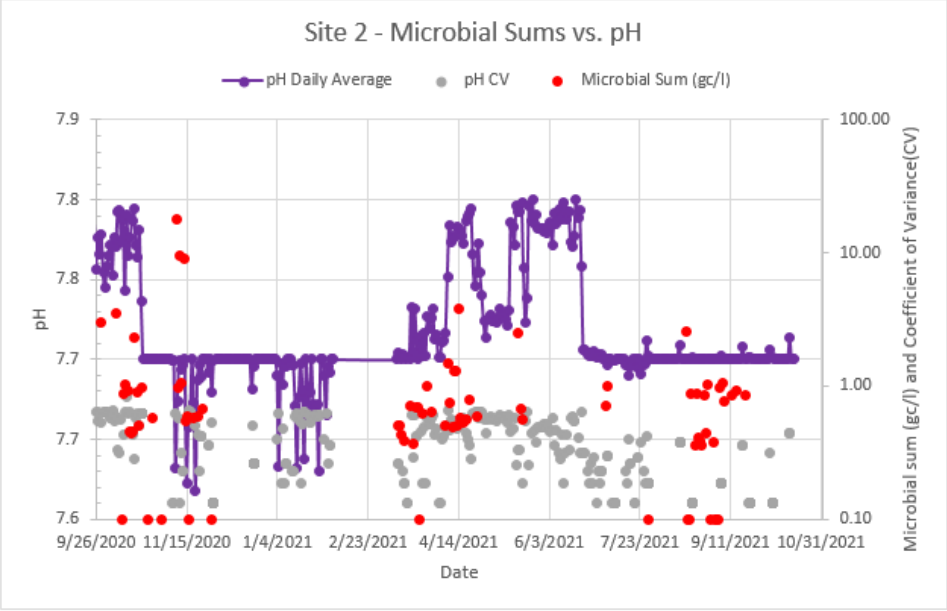

Figure 33. Observations of pH at Site 2.

Aside from the observations about specific conductance, temperature and pH noted above, the other data from the water quality sondes yielded significant noise and lack of sensitivity to the parameters being detected and are not discussed further in this report.

Chemical and isotopic results

The results from the whole water samples showed that the well water samples fell along mixing line 1 in Figure 34, indicating that the water was impacted by halite. Possible sources within the well capture zone include Highway 371, located east of the site, and the on-site septic systems. Water softening is employed on site, and the effluent from the water softener would have a comparable signature to road salt. Given the frequency of microbial detections observed at this well, and the similarity between the chloride/bromide signature of the well and the northern septic system, we are assuming that the septic system is the dominant source, although contribution from roadways to the east cannot be ruled out. In addition, comparison with individual well samples taken during the 2014-2016 study phase show that the results from this period were consistent with what was observed previously, although towards the higher end of that range (Figure 34).

Although no clear relationship was observed between the chloride/bromide ratios and microbial detections generally, the three samples with the highest microbial sums were closely coincident in time with relatively high chloride/bromide values for the well (1,862-1,900 compared to the average well value of 1,790, Figure 35). This suggests that those microbial detections were associated with volumetrically small and short-lived pulses of relatively elevated chloride/bromide water that was likely impacted by a septic source. The addition of less than 5% by volume of wastewater with the highest chloride/bromide value measured from the well during this study (4420) would be enough to raise the well water value into the elevated range noted for the highest microbial sum samples. It's also worth noting that the average Cl/Br value noted from this study period of 2,118 significantly exceeded that of the 2014-2016 study period (1,274), indicating increased water quality degradation over time.

Chloride values ranged from approximately 21.5 to 29.7 mg/l and averaged 23.8 mg/l, exceeding the average from 2014-2016 of 22.6 mg/l, again suggesting water quality degradation over time (Figure 36). Addition of 2.3% by volume of wastewater with the average value observed in this study between the northern and southern septic systems (75 mg/l) would raise the 2014-2016 average value to the average value seen in this study phase. In general, chloride values rose over the course of the study and within each sampling event, except for the final ones noted in the summer and fall of 2021 over which chloride values remained flat.

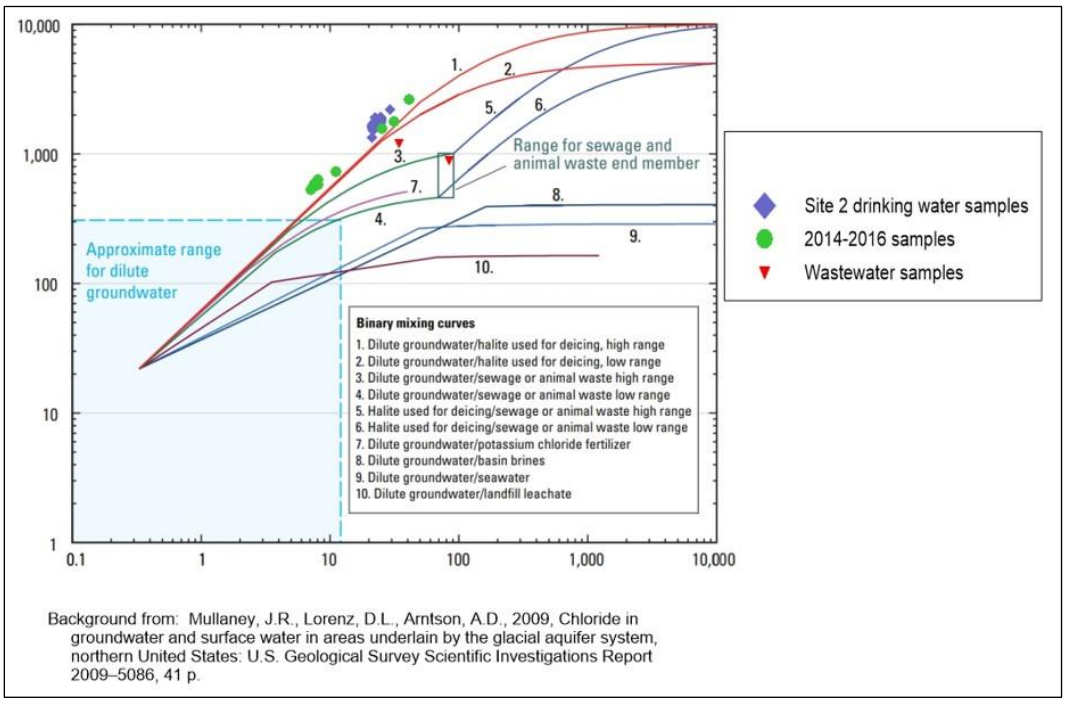

Figure 34. Chloride vs. chloride/bromide results for Site 2 compared to the fields shown in Mullaney et al., 2009.

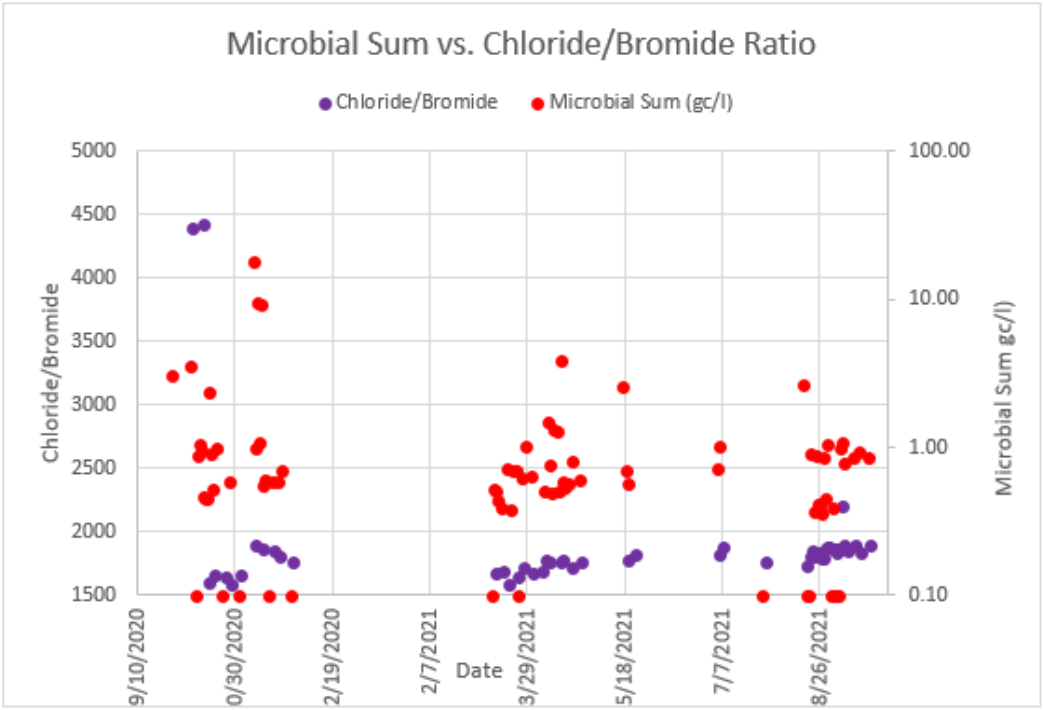

Figure 35. Chloride/bromide ratios from whole water samples at Site 2 compared with microbial detections. Microbial non-detections were converted to values of 0.10 for the purpose of plotting on the log scale.

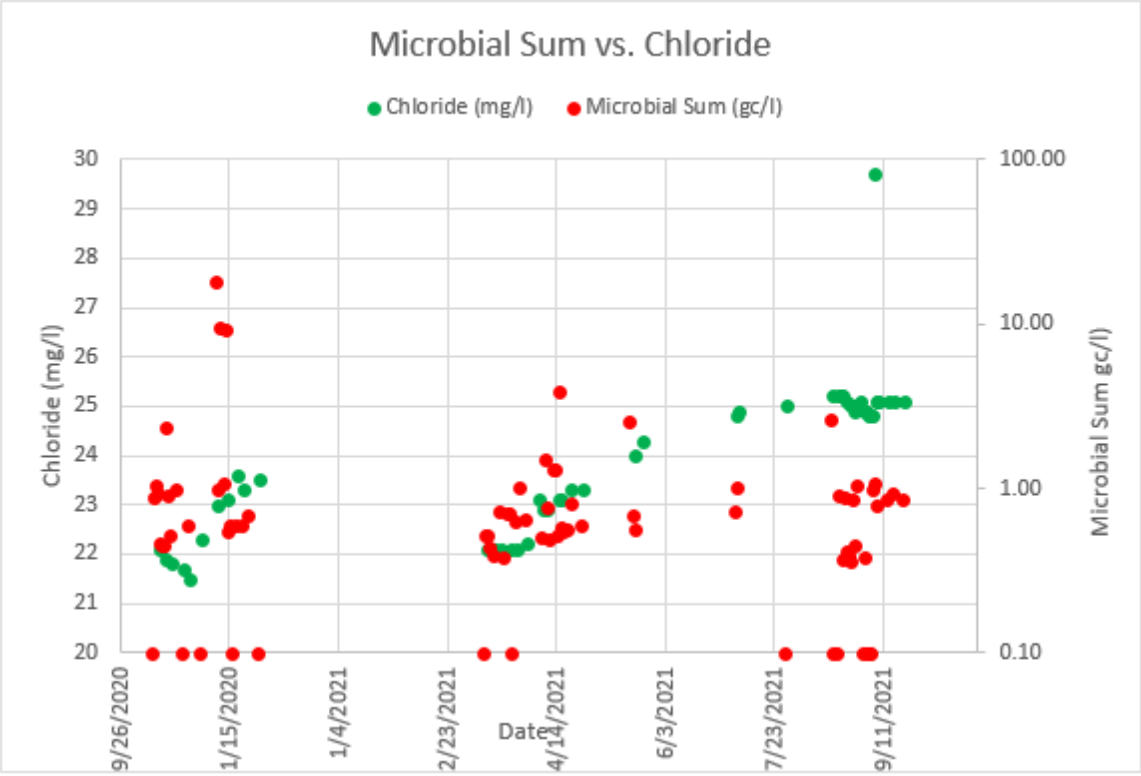

Figure 36. Chloride values versus microbial sums at Site 2. Microbial non-detects converted to values of 0.1 for plotting.

The stable isotopes of water showed no evidence that this well captured any significant quantities of evaporated surface water during the study. All samples cluster near the MWL of Landon et al (2000)., with only one of the fifty samples showing any significant deviation from the line based on a line-conditioned excess value less than -1.0 (Landwehr and Coplen 2004). This confirms that the lakes in the vicinity of this well were not significant sources of water to the well capture area. The average water isotopes result was relatively consistent over time (within 1 per mil for the samples collected during the study), which is consistent with a higher degree of mixing within the thicker unsaturated zone.

The variation in oxygen-18 and deuterium observed during the study showed no consistent patterns, other than trending on average isotopically lighter later in the study (Figure 37), reflecting colder recharging waters.

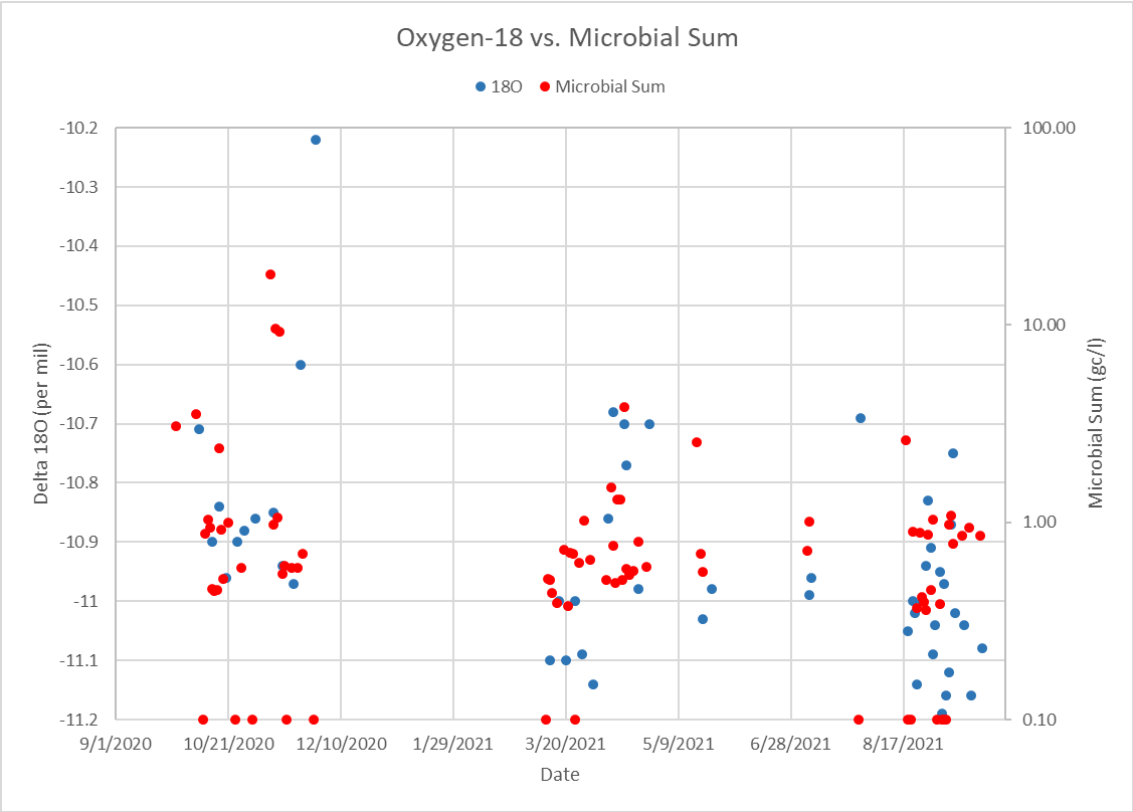

Figure 37. Comparison between oxgen-18 values and microbial detections at Site 2. Microbial non-detections were converted to values of 0.1 for plotting purposes.

Comparison with wastewater samples

Human *Bacteroides* (HF183/R287), Human adenovirus Groups A-F, pepper mild mottle virus and *Bacteroidales*-like HumM2 were detected in both the drinking water and wastewater samples, the latter two closely coincident in time with the drinking water detections for these organisms during the final sampling event in fall 2021 (Figure 38). This suggests that the onsite wastewater systems are impacting water quality at the well, consistent with the observations noted above for chloride and chloride/bromide. However, while *Giardia* was detected consistently in the drinking water samples, it was not observed in the single samples from the two septic systems. It's unclear if this was due to those single samples being unrepresentative of the full suite of wastewater discharged over time at the site, or if the *Giardia* is originating at a different source. In the latter case, it's unclear what that source may be, especially given its persistence both in this phase of the study and the 2014-2016 phase. Assuming a human origin, *Giardia* measured during this study may reflect past site conditions. It's possible that enhanced septic system source from the broken sanitary lines and/or the loading of the daycare facility provided a substantial pathogen load to the relatively thick vadose zone at this site, which is slowly releasing to the water table and well over time.

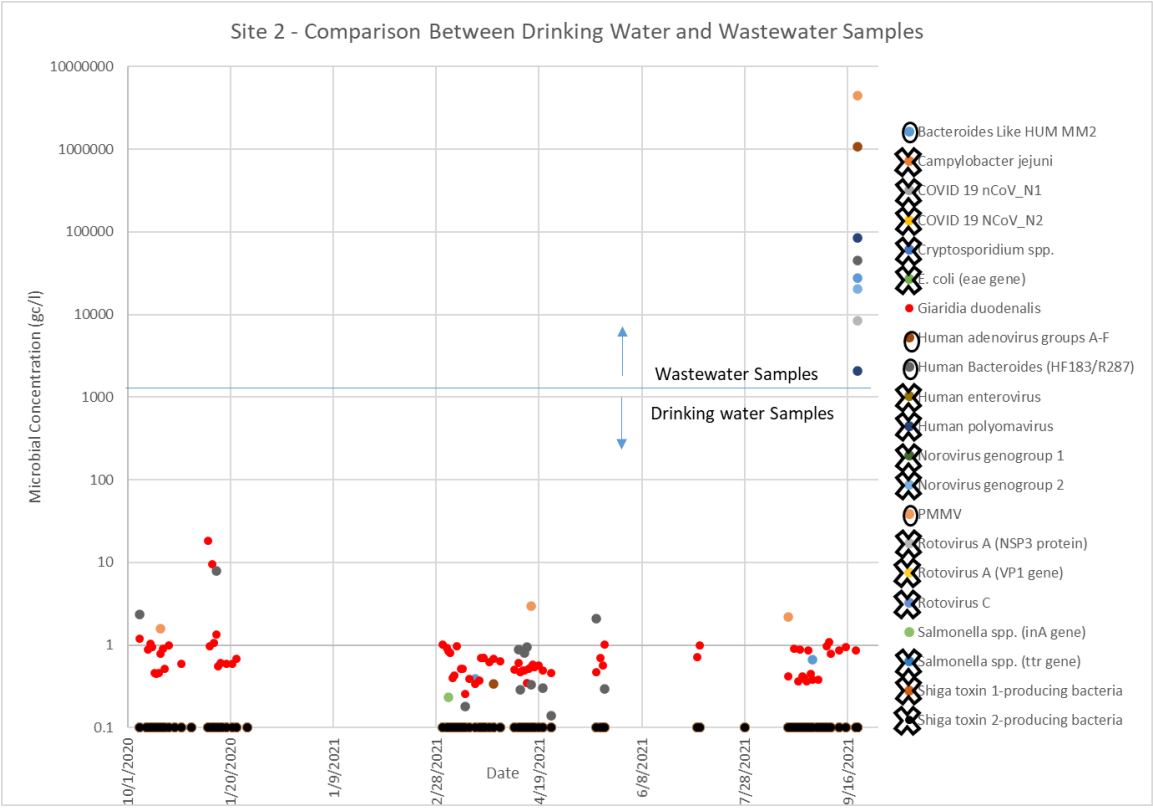

Figure 38. Comparison between drinking water samples and wastewater samples microbial results. Results below detection were converted to 0.1 for plotting purposes. Circled organisms were detected in both the drinking water and wastewater. Organisms with an "X" were not detected in either source. The remaining organisms were detected in only drinking water or wastewater, not both.

Site 2 - Groundwater age dating

Samples were collected for SF6 and dissolved gas and tritium analysis on October 19, 2021 and analyzed at the University of Utah Department of Geology and Geophysics Dissolved Gas lab. Age estimates could only be determined from the dissolved gas/tritium method, as the samples were contaminated with SF6. The results showed that the bulk age for the well water was approximately 30 years (range of 31.3-32.9 years), suggesting most of the water entered the ground around 1990. However, the microbial, chemical, and isotopic response of the well water to precipitation events suggest that there is a component of very young water mixing with this body of much older groundwater. Lag time analysis suggests that this young water fraction recharges the aquifer on time frames of days. Volumetric estimates based on conservative parameters such as specific conductance, chloride/bromide, chloride, and water isotopes indicate that recharge pulses, sometimes accompanied by microbial DNA and wastewater signatures, account for approximately 10% or less of the overall well water volume but likely result in the microbial detections noted in this study.

Site 2 – Tracer Studies (extracted from Barry [2022b])

Tracer studies were conducted at this facility by the Minnesota DNR and began with dye tracing of the wastewater system on the west side of the main building (Figure 39). Dye tracing focused

on the immediate area around the two cleanout connections that were determined to have failed. Since the connections were repaired immediately, the DNR augered to the depth of the repaired cleanout piping to introduce dye at these potential source locations. The northern cleanout piping was encountered approximately 20" below grade and the southern was roughly 6"-8" below grade. Soils at the northern location were fine to medium silty sand with organics. Southern soils were silty sand.

Eosin dye was introduced into the northern auger pit and sulforhodamine B was introduced into the southern auger pit. Dye in each pit pooled due to low infiltration rates from loamy textured soils. The DNR created one additional pit near the northern and southern locations to determine soil properties at depths greater than the cleanout depths where the dyes were introduced. Coarser soils were encountered with depth at each location. Two-inch PVC standpipes were installed in each of the exploratory pits for additional dye input the following day (following discussion and approval from MDH collaborators). On September 16, 2020, additional dye was poured into the auger standpipes to ensure that dye was introduced into the coarse textured soils below the wastewater piping elevations. Dye input locations, date/time of pour, types, and liquid mass are summarized in Table 6.

Table 6. Site 2 tracer injection summary

Date	Time	Location	Tracer	Dye Mass (Liquid pounds)	Description
15Sept2020	15:46	northern clean out	Eosin	4.0	augered pit
15Sept2020	16:01	southern clean out	sulforhodamine B	8.0	augered pit
16Sept2020	10:30	northern clean out	Eosin	2.3	PVC pipe in augered pit
16Sept2020	10:50	southern clean out	sulforhodamine B	4.0	PVC pipe in augered pit

Additional tracing at this site began on September 16, 2020, using an approximate 1% sodium chloride brine solution. Five shallow soil pits were created parallel to the northern wastewater piping between the failed cleanout and the solids tank (Figure 39). The most western of the holes, near the solids tank was 5 feet deep, all others were less than 3 ft deep. Soil classification of each pit, except the middle one, was predominantly sand and gravel. The center pit was classified as silty sand and gravel. Beginning at 11:20 a.m. September 16, 2020, a mixed sodium brine solution was poured continuously into the shallow soil pits. Brine was introduced from the eastern pit moving westward and repeated until 12:50 (Table 6). An approximate 220 gallons of brine was introduced in total. Following liquid introduction, sodium chloride pellets were introduced into each pit and then the pits were backfilled with native soils.

Figure 39. Brine and dye injection locations and associated stormwater conveyance infrastructure. Black dots represent on-site wells. Well 500605 was sampled for this study, while 850447 was used for water level observation. Image courtesy of Crow Wing County.

Since the cleanout failures were repaired, loading to the dye input locations was mimicked using solenoid timers and soaker hoses. Garden style soaker hoses were set up along the path of waste line (above backfilled brine pit locations) and additional soaker hose was hose coiled above the dye introduction areas. Hose timers were set to cycle water on four times per day for 40 minutes per cycle. Water "on" times were set to 7:00, 13:00, 19:00, and 1:00; with Zone A controlling southern hoses and Zone B controlling the northern hoses. Artificial recharge via the timers and hosing ran for several weeks before air temperatures fell below freezing and artificial recharge was terminated.

Dye tracing of the wastewater conveyance system here found no rapid or slow breakthrough of the eosin or sulforhodamine B dyes and no evidence of rapid brine breakthrough. Possible explanations for not detecting the tracers include:

- The dyes were attenuated or degraded within the underlying glacial deposits. Based on presence of fluorescein detected in the background analysis, eosin and sulforhodamine B dyes were used. Eosin has high resistance to adsorption, however sulforhodamine B loss to adsorption is high (OUL, 2019). Sulforhodamine B loss to adsorption increases in settings

where dye travel is through soil and residuum, organic matter is elevated, bacterial activity is elevated, and water flow is dispersed and may have affected outcomes (OUL, 2019).

- The eosin and sulforhodamine B dyes traveled somewhere else and were not intercepted by wells 500605 and 850447. There may be some credence to this, as onsite geology is likely heterogenous and may include low permeability layers that aren't evident through county scale mapping or detailed in the site well logs (500605 and 850447). Fine-grained soils with relatively slow infiltration rates were encountered during dye introduction and may have impeded vertical recharge in areas where they exist. A possible perched wetland exists on the south side of the project site (evident as a wet ditch with cattails on each of the DNR visits) and may be additional evidence of unmapped lower permeability soils (Figure 39).
- The dye took longer than the sampling period to reach the well intake. This seems unlikely, as hydrograph response and microbial detections imply time of travel through the vadose zone is approximately two days. In addition, the dye inputs were in close proximity to the well, within the delineated one-year time of travel capture area (Figure 24).

Alternatively, the absence of a positive tracer result may simply reflect that the pathogen source at this site was not tested. This could be the case if the pathogen source was the septic tanks and drainfields rather than the sewer piping. The short vertical times of travel noted at this site would be promoted by the consistent flow of water and contaminants to the vadose zone from drainfields or leaky septic tanks rather than intermittent pulses of recharge associated with precipitation events. Finally, if the broken sewer lines were the ultimate source, it's possible that the attempts to simulate recharge via the use of sprinklers was not adequate for replicating the volumes of water that may have flowed past these sites based on roof runoff over time.

Site 2 - Annular Space Test

The competency of the grout seal in the annular space between the well casing and borehole wall was tested using a brine solution deployed at the surface and specific conductance measurements conducted in the well water after methods described in Walsh (2018). Approximately 100 gallons of a 1% NaCl solution with an average specific conductance of approximately 16,000 µS/cm was allowed to soak into the approximately 2-inch annular space between the well casing and borehole wall that is grouted with cement to a depth of 30 feet. It was calculated that if 50% of this solution were to permeate the grout seal and make it to the well bore, it should raise the specific conductance of the well water to at least 500 µS/cm, which would significantly exceed any measurement noted during the study. This solution was deployed continuously from 8:37-16:40 on September 22, 2021, and specific conductance was measured at 15-minute intervals at the raw water tap used for the microbial sampling via the water quality sonde deployed in the autosampler. Specific conductance measurements continued for six weeks following the end of brine deployment, ending on November 3, 2021. No rise in specific conductance beyond the range observed during the study was noted, suggesting that rapid movement of surface water along the annular space of the well was not a likely pathway for the microbial detections observed in this study.

Site 2 - QMRA

Site 2 pathogen detections are characterized by frequent (78 out of 92 samples), low-level detections of *Giardia*. The highest detections of 18.2 and 9.62 gc/L were found on 11/9/2020 and 11/11/2020 respectively. The estimated risk for these detections were .33 and .19 respectively.

The population currently served by Site 2 is transient in nature, and on average likely drinks less than the 1.1 L used for calculating risk during each visit to the site. That said, the frequency of detections means that there is a good chance for infection during any visit, and that only continuous treatment of the water supply or switching to a new source will be effective tools at reducing risk.

Site 2 - Conclusions

The well at Site 2 showed a high percentage of samples with microbial detections, strongly dominated by one organism (*Giardia*) and with consistently short average lag times from precipitation events, suggesting the well is impacted by a relatively consistent *Giardia* source with fast travel times to the well intake. Although *Giardia* was not detected in the single samples from the wastewater system, those samples may not have been representative of either the current or historical wastewater load at this site. In a relatively protected environment free from predation, the *Giardia* cysts may persist in the unsaturated zone and enter the aquifer and well during recharge events. This conceptual model, of *Giardia* loading to the vadose zone followed by slow release and degradation, is consistent with the decrease in microbial concentrations between this study and that conducted in 2014-2016, although the somewhat minor reduction may be attributable to other factors such as sampling frequency and differing water use and precipitation regimes.

Microbial occurrence at this site was accompanied by small-scale changes in water quality parameters such as specific conductance, chloride/bromide, chloride, and water isotopes. Mass-balance estimates based on these parameters suggest that recharge pulses associated with these small-scale water quality variations may account for as little as 2-10% of the overall well water volume, but likely result in the microbial detections noted in this study. These results match a conceptual model of small volumes of fast-moving recharge, driven by precipitation events and with travel times on the order of days, mixing with a reservoir of older, relatively unimpacted groundwater with a bulk residence time on the order of 30-years, in the aquifer tapped by this well. The exact pathways traveled by these pulses of young recharge are unknown, but the absence of any obvious problems with well construction or the grout seal at this well suggests they are not specifically well-related and may instead be naturally occurring within the groundwater system. Examples may include small-scale features such as spatially limited gravel lags within the glacial outwash strata. Reducing the microbial threat to this well might be achieved by relocating the septic systems outside of the well capture zone if possible, and/or constructing a new well that is less directly connected to the septic systems.

Site 3 - Hydrogeology

Site 3 is in north-central Minnesota, approximately three quarters of a mile from the Mississippi River which is the dominant discharge feature in the area (Figure 40). The site includes two

wells located 100-feet apart that serve a small community of approximately 120 people. The surrounding land use was dominated by iron mining from 1912 to 1962, with two surface mines (the Rowe and Sagamore), now water-filled and prominent features of the local landscape. These exist amongst a series of shallow natural lakes (30-feet deep or less), the nearest of which is located less than 500-feet downgradient of the city wells. Current land use is dominantly residential and forested, with several wetlands surrounding the lakes.

The surficial geology of the site is characterized by approximately 30-40-feet of unconsolidated sediment that ranges from clay-rich till to sand and gravel, and which may include glacial sediments excavated from the nearby Rowe mine during overburden removal in the early 1900's (Figures 40 and 41). Below this depth, sand and gravel that is presumably native to the site is encountered to depths of approximately 65-75 feet. This rests on clay-rich till, below which lies weathered Precambrian bedrock/saprolite. The two wells are screened at depths of 53-68 and 48-78 feet, respectively. The surficial sediments are derived from the St. Louis sublobe, while the outwash is related to the St. Croix Phase of the Rainy Lobe (Knaeble, Meyer, and Hobbs, 2004).

Depth to water is approximately 35-feet below the land surface at the well sites and the potentiometric surface dips steeply toward the Mississippi River and lakes connected to it (Figure 40). Vertical hydraulic gradients are not well known locally due to a lack of observation wells, but comparison with the nearest surface water features suggests it is downward. The 1-year and 10-year time of travel capture zones for this well are shown in Figure 40. These were determined using the analytic element model MLAEM (Strack, 1999).

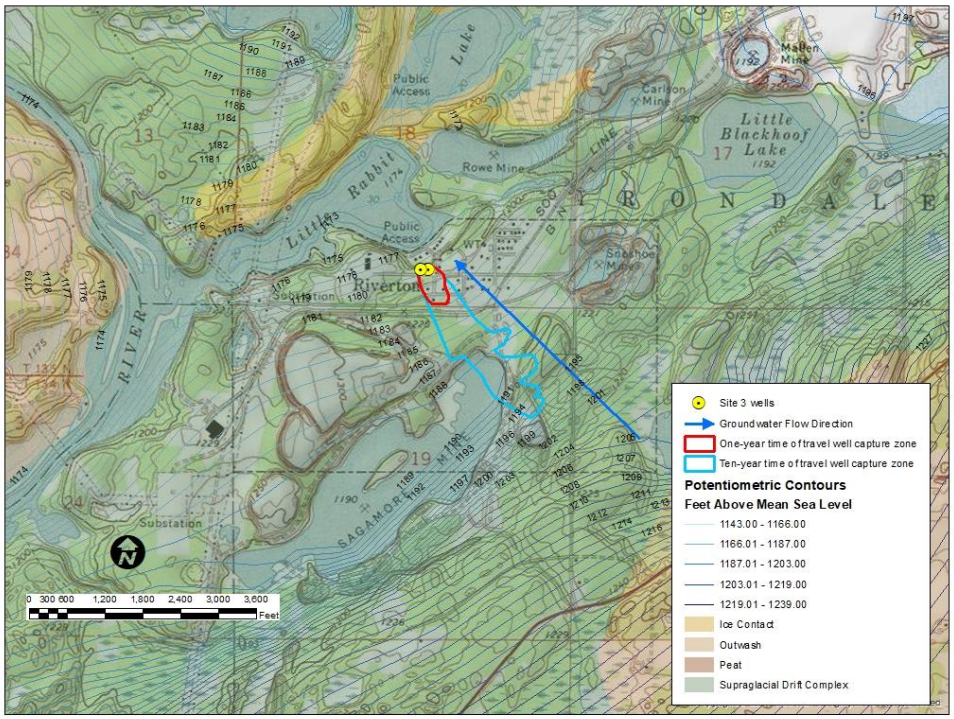

Figure 40. Site 3 hydrogeologic setting.

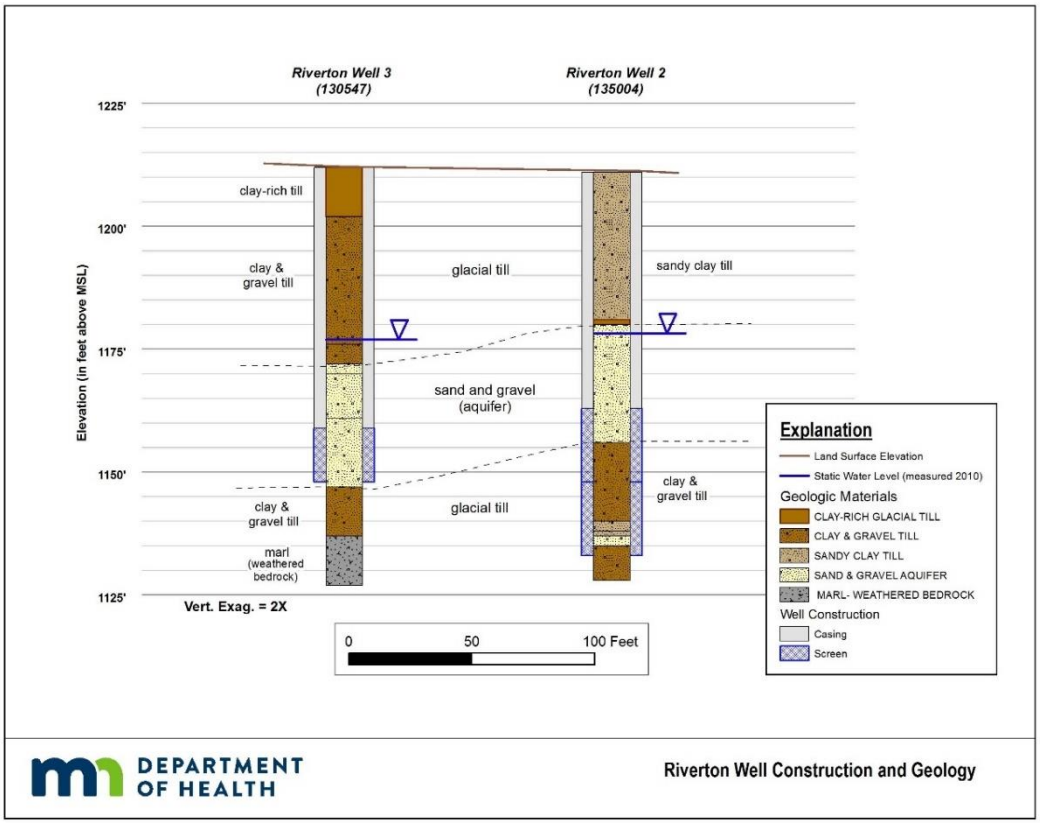

Figure 41. Well construction and stratigraphy at Site 3.

Site 3 - Potential Contaminant Sources

An inventory of potential contaminant sources located near the public supply wells at this site show several possible pathogen sources. Five private septic systems consisting of septic tanks and drainfields are present within the wellhead protection area; the two nearest are 130' (south) and 180' (east) of the wells, the others being 250' to 650' distant, with three of the four falling within the one-year time of travel capture zone for the city wells (Figure 42). An additional drainfield had existed approximately 140-feet north (downgradient) of the city wells, but that was replaced with a sewage lift station that now pumps effluent from this small residential area to the municipal sewage system. Most of the city's sanitary sewer system lies east of the wells; the closest components are the two manholes (at ends of sewer runs) located approximately 550' and 650' to the east. In addition, a 12-inch concrete storm sewer is located as close as 26-feet south of the easternmost well and flows to a manhole structure located 75-feet to the east where it joins additional storm water piping before flowing through an 18-inch pipe to the outlet approximately 750 feet to the northeast. Approximately 330-feet of stormwater piping exist within the one-year time of travel well capture zone.

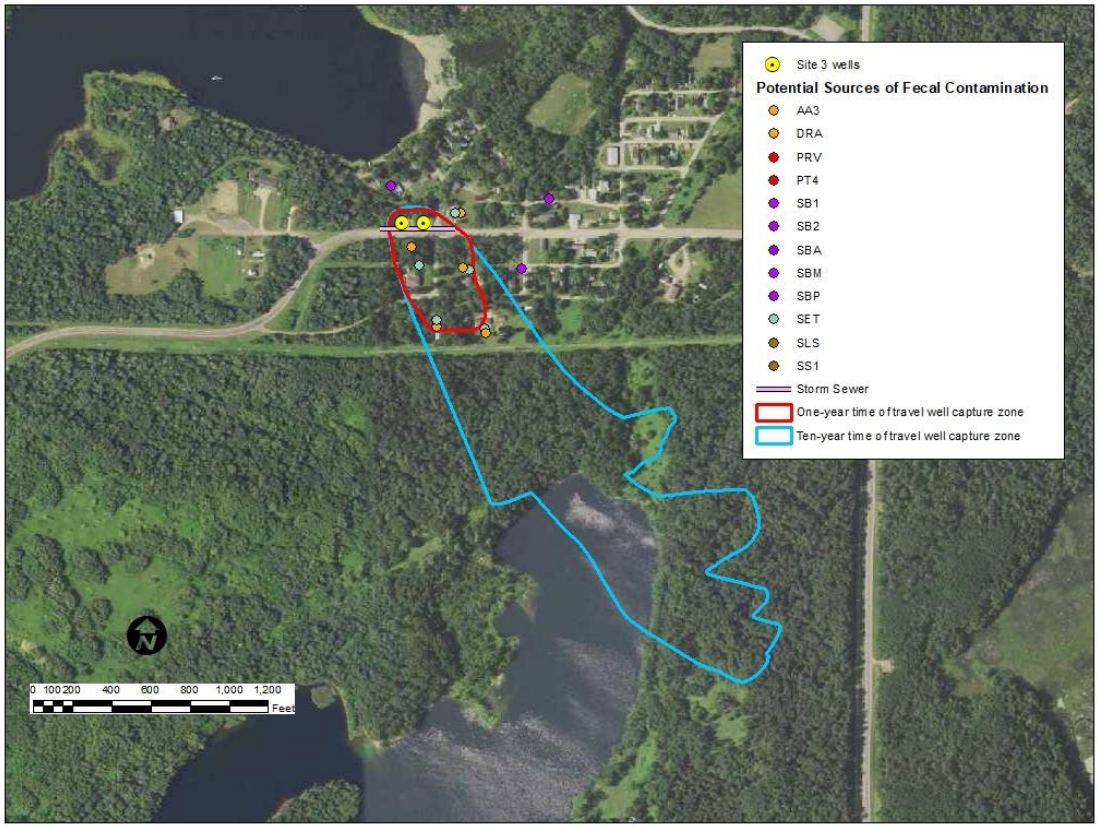

Figure 42. Location of possible pathogen sources with respect to Site 3 wells and capture zones.

Site 3 - Monitoring Setup

The monitoring setup at this site matched the general description noted under the discussion of study design, with these site-specific details:

- The autosampler at this site was attached to an untreated water tap from the study wells that followed a 1500-gallon hydropneumatic tank. The wells alternated on a regular basis, so the sampler was receiving water from both wells blended within the tank throughout the study. Analysis of the water quality data from this study compared with single-well sampling conducted previously suggests that the blend was approximately a 50-50 mixture of the two wells. Flow through the autosampler system was disrupted several times during the project, each for an extended period due to blockage of valve components by iron oxide precipitation, which required replacement or cleaning of these components.
- The observation well for this site was the backup well for the city, completed to the same depth as the other city wells and located 460-feet east of the easternmost primary well. The hydrograph for this well was strongly influenced by pumping of the active city wells, confounding analysis of recharge trends.
- The USGS weather station for this site was co-located with the observation well noted above.

- The wastewater sampling site at this facility consisted of a municipal sewer access point located 525-feet southeast of the city wells.

Site 3 – Comparisons with water use and precipitation regimes from preceding water years and study periods

The months during which sampling occurred during this study were evenly split between wet and dry ratings, with two normal values (WETS, Minnesota DNR, 2022). The months preceding sampling events were dominated by dry ratings, with normal and wet ratings showing only twice each. For comparison, the preceding sampling months in the 2014-2016 study were evenly split between wet, normal, and dry.

Water use from the study period slightly exceeded historical averages. Water use during the 2014-2016 study period averaged 2.4 million gallons per year, whereas nearly 2.9 million gallons was recorded during 2020.

Site 3 – Description of Sampling Events

Six precipitation events were monitored at Site 3 during this study (Table 7 and Figures 43-45). Events 1 and 2 captured a series of late fall rains that followed a dry preceding month (Figure 46). These rainfall events were essentially continuous, spanning October 7-November 28, 2020, with a one-week period (November 1-November 8) separating them. Total rainfall during this period equaled approximately six inches and resulted in a net water level rise of 0.22 feet on a generally rising hydrograph, with peaks and valleys ranging from 0.1-0.2 feet throughout the event based on pumping influences from the nearby wells.

Events 3 and 4 also ran together and spanned from March 5-April 25, 2021, with the period March 31-April 6 separating them (Figure 47). These events captured the onset of early spring warmth accompanied by the complete loss of approximately six inches of snowpack and accompanied by rain totaling 3.3 inches. A water level rise of 0.2 feet was observed during this period on a generally rising hydrograph that reversed a falling trend observed in January and February, with peaks and valleys ranging up to 0.3 feet based on pumping influences. This rise was noted during a time when at least partial frozen ground conditions were suggested by standard indicators, such as the presence of lake ice and frozen soil beneath area highways, revealing the shortcomings of those indicators and/or the importance of recharge via macropore flow in partially frozen ground (Mohammed et al., 2019).

Events 5a, 5b and 5c were “false starts” based on forecast rainfall events that failed to materialize. The first ran from May 17-May 21, 2021 and captured 0.13 inches of rainfall with an essentially flat water level response on an otherwise falling hydrograph. The second ran from July 5-6, 2021, was not accompanied by any measurable rainfall, although approximately 0.3 inches had fallen on June 28. Water levels dropped 0.1 feet over this time on a generally declining hydrograph, reflective of the drought summer of 2021. The single sample collected on July 28 for Event 5c followed 0.46 inches of rain on July 24-25 and the resulting hydrograph continued to drop during this period, losing 0.03 feet.

Event 6 ran from August 18-September 22, 2021 and captured 7.9 inches of late summer-fall rains that followed a significant drought. Water levels during this period began to stabilize and

rose slightly, exceeding that of the beginning water level by 0.05 feet and signaling a rising trend that continued to the end of the monitoring period later that fall, although never recovering to the levels seen at the start of the study, falling short by 0.37 feet.

Table 7. Summary of precipitation events monitored at Site 3.

Event	Date	Type	Cumulative Precipitation During Event (in)	Net Water Level Change from Baseline During Event (ft)	Precipitation History from Current/ Prior Month	Number/% of Samples Positive for Any Microbial Parameter	Lag Time in Days Between Precipitation and Microbial Detections (Shortest/Longest/Avg)	Microbes Detected (pathogens in red)	Maximum Concentration (gc/l)
1	10/7-11/1 2020	Fall Rain	4.0	+0.05	Normal/Dry	7 (46%)	0/6/2.3	Crypto, Salmonella, Giardia	1.48
2	11/8-11/29 2020	Fall Rain	1.49	0	Wet/Normal	6 (50%)	0/4/1.7	HB, Crypto, Giardia	26.24
3	3/5-3/31 2021	Spring Thaw, Snowmelt and Rainfall	1.5 on top of melting of approximately 6-inches of snowpack	+0.26	Wet/Dry	12 (63%)	0/7/1.5	HB, Crypto, Norovirus, Salmonella	4.35
4	4/5-4/25 2021	Spring Rain	1.8	+0.38	Wet/Wet	5 (38%)	0/3/1.2	B-like Hum, HB, Crypto	12.4
5a	5/17-5/21 2021	Late Spring/Early Summer Rain	0.13	-0.05	Dry/Wet	1 (25%)	0/0/0	HB, Crypto	0.23
5b	7/5-7/6 2021	Summer Rain	0 (0.3 preceded event)	-0.11	Dry/Dry	1 (50%)	7/7/7	Crypto	1.04
5c	7/28-7/29 2021	Summer Rain	0.46	-0.03	Dry/Dry	0 (0%)	NA	NA	NA
6	8/18-9/21 2021	Fall Rain	7.9	+0.05	Normal/Dry Wet/Normal	5 (21%)	1/17/5.2	HB, Crypto	2.24

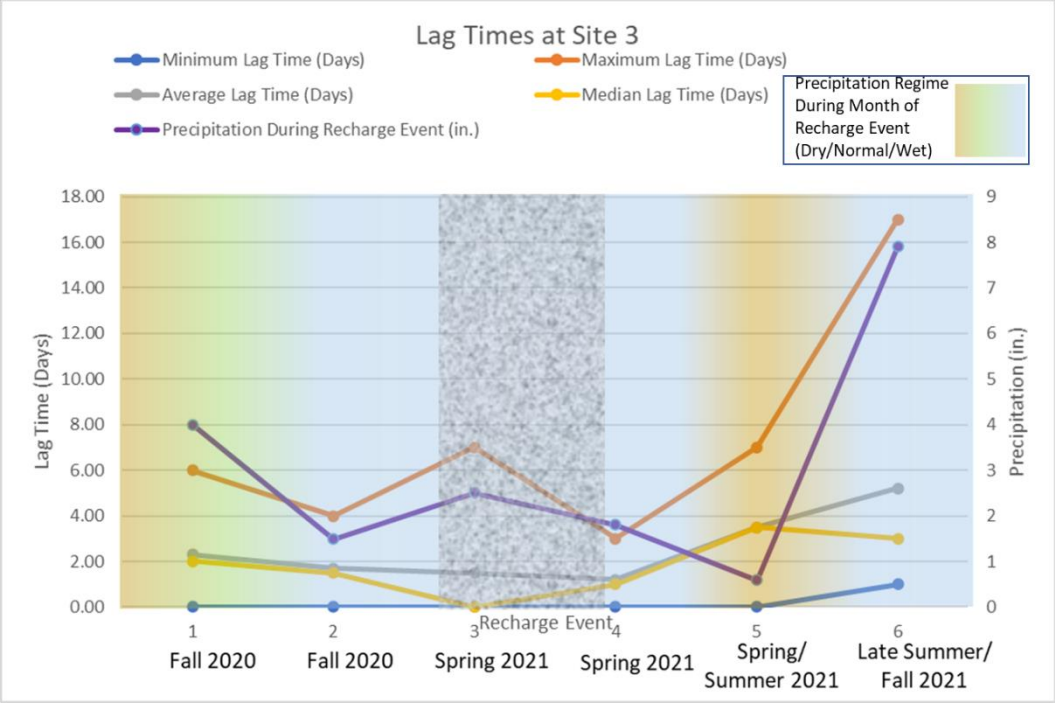

Figure 43. Summary of lag times at Site 3. Stippled pattern indicates period of possible frozen ground conditions based on indicators such as lake ice and frost depth beneath area highways. Precipitation regimes from MDNR Climatology (2022).

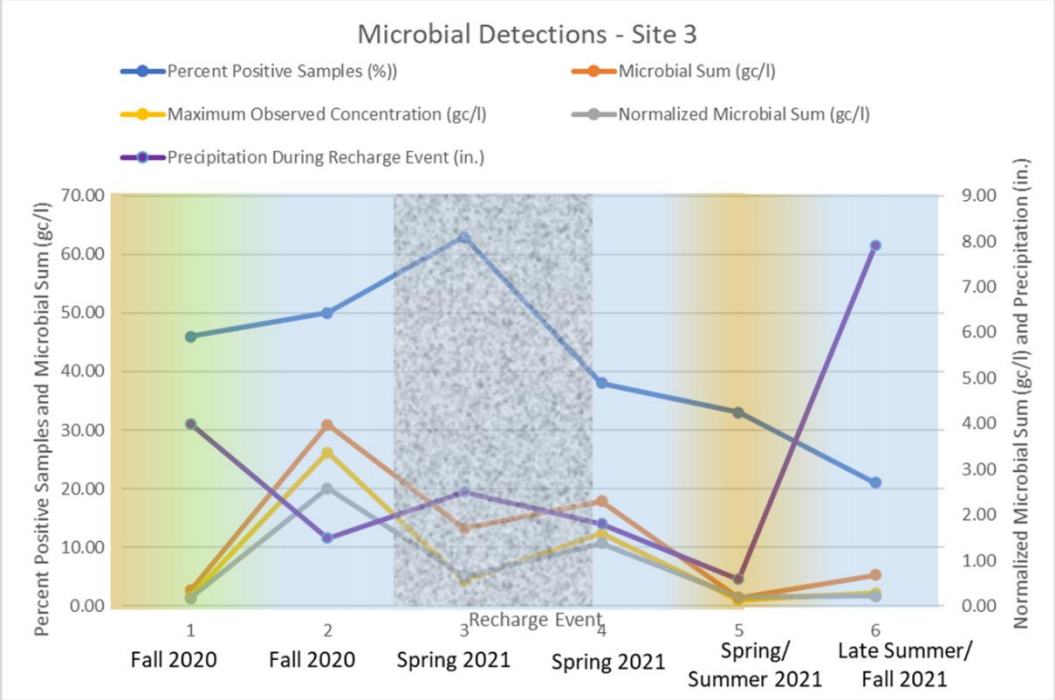

Figure 44. Summary of microbial detections at Site 3. Stippled pattern indicates period of possible frozen ground conditions based on indicators such as lake ice and frost depth beneath area highways. Precipitation regimes from MDNR Climatology (2022).

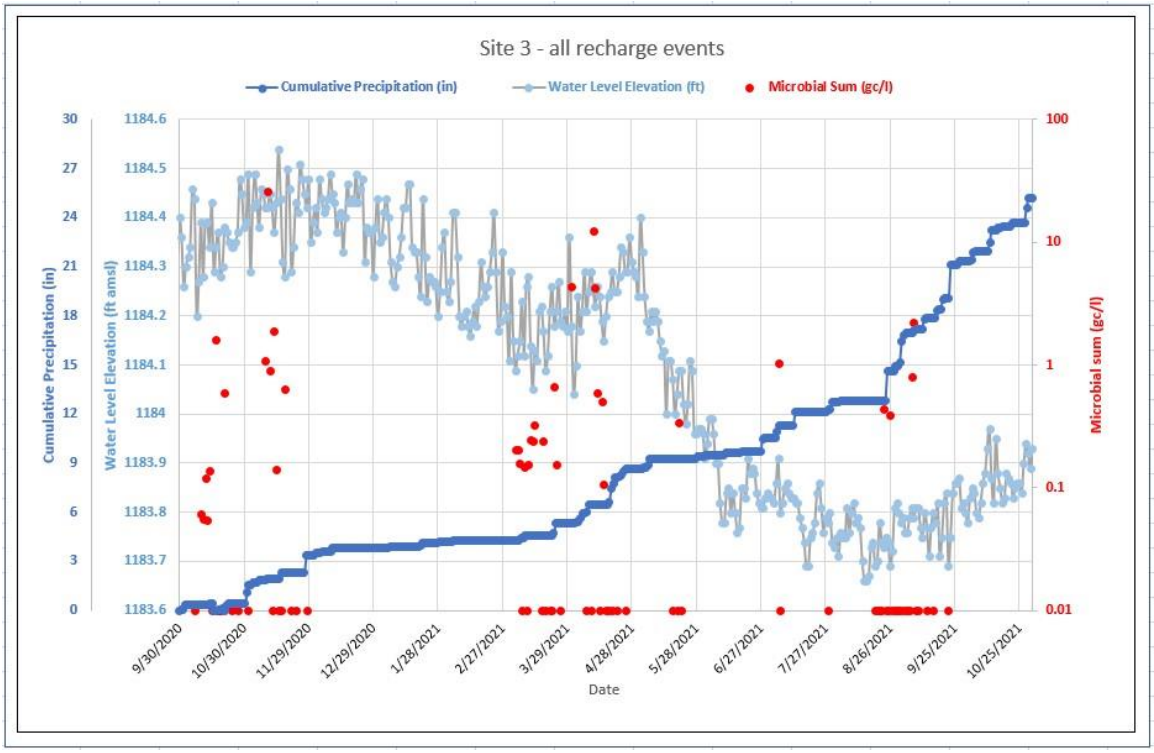

Figure 45. Precipitation monitoring events at Site 3. Microbial non-detections were converted to values of 0.01 gc/l for plotting on log scale.

Site 3 – Monitoring Results

Microbial results

Of the 93 samples taken from these wells, 40 (43%) showed some level of microbial detection, representing 45 overall positive results (i.e., five samples of the 40 were positive for more than one organism). Most were very low concentrations, averaging 0.83 gc/l, and *Cryptosporidium* the most commonly detected organism, representing 28 of the 45 positive results. Human *Bacteroides* was the next most detected organism (8 times). For comparison with the 2014-2016 study, 9 of 14 samples were positive (64%). Six of the organisms detected during this study (*Cryptosporidium*, *Giardia*, norovirus, *Salmonella*, Human *Bacteroides* and *Bacteroidales*-like HumM2) were also detected in 2014-2016, but adenovirus and enterovirus, detected in 2014-2016, were not detected in the current study (Ruminant *Bacteroides,* detected during 2014-2016, was not analyzed in the current study). The highest concentration observed during the earlier study phase, 221.9 gc/l for norovirus, was nearly ten times greater than the highest observed in this phase (26.2 gc/l for *Cryptosporidium*). The differences in detection frequencies and concentrations may relate to different sampling frequencies and total number of samples, as well as different precipitation regimes. The 2014-2016 study period was slightly wetter, with 71% of the sampling dates occurring during wet or normal precipitation months, whereas 63% of the sampling events in this study phase were within those regimes.

The lag times between precipitation events and microbial detections at Site 3 were relatively consistent for much of the study, averaging 1-2 days during the first four events (Table 7 and

Figure 43). The shortest lag times were observed during the spring thaw events (3 and 4), and many same-day detections were noted (Figure 47). Detection frequency also peaked during the spring, with 63% of samples showing a detection during Event 3, compared with 50% or less in all other events, and with an apparent strong response to the onset of elevated air temperatures accompanied by snowmelt in the absence of additional precipitation (Figure 44, 45 and 47). The onset of drought conditions in the summer of 2021 was accompanied by limited sampling, but those results suggest a general reduction in microbial detections and the start of longer lag times, especially towards the end of the summer and into the fall. The final precipitation event (#6) brought an end to drought conditions and halted the falling hydrograph (Figure 45). A relatively low detection frequency was noted during this event, with 21% of samples being positive. These results suggest that extended dry periods reduce microbial mobility in this groundwater system, even when followed by a return to near-normal precipitation patterns and may signal a lag time that is related to re-wetting of subsurface transport pathways that had temporarily dried.

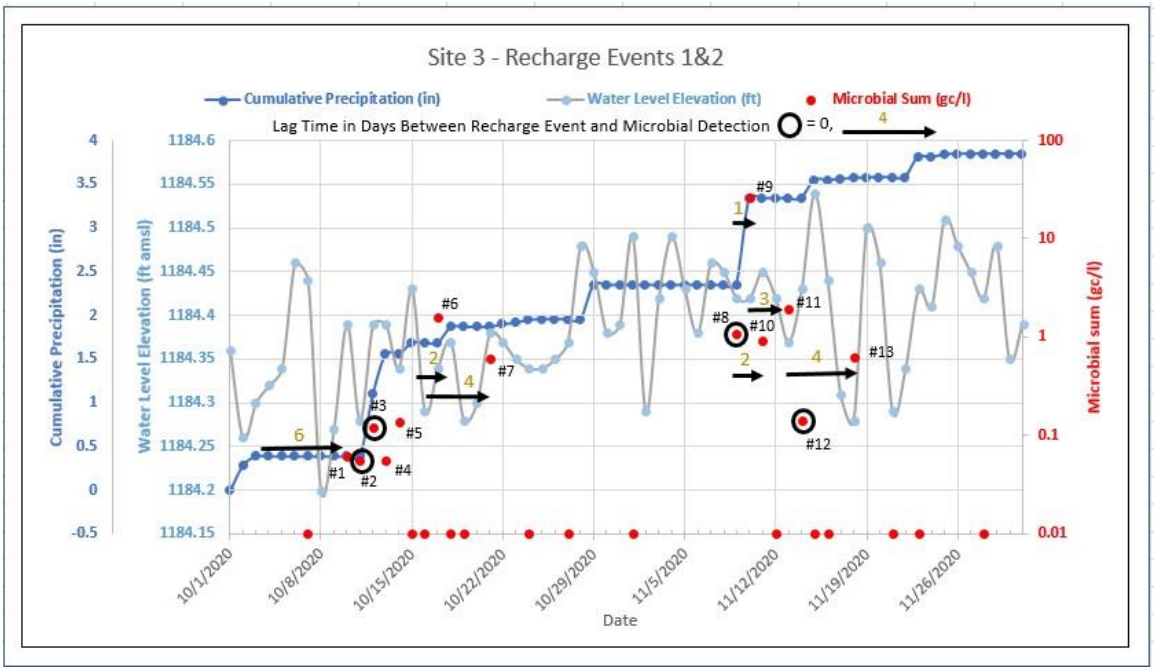

Figure 46. Microbial detections compared to cumulative precipitation and water level changes during Precipitation Events 1 and 2. Microbial non-detections were converted to values of 0.01 for plotting in log space.

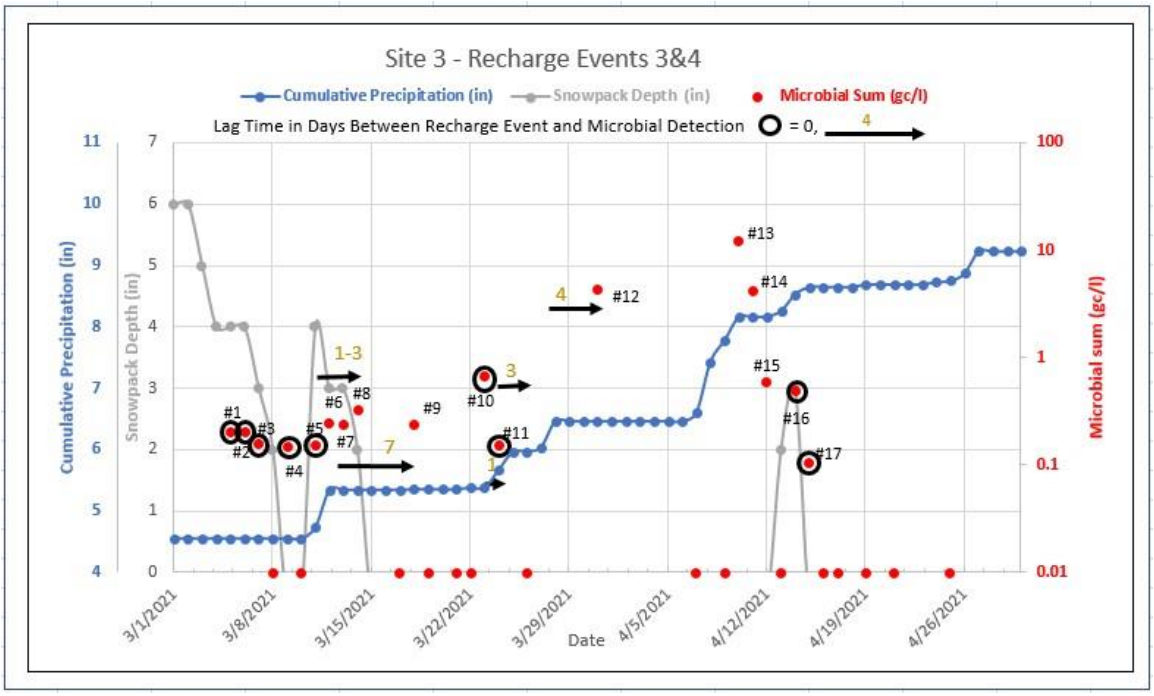

Figure 47. Precipitation monitoring during spring thaw at Site 3.

Data Logger Results - Water level and chemical responses to precipitation

Water level hydrographs were confounded by the pumping effects of the nearby city wells, but still showed trends that tracked precipitation patterns, suggesting a relatively direct hydraulic connection between the land surface and the buried aquifer used by the study wells (Figure 45). This is reinforced by the observed microbial detections, which together suggest the presence of fast-flow pathways in the groundwater system, despite the presence of clay-rich strata reported in the upper 30-feet in construction records for these wells.

Specific conductance values dropped early in the study, decreasing from 515 µS/cm on October 1, 2020 to a minimum of 487 µS/cm observed on October 24, 2020 (Figure 48). This was followed by a general rise in daily average values, which temporarily peaked in late April 2021 at 542 µS/cm. After this time, average daily values ranged between 522 µS/cm and 544 µS/cm, with no clear trend observed, although the rising trends noted above roughly correlated with water level data from the observation well (Figure 45). Analysis of this and other water quality sonde data for this site was confounded by extended periods of no-flow through the data logger, most notably late December 2020-late January, 2021, early February to early March, 2021, and mid-May to late July, 2021. These breaks were due to mechanical issues with the flow-through system caused by iron oxide precipitation on valve components.

A relatively high level of daily variation in specific conductance was observed at this site, with an average coefficient of variation of 9% (Figure 48). This is likely due to the alternate pumping of the two study wells throughout the project. The wells would cycle on and off several times in a single day, and the average specific conductance historically has varied between the two wells. Based on the 2014-2016 monitoring study, Well 2 averaged 386 µS/cm and Well 3 averaged 464 µS/cm. Presumably one or both produced higher values during the current study

to yield the ranges noted above. No obvious correlation was noted between specific conductance and microbial detections, which may in part stem from the blended nature of the conductance readings at this site and resulting high daily variance.

A short-term, low-level spike in specific conductance was observed during a brine test on the stormwater piping that runs past the city wellfield (Figure 49), suggesting the presence of a short time of travel but small volume pathway for contaminants to travel from this infrastructure to the city's aquifer and wells (Barry, 2022a).

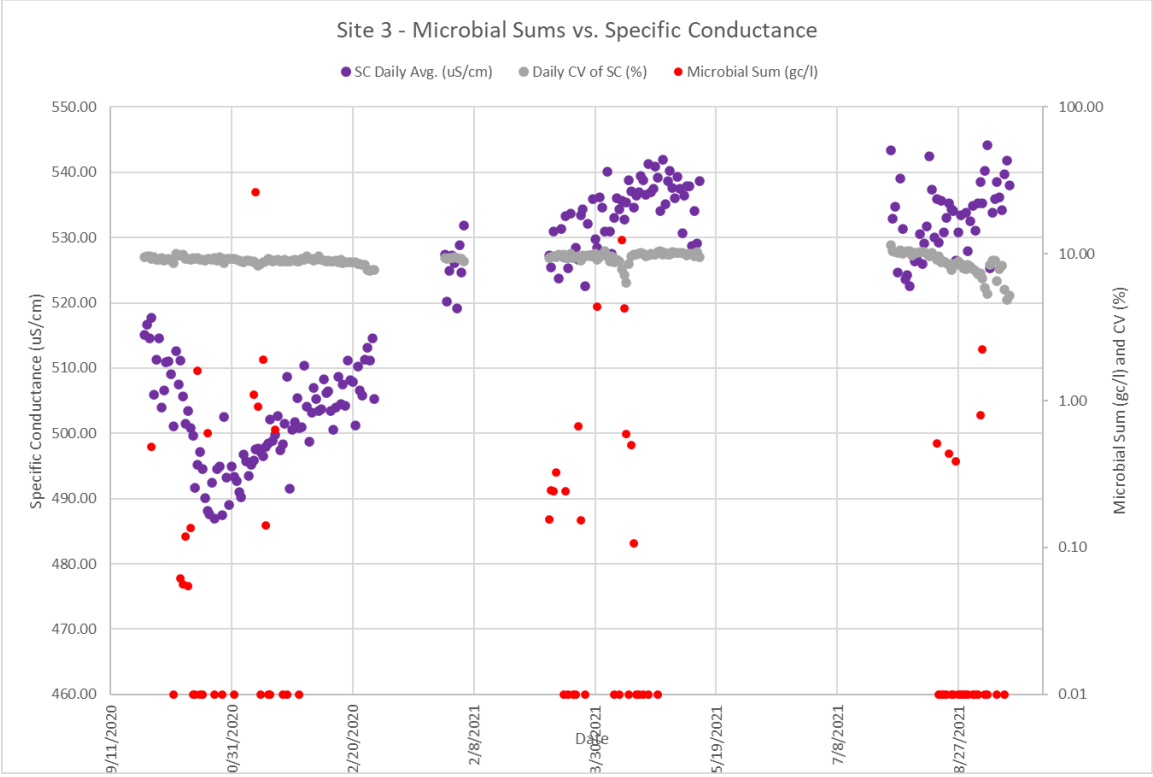

Figure 48. Specific conductance daily average values and variability during the monitoring study compared with microbial detections.

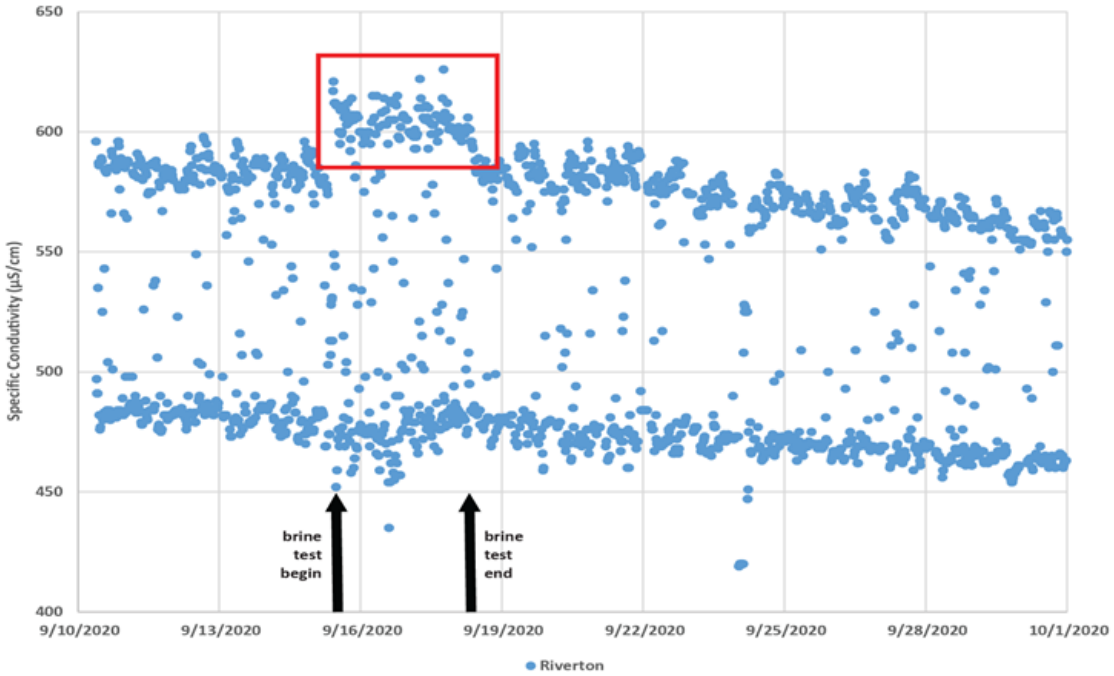

Figure 49. Specific conductivity composite of Wells 2 and 3 recorded during the stormwater piping brine test. Arrows mark the beginning and end of brine testing that occurred during continuous well pump cycling (15Sept2020 to 18Sept2020). From Barry (2022a).

Small-scale water temperature increases as measured at the water quality sonde were noted in relation to several strings of microbial detections (Figure 50), whereas consistent streaks of microbial absence seemed related to lower average water temperatures. Notable exceptions to these trends were the numerous microbial absence results from the final precipitation event in late August and early September of 2021 that were more closely related to relatively high or rising water temperature values. This period saw the highest water temperature values recorded in the study (14.08 °C), which may reflect an increase in ambient air temperature in the well house or decreased flow through the water quality sonde because of iron oxide precipitation as noted previously. These mechanisms are suggested by comparison with the water temperature data from the observation well, which was nearly flat throughout the study at around 9.0°C (Figure 50). It's unclear if all deviations from this temperature as measured at the sonde were due to issues of artificial warming, or if any could be related to leakage immediately around the pumping wells. Water temperature was less variable than specific conductance, with an average CV 0f 3.4% (Figure 50). This variability may be related to the well water blending noted previously about specific conductance.

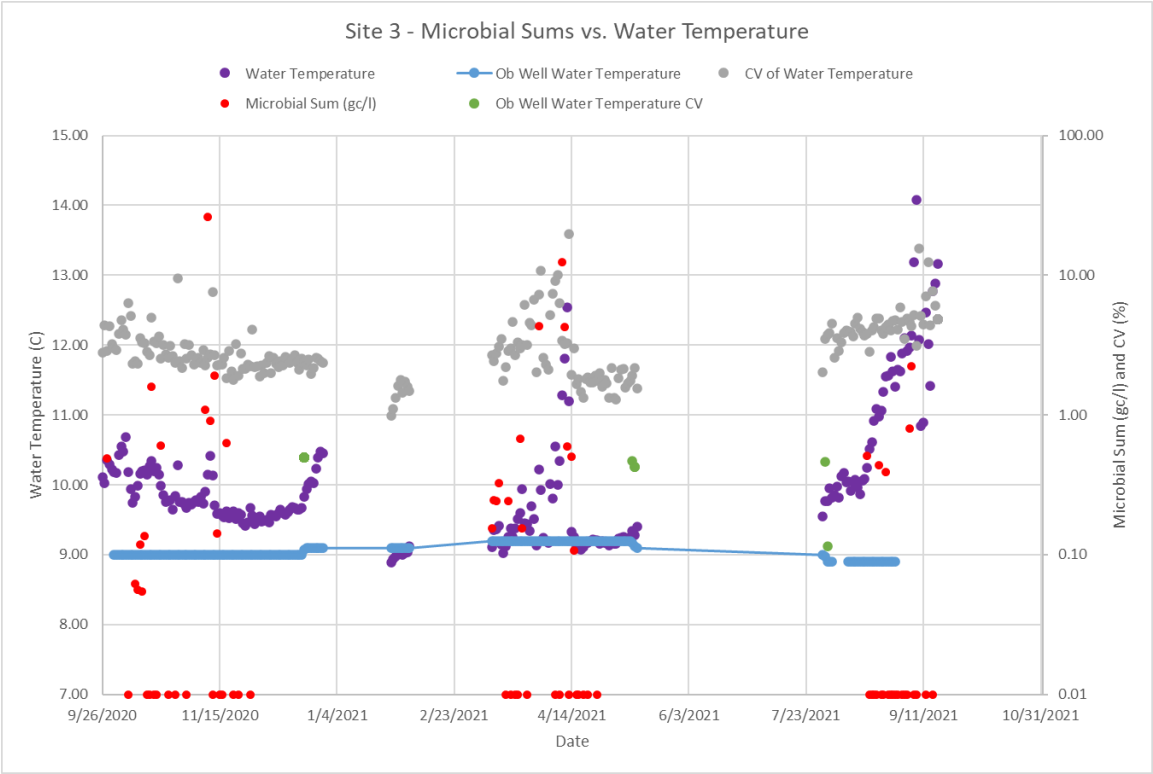

Figure 50. Water temperature variations during the monitoring study at Site 3 as measured at the sonde and observation well at a depth of 43.5 feet.

Well water pH varied between approximately 6.9 and 7.1 over the course of the study, with relatively little daily variation (daily CVs averaged 1.2%). There was no clear relationship observed between pH of the well water and microbial occurrence, although a rising trend was observed during the spring sampling events of 2021 (Events 3 and 4), which recorded the highest percentage of microbial detections of the study. (Figure 51).

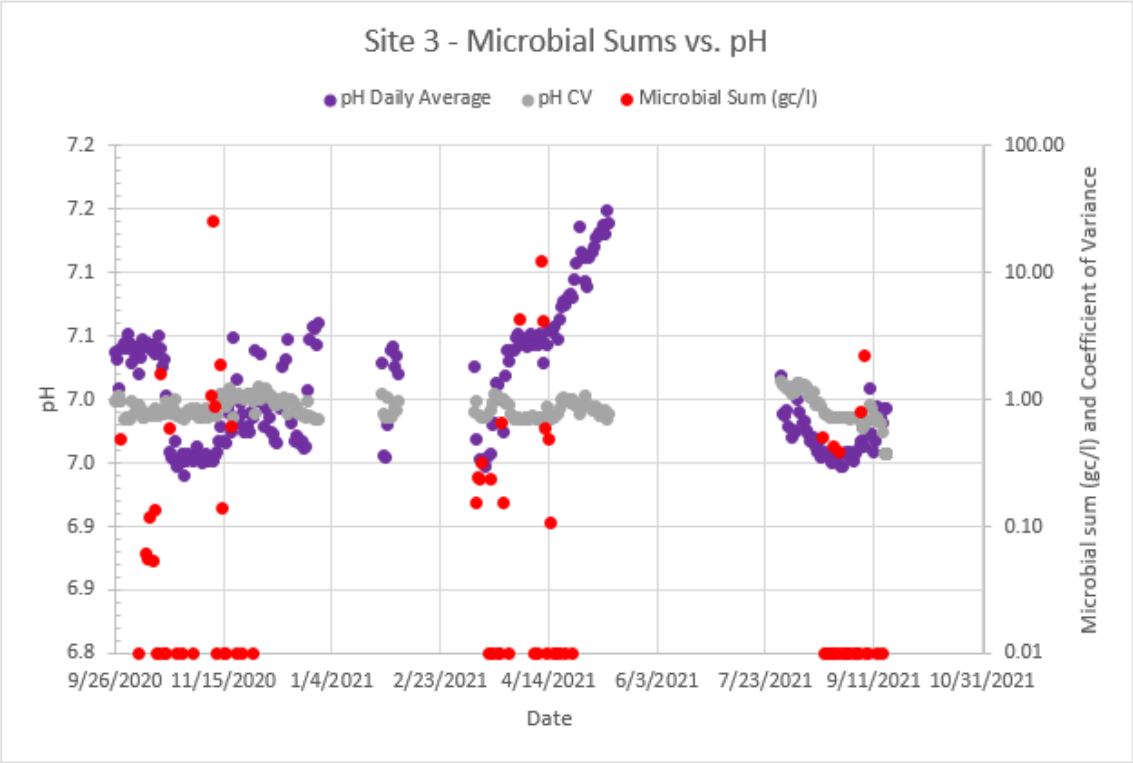

Figure 51. Observations of pH at Site 3.

Aside from the observations about specific conductance, temperature and pH noted above, the other data from the water quality sondes yielded significant noise and lack of sensitivity to the parameters being detected and are not discussed further in this report.

Chemical and isotopic results

The chloride and bromide results from the whole water samples showed that the well water samples fell within the range of the 2014-2016 study data and along mixing line 1 in Figure 52, indicating that the water was primarily impacted by halite. The most likely source is deicing salt used on area roadways. A storm sewer passes within 26-feet of one of the wells and the results of a brine tracer test on this sewer correlated with a near-immediate rise in specific conductance at the wells which returned to baseline four days after brine introduction, suggesting relatively direct hydraulic connection between the storm sewer and well(s) (Figure 51, Barry, 2022a). However, the amount of exfiltration from the storm sewer was likely small, as little as 0.3% by volume relative to the water in the pressure tank to which the wells flow. The fact that the chloride/bromide data from the wastewater samples collected for this study plot in a different space on this graph suggests that these were not as strong of a source impacting the wells compared to the stormwater system, although some contribution from the municipal sewer overprinted by road salt contribution cannot be ruled out. The single point that plots outside the graph window stems from one of the wastewater samples and shows that some high chloride and chloride/bromide values are possible from the sewer system but may not be the norm.

Chloride/bromide values generally declined during the fall 2020 precipitation events, before rising consistently during spring 2021. The fall 2021 precipitation events did not show any significant trend, first falling and then rising. Chloride/bromide ratios were not clearly correlated with detections, and many of the non-detection samples were closely related in time with some of the higher observed ratios (Figure 53). The lack of a clear positive correlation may in part be due to the blended nature of the samples here, which likely muted observations from the individual wells and delayed response times.

Chloride values for the well water ranged from 17.1 to 23.1 mg/l during the current study, which fell within the range observed from 2014-2016 of 7.5-41.1 mg/l, again suggesting that the samples from this study were a relatively even blend of water from the two wells (Figure 54). The same observations noted above about chloride/bromide generally pertain to the chloride values, but the monotonic rise in spring 2021 values is more striking and seems to point to regular contributions to the well water from a high-chloride source, presumably road salt.

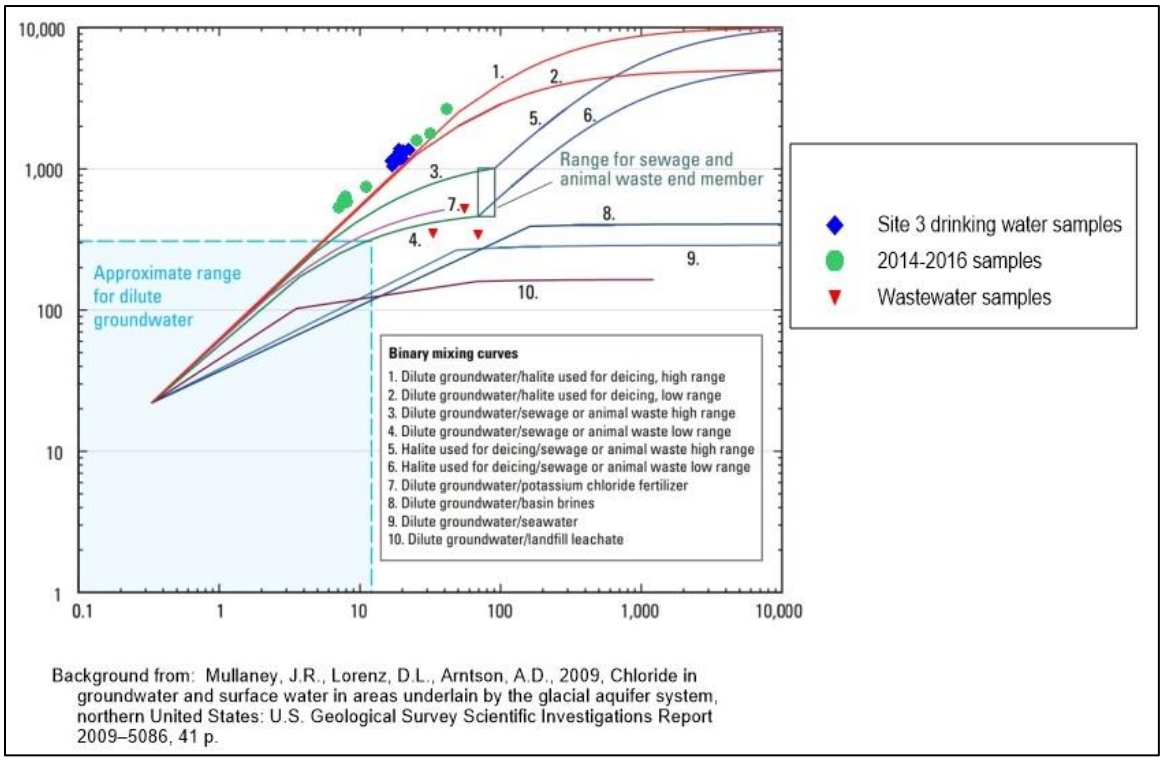

Figure 52. Chloride vs. chloride/bromide results for Site 3 compared to the curves shown in Mullaney et al., 2009.

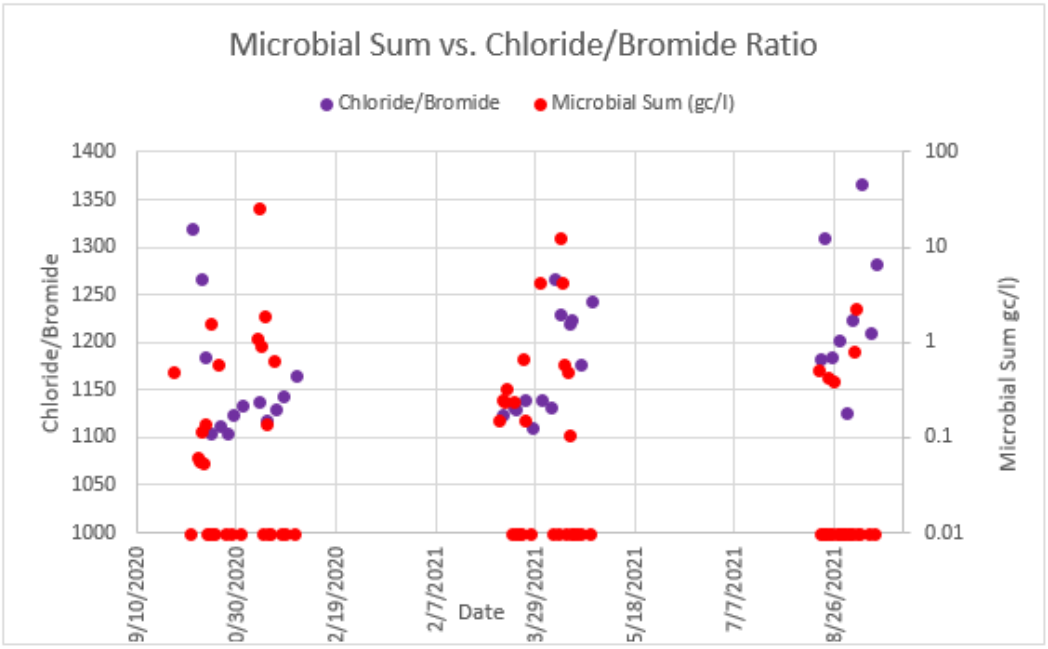

Figure 53. Microbial sum vs. chloride/bromide ratio for well water from Site 3. Microbial non-detects converted to values of 0.01 for plotting.

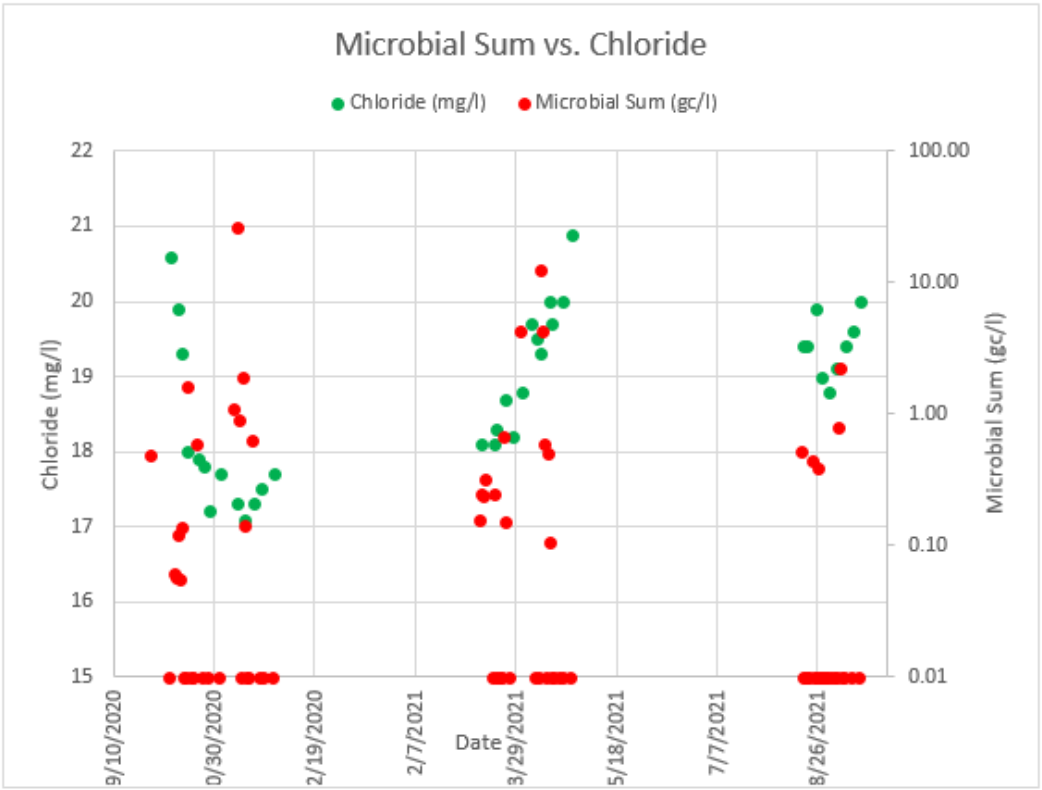

Figure 54. Chloride values versus microbial sums at Site 3. Microbial non-detects converted to values of 0.01 for plotting.

The stable isotopes of water showed little evidence that these wells captured any significant quantities of evaporated surface water during the study. All samples cluster the MWL of Landon et al. (2000), other than a single sample from August 21, 2021, that deviates below it. This confirms that the nearby lakes and wetlands were generally not significant contributors to the wells. The single sample that showed a slight evaporative signature was taken during the drought of summer 2021 and may reflect on a transient dynamic related to that event. However, samples taken a few days before and after that sample showed no deviation from the MWL and so this may represent a spurious result.

The variation in oxygen-18 and deuterium observed during the study showed no consistent patterns relative to microbial occurrence (Figure 55). However, average values noted during the first four sampling events were isotopically lighter than the estimated annual average for precipitation at this location (Bowen and Revenaugh, 2003). This may reflect the importance of isotopically light sources of recharge such as snowmelt and spring rain during these events. The fall 2021 sampling event was isotopically heavier than the preceding events, averaging close to the predicted annual value and likely reflecting an influx of summer precipitation.

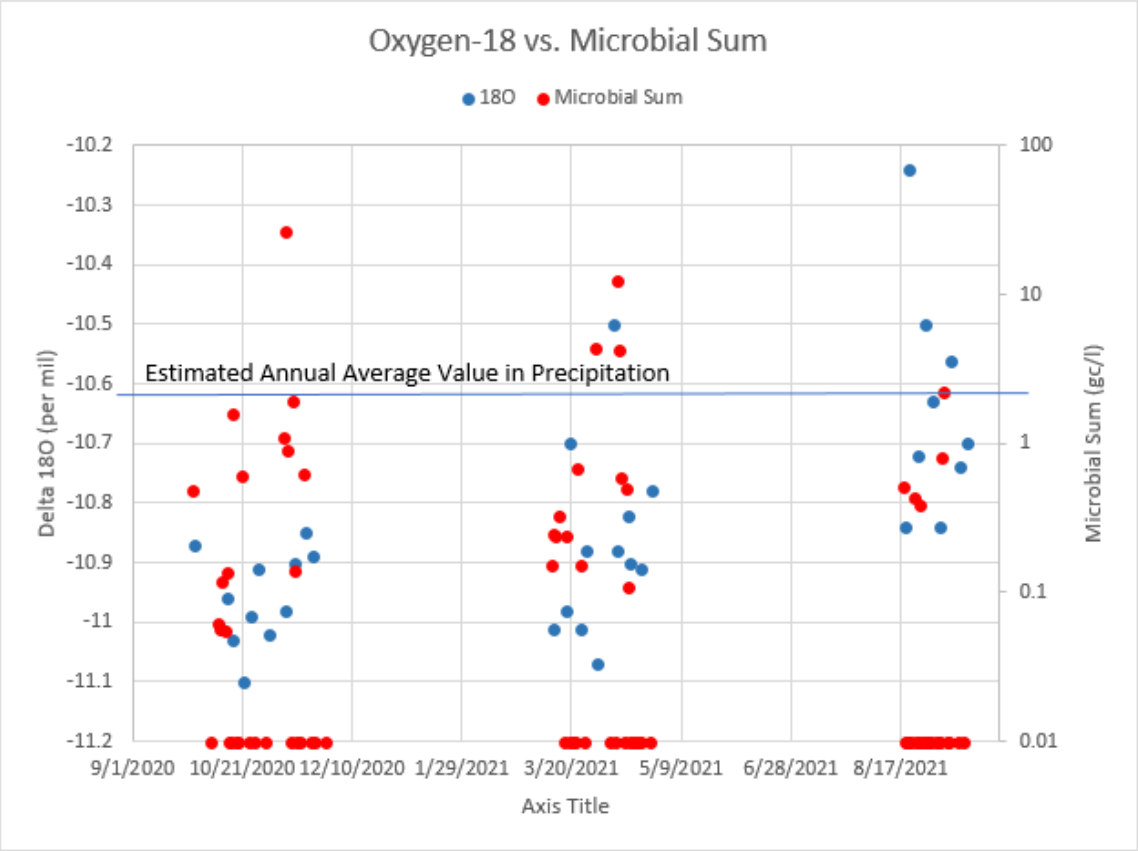

Figure 55. Comparison between oxgen-18 values and microbial detections. Microbial non-detections were converted to values of 0.01 for plotting purposes at Site 3.

Comparison with wastewater samples

Human *Bacteroides* (HF183/R287) was found consistently at high levels in the wastewater and was the most commonly observed indicator organism in the drinking water samples, though at

much lower concentrations (Figure 56). Pepper mild mottle virus was also commonly detected in wastewater but was not detected in drinking water. *Cryptosporidium* was only detected a single time in wastewater, at relatively low concentration, but was detected repeatedly in drinking water. *Salmonella* and norovirus were only detected in drinking water. The discordance between these results, and similarity in chemistry between the drinking water samples and deicing salts, suggests that stormwater might be a stronger impact on the well water quality than the sanitary sewer system, but some contribution from the latter cannot be ruled out.

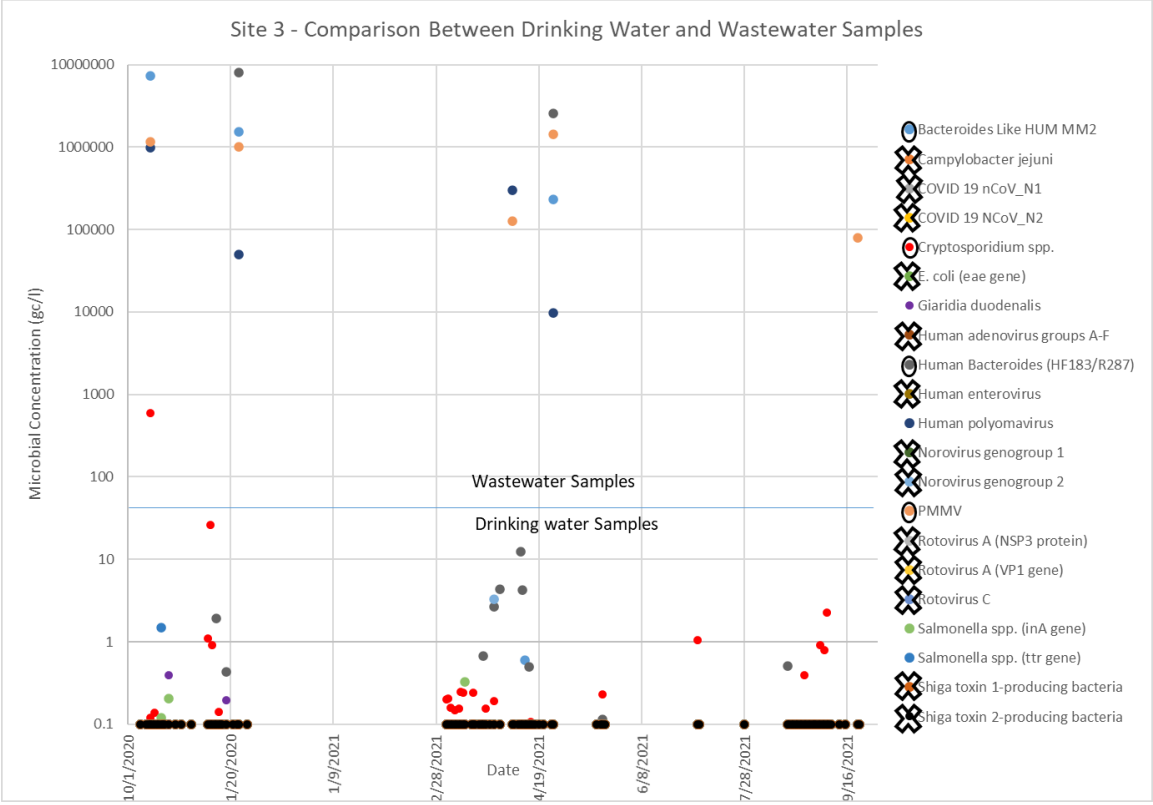

Figure 56. Comparison between drinking water samples and wastewater samples microbial results. Results below detection were converted to 0.1 for plotting purposes. Circled organisms were detected in both the drinking water and wastewater. Organisms with an "X" were not detected in either source. The remaining organisms were detected in only drinking water or wastewater, not both.

Site 3 - Groundwater age dating

Samples were collected from Well 3 for SF6 and dissolved gas and tritium analysis on September 28, 2021 and analyzed at the University of Utah Department of Geology and Geophysics Dissolved Gas lab. The results showed that the bulk of the water in this well was approximately 15-years old, with most of the recharge having entered the ground around 2006. However, the microbial, chemical, and isotopic response of the well water to precipitation events suggest that there is a component of very young water mixing with this body of older groundwater. Lag time analysis suggests that this young water fraction recharges the aquifer on time frames of hours to days. Results of a brine tracer study conducted on the stormwater piping near the city wells suggest that exfiltration appears quickly at the wellheads, and losses

as small as 0.3% of the overall well water volume may have accounted for the short-term rise in specific conductance observed there (Barry, 2022a).

Site 3 - Tracer Studies (extracted from Barry [2022a])

In conjunction with the recharge monitoring study, a series of tracer studies was conducted by the Minnesota DNR dye trace team to assess possible pathogen sources, flow pathways and times of travel (Barry, 2022a). Possible contaminant sources that were investigated included the stormwater piping that runs past the city well field and three nearby private septic systems. Testing ran from November 2019 to March of 2022, inclusive of all tracer releases and subsequent monitoring. No dyes were detected, suggesting that the private septic systems were not impacting city wells within the timeframe of the study. An alternate possibility is that the dyes were degraded or retarded, either by adsorption within the septic systems or by native geologic materials in the subsurface. The brine trace at the stormwater piping showed a rapid but small-scale rise in specific conductance at the city wells, suggesting a relatively direct but volumetrically small contribution from exfiltrating stormwater. Volumetric estimates suggest this contribution amounted to no more than 0.3% of the overall volume of water in the pressure tank to which the city wells flow (Barry, 2022a).

Site 3 - Annular Space Test

The competency of the grout seal in the annular space between the well casings and borehole walls was tested using a brine solution deployed at the surface and specific conductance measurements conducted in the well water after methods described in Walsh (2018). Approximately 200 gallons and 120 gallons, respectively, of a 1% NaCl solution with an average specific conductance of approximately 16,000 µS/cm was allowed to soak into the annular space outside the well casings. It was calculated that if 50% of this solution were to permeate the grout seal and make it to the well bore, it should raise the specific conductance of the well water at either well to at least 750 µS/cm, which would significantly exceed any measurement noted during the study. This solution was deployed continuously from 08:00-17:00 on September 21-24, 2021 at Well 3 and from 08:00-17:00 on September 27-31, 2021 at Well 2, and specific conductance was measured at the blended raw water tap used for the microbial sampling via the water quality sonde deployed in the autosampler from September 21-October 4, in addition to hand-measurements taken on individual well discharge from October 4-18. The latter readings were employed due to valve failure in the autosampler, which cast some doubt on the quality of the readings obtained from the water quality sonde during the early part of this study. Specific conductance measurements showed no rise beyond the range observed during the study, suggesting that rapid movement of surface water along the annular space of the well was not a likely pathway for the microbial detections observed in this study.

Site 3 - QMRA

The most concerning pathogen detections at Site 3 were the frequent (28 out of 93 samples) detections of *Cryptosporidium*, resulting in daily risk estimates consistently above .001 for most detections, and as high as 0.64 on November 10, 2020, when the concentration was 26.2 gc/L. Since this system serves a residential population, it is likely that a resident will be exposed to risk from *Cryptosporidium* multiple times during the year. Given that the risk is still relatively

low (the risk estimate of .001 could be viewed as 1 infection per 1,000 people), and that not every infection leads to illness, any health impacts may still not be visible in the community. As for Site 2, given the frequency of detections, treatment of the water supply or use of an alternate source will be the best ways to reduce risk.

Site 3 - Conclusions

The wells at Site 3 showed microbial detections that lagged precipitation events by 5-6 days on average during the fall of 2020, but which became more coincident in time once wetter precipitation regimes were in place (Figure 43). The spring 2021 sampling events showed lag times that averaged two days or less, and recorded the highest frequency of microbial detections, 63% compared with 50% or less in all other sampling events (Figure 44). The highest concentration was observed in the latter part of fall, 2020, when the precipitation regime had gone from normal values the preceding period to wet values. Together, these observations suggest that the wells are most susceptible to microbial contamination during wet periods, especially during spring snowmelt and shortly thereafter. The chloride/bromide ratios observed from the well water showed strong influence from road salt, which, combined with the positive results of a brine tracer test on the stormwater infrastructure near the wells, suggest that this infrastructure may be a primary threat to water quality at these wells.

The study results match a conceptual model of small volumes of fast-moving recharge driven by precipitation events and mixing with a reservoir of older, relatively unimpacted groundwater in the aquifer tapped by the wells. For example, the results of the brine test on the stormwater piping near the city wells suggest that exfiltration of only 0.3% by volume may result in short-term impacts to the water quality at the city wells (Barry, 2022a). The exact pathways traveled by these pulses of young recharge are unknown, but the absence of any obvious problems with well construction or the grout seal at these wells suggests they are not specifically well-related and may instead be naturally occurring within the groundwater system. Such features may consist of naturally occurring areas of high permeability within the upper portion of the package of glacial sediments here or may be related to human-caused connections stemming from potential deposition of mining overburden in the area.

Reducing the threat to this water supply might be achieved by actions that seek to break the apparent connection between the stormwater infrastructure and well(s), such as lining the stormwater piping in the stretch close to the wells to eliminate any localized exfiltration. Pressure testing of these sewer lines in advance of any mitigation efforts could be helpful for confirming the results of the tracer study and for pinpointing mitigation efforts. Additional water treatment may also provide protection from microbial threats, particularly if coincident with microbial pulses that seem tied to wet periods, especially spring thaw. Finally, increased water storage could allow for greater flexibility in responding to forecast precipitation events by pumping to storage before such events and then relying on the stored water until the lag times observed in the study have passed, although uncertainty about exact time periods to avoid plus possible issues with stagnation of excess stored water may minimize the attractiveness of this option.

Site 4 - Hydrogeology

Site 4 is in the southeastern portion of the Twin Cities Metropolitan Region (TCMR), approximately one-half mile from the Mississippi River, which is the dominant discharge feature in the area (Figure 57). The public water supplier serves a nontransient population of approximately 175 that includes a daycare and church. The surrounding land use is dominantly agricultural, mostly hay and pasture with some cultivated crops, as well as low to medium intensity development in the form of roadways and a nearby golf course.

The geology of the site is characterized by approximately 40-feet of unconsolidated Pleistocene sediment of Superior Lobe provenance, consisting of coarse-grained glaciofluvial material of the Cromwell Formation, overlying Ordovician limestone of the Prairie du Chien Group (Bauer, 2016). Combined with the underlying Jordan sandstone, these rocks constitute the most heavily used aquifer system in the TCMR. The well at this site is completed to a depth of 258-310 feet and open to dolomitic siltstone, sandstone and shale of the St. Lawrence Formation and sandstone of the Mazomanie Formation of the Tunnel City Group, which conformably underlie the Jordan sandstone (Figure 58). The St. Lawrence Formation is a regional confining unit, but locally functions as an aquifer. Several high-angle normal faults have been mapped in the area, all trending southwesterly, roughly coincident with the dominant groundwater flow direction. The closest of these is approximately 1,000-feet southeast of the site. Low-amplitude folds have also been mapped in the area, trending northwesterly. The terrain is relatively flat at the well site, but steps down to the Mississippi River to the southeast in a series of terraces.

Depth to water is approximately 180-feet below the land surface at the well site and the potentiometric surface dips steeply toward the Mississippi River, dropping another 25-feet over the ½-mile separating them (Figure 57). Vertical hydraulic gradients are strongly downward locally. The 1-year and 10-year time of travel capture zones for this well are shown in Figures 57 and 59. These were determined using the Metro Model 3 in Modflow (Metropolitan Council, 2014).

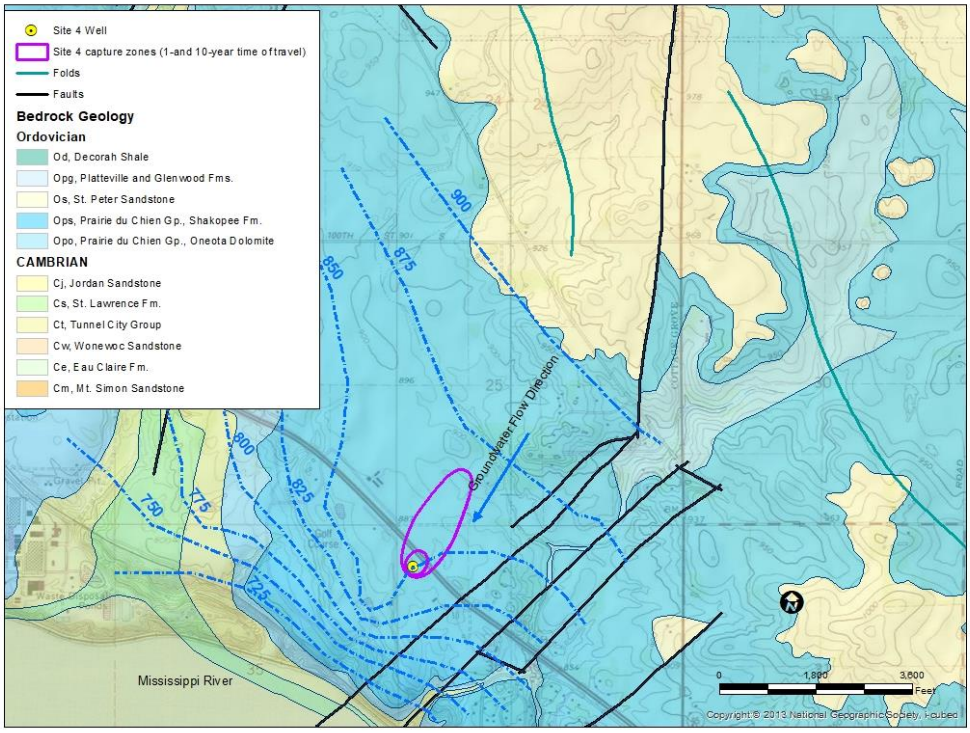

Figure 57. Site 4 hydrogeologic setting. Dashed lines are water table surface elevations in feet above sea level.

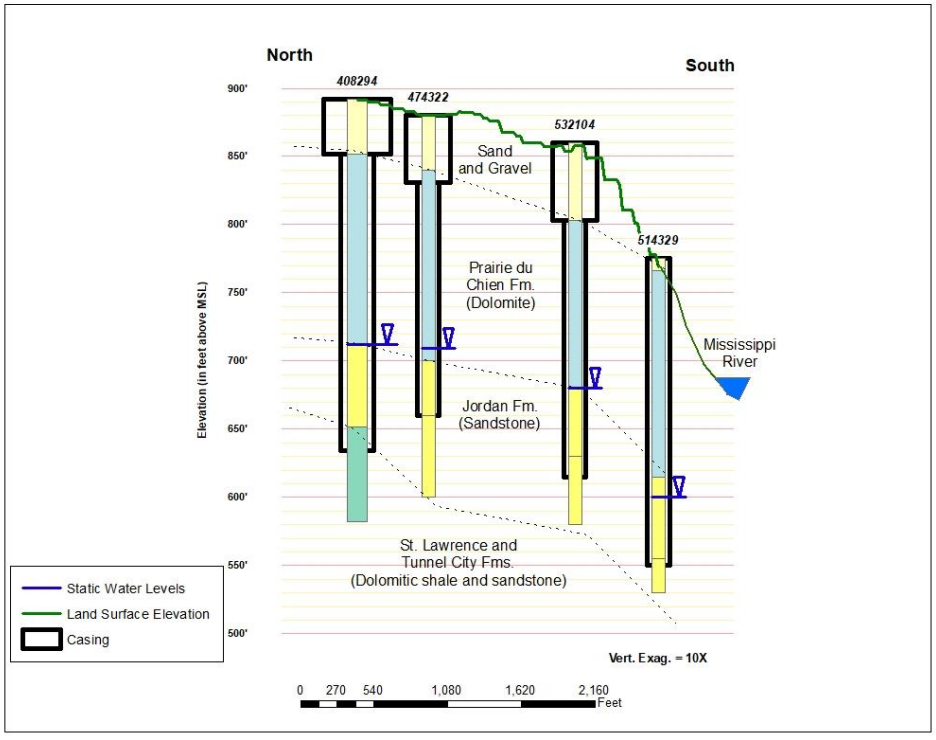

Figure 58. Geologic cross-section through Site 4, looking east. The sampled well is labeled 408294.

Site 4 - Potential Contaminant Sources

An inventory of potential contaminant sources located within 200-feet of the public supply well at this facility show that a septic tank located 56 feet north (upgradient) of the well constitutes the only identified pathogen source (Figure 59). This location falls within the one-year time of travel capture zone for this well. It is unknown whether manure is applied on upgradient farm fields thereby constituting another possible source.

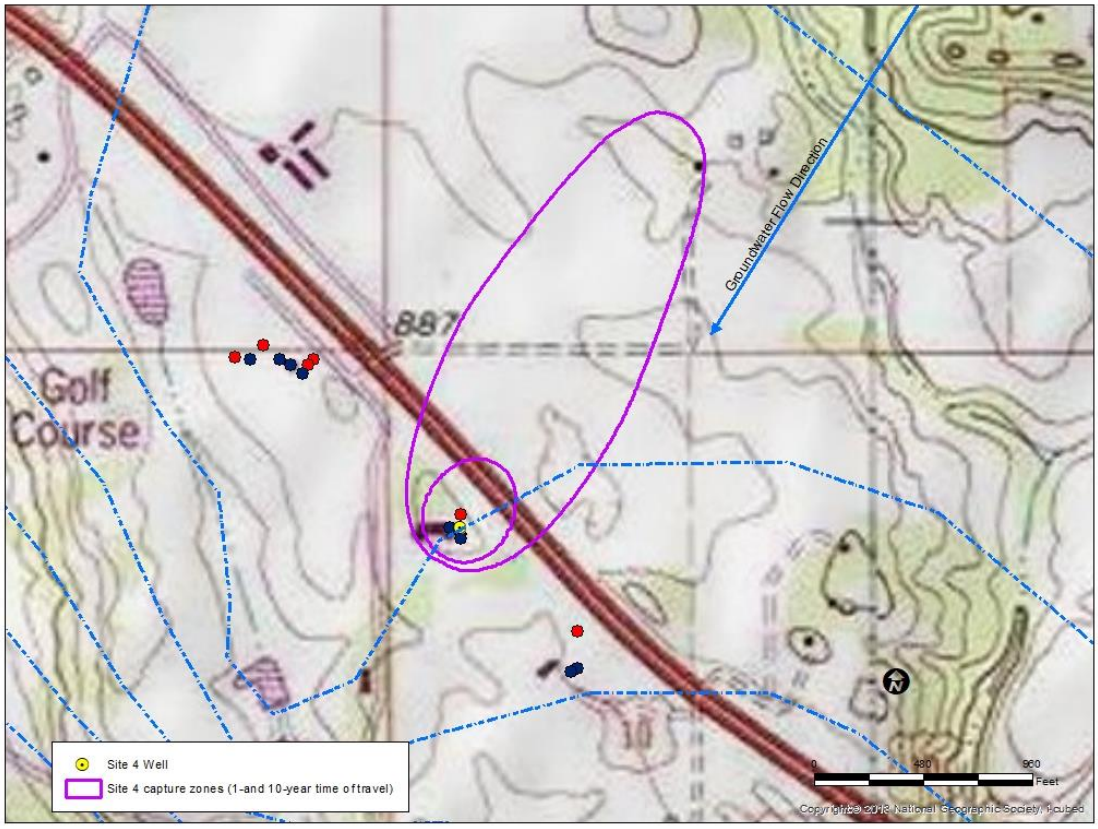

Figure 59. Location of possible pathogen sources with respect to Site 4 well and capture zones. Red dots represent possible pathogen sources, dark dots represent other contaminant types.

Site 4 - Monitoring Setup

The monitoring setup at this site matched the general description noted under the discussion of study design, with these additions:

- The autosampler at this site was attached to an untreated water tap from the study well that followed a series of two hydropneumatics bladder tanks with individual capacities of 86 gallons. Flow through this setup was continuous throughout the duration of the study except for a few brief maintenance periods.
- The official observation well for this site was completed in the Jordan Aquifer and located approximately 4-miles west of the study well. No nearby observation wells were available that were completed in the Tunnel City Group. Because the Jordan Aquifer is heavily used

for water supply in the Twin Cities Metropolitan Area, the hydrograph for this observation well was strongly influenced by pumping, making trend observations difficult. For determination of water level response to recharge events, a well completed in the Pleistocene unconsolidated sediments and located 5.7 miles to the north was used.

- The official USGS weather station for this site, which was co-located with the official observation well noted above, was not available for the full study period due to the late addition of this site (it replaced another site that had already been established and which was removed from the final site roster due to changed conditions). Instead, weather data from the US Weather Service site at Hastings Lock and Dam 2 (Station ID 213567) located approximately two miles away was used.
- The wastewater sampling site at this facility consisted of a septic tank located 56 feet from the well that was sampled once during each sampling event.

Site 4 – Comparisons with water use and precipitation regimes from preceding water years and study periods

The months during which sampling occurred during this study were evenly split between wet, normal, and dry ratings (WETS, Minnesota DNR, 2022). The preceding months were equally mixed between wet and dry ratings, with normal ratings showing only twice. For comparison, the preceding sampling months in the 2014-2016 study were dominated by normal months (eight), with two each of wet and dry months also represented.

Water use is not metered at this facility, so any usage comparisons are uncertain. However, reduced attendance at the church, day care and school associated with this facility during the time of COVID-19 restrictions likely means that water use during the study period was down from historical averages (Tim Charles, personal communication, 2022).

Site 4 – Description of Sampling Events

Six precipitation events were monitored at Site 4 during this study (Table 8 and Figures 60-62). Events 1 and 2 captured a series of late fall rains that followed a dry summer and early fall. These were essentially continuous, spanning October 8-November 28, 2020, with a one-week period (November 2-November 6) separating them. Total rainfall during this period equaled approximately 4 inches and resulted in water level rises of only a few tenths of foot on an otherwise falling hydrograph, reflective of the prevailing dry conditions (Figure 63). Events 3 and 4 also ran together and spanned from March 1-April 26, 2021. These events captured the onset of early spring warmth accompanied by the complete loss of approximately 7-inches of snowpack and accompanied by rain totaling 2.8 inches. A water level rise of 1.39 feet was observed during Events 3 and 4. This rise was noted during a time when at least partial frozen ground conditions were suggested by standard indicators, such as the presence of lake ice and frozen soil beneath area highways, revealing the shortcomings of those indicators and/or the importance of recharge via macropore flow in partially frozen ground (Mohammed et al., 2019). Event 5 ran from May 17-June 15, 2021 and captured late spring/early summer rain totaling 2.5 inches (Figure 64). A water level rise of 0.4 feet was noted. Event 6 ran from August 5-September 12, 2021 and captured 4.8 inches of late summer-fall rains that followed a significant drought. Limited sampling also occurred from July 5-July 15, 2021 related to a 0.6-

inch rainfall. That sampling was labeled Event 6a and was discontinued due to less than expected rainfall. Water levels during these periods were generally declining, although rises of 0.1 and 0.55 feet were noted during the August and September events.

Table 8. Summary of precipitation events monitored at Site 4.

Event	Date	Type	Cumulative Precipitation During Event (in)	Precipitation History from Current/ Prior Month	Water Level Change from Baseline During Event (ft)	Number/% of Samples Positive for Any Microbial Parameter	Lag Time in Days Between Precipitation and Microbial Detections (Shortest/Longest/Avg)	Microbes Detected (pathogens in red)	Maximum Concentration (gc/l)
1	10/8-11/2 2020	Fall Rain After Dry Summer	3.18	Wet/Dry	-1.31	0 (0%)	No detections	No detections	No detections
2	11/7-11/29 2020	Continued Fall Rain	0.4	Normal/Wet	-0.14	2 (14%)	9/14/11.5	HB	2.94
3	3/1-4/7 2021	Spring Thaw, Snowmelt and Rainfall	1.4 on top of melting of approximately 7-inches of snowpack	Wet/Dry	+1.31	4 (18%)	1/9/3.8	HB, B-like Hum, PMMV, Noro	17.93
4	4/7-4/26 2021	Spring Rain	1.4	Normal/Wet	+0.08	2 (18%)	0/8/4	HB, B-like Hum	2.96
5	5/17-6/15 2021	Early Summer Rain	2.5	Normal-Dry/Normal	+0.4	3 (25%)	4/19/13.7	HB, Noro	6.83
5a	7/5-7/15 2021	Summer Rain	0.6	Dry/Dry	-0.24	2 (40%)	7/8/7.5	HB, B-like Hum, Adeno	1.04
6	8/5-9/13 2021	Late Summer/ Early Fall Rain	4.8	Wet-Normal/ Dry-Wet	-0.18 overall, with rises up to 0.55	2 (28%)	0/8/4.7	HB, B-like Hum, PMMV, Noro, Crypto	1.59

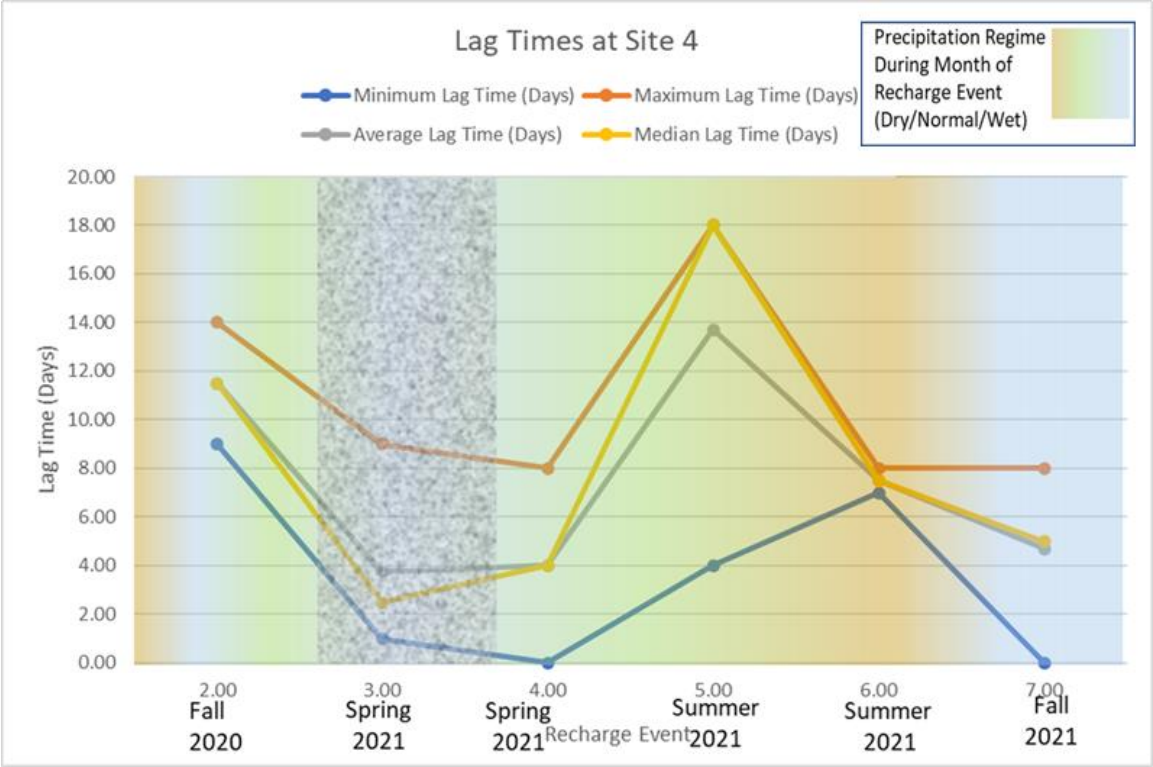

Figure 60. Summary of lag times observed at Site 4. Stippled pattern indicates period of possible frozen ground conditions based on indicators such as lake ice and frost depth beneath area highways. Precipitation regimes from Minnesota Climatology (2022).

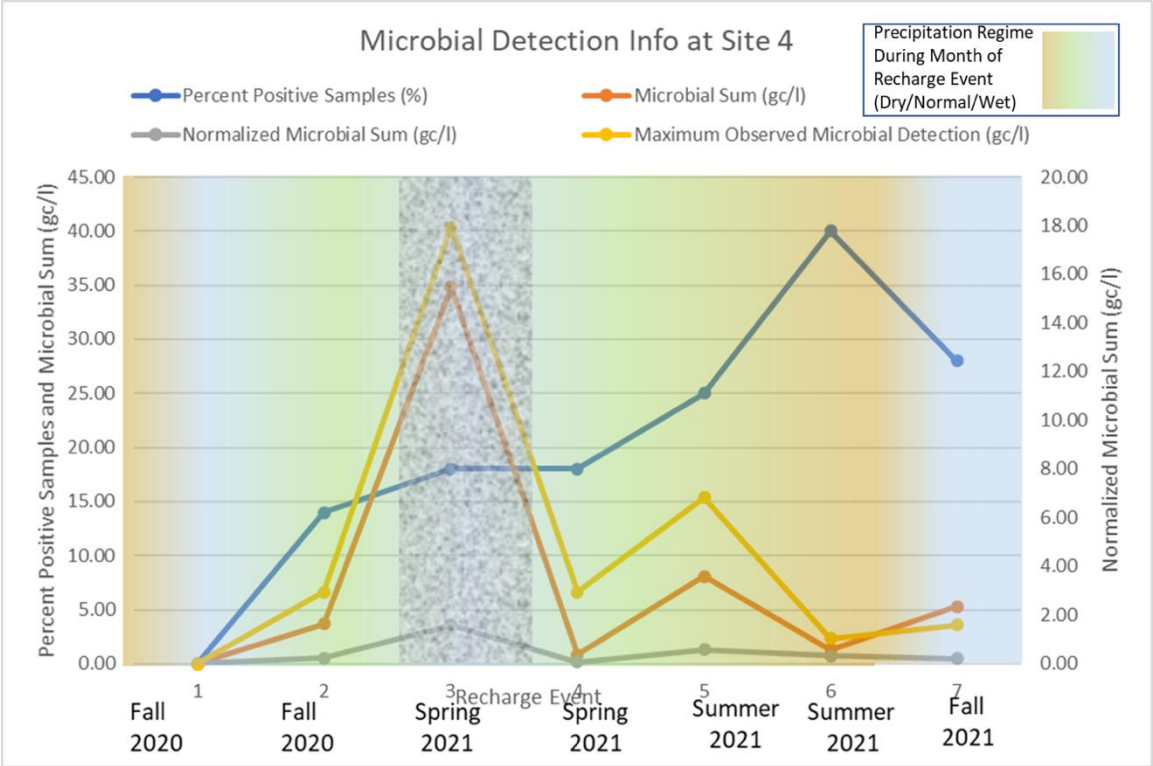

Figure 61. Summary of microbial detections at Site 4. Stippled pattern indicates period of possible frozen ground conditions based on indicators such as lake ice and frost depth beneath area highways. Precipitation regimes from Minnesota Climatology (2022).

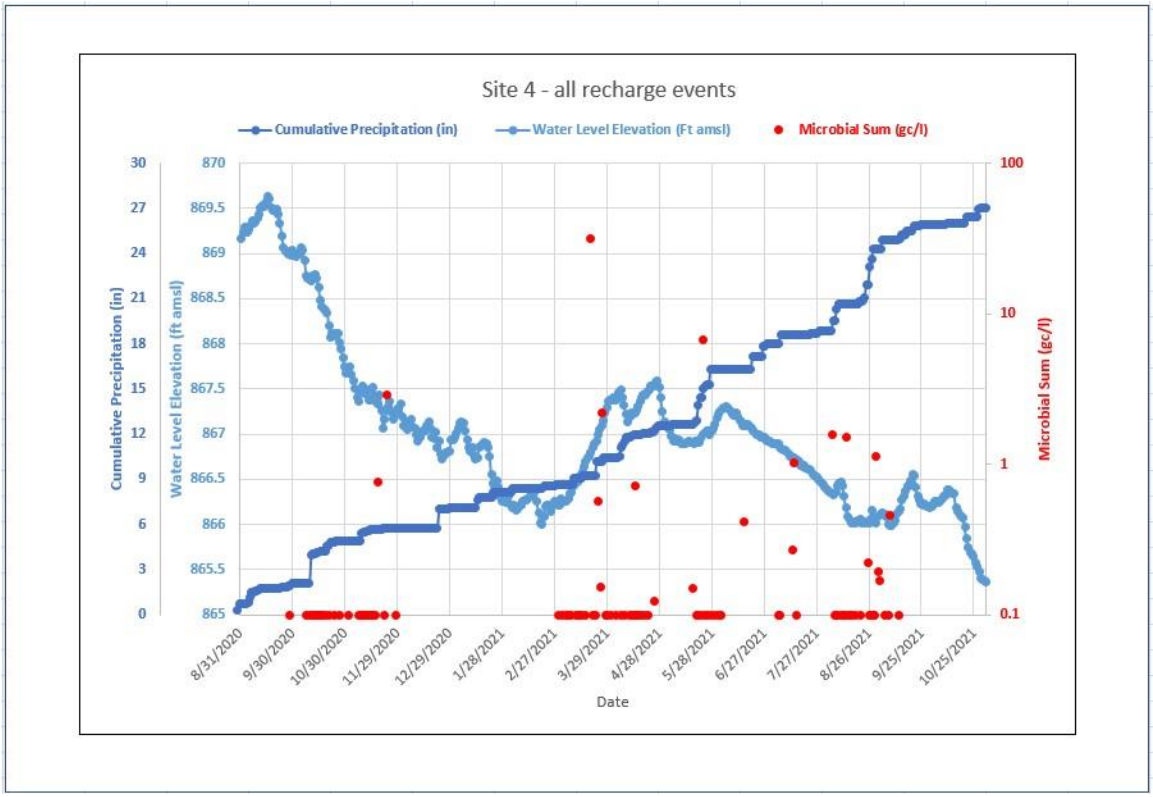

Figure 62. Precipitation monitoring events at Site 4. Microbial non-detections were converted to values of 0.1 gc/l for plotting on log scale.

Site 4 - Monitoring Results

Microbial results

Of the 109 samples taken from this well, 21 (19%) showed some level of microbial detection representing 23 overall positive results (i.e., two samples of the 21 were positive for more than one organism). Most were very low concentrations, around 1 gc/l, and were from non-pathogenic indicator organisms (Human *Bacteroides*, *Bacteroidales*-like HumM2 and pepper mild mottle virus). There were a few low-level detections of pathogens like adenovirus and norovirus, and a single low-level detection of *Cryptosporidium*. For comparison with the 2014-2016 study, 6 of those 12 samples were positive (50%), again with most of the detections coming from the indicator parameters Human *Bacteroides* and *Bacteroidales*-like HumM2. The differences in detection frequencies may relate to different precipitation regimes, with the 2014-2016 study period representing a wetter period than the current study. *Cryptosporidium* was detected once at a low-level during both study phases. *Salmonella* was detected during the 2014-2016 sampling period but not during this phase, and adenovirus and norovirus were detected during this study but not previously. The highest concentration observed during both study phases was similar, around 17 gc/l for Human *Bacteroides* in the earlier study, and for pepper mild mottle virus in this phase. Most of the other detections were 1/10th of that or less.

Microbial detections from Site 4 showed relatively long lag times initially, followed by shorter lag times during subsequent events before rising again during the early part of the drought summer of 2021 (Figure 60). The first sampling event showed no detections, and the median lag

time for detections during Event 2 was nearly 12 days. Subsequent sampling events showed lag times that generally averaged around 4-8 days, before increasing to nearly 14-days during the early summer months that preceded drought conditions. Average lag times decreased during the drought before returning to values more typical for the study. Microbial detection percentages also peaked in the summer of 2021, although the highest microbial sum was observed in the spring of 2021, driven largely by a single high value for pepper mild mottle virus (Figure 61). These results suggest lag times and microbial flux in the subsurface at this site are a function of moisture conditions, but with a lagged response overall, perhaps due to the very thick unsaturated zone at this location (180-feet). Longer lag times seem related to time-integrated antecedent moisture conditions more so than conditions present at the time of sampling, perhaps signaling the time required for wetting fronts in the vadose zone, accompanied by microbial genetic material, to propagate to the water table (Bradbury et al., 2008).

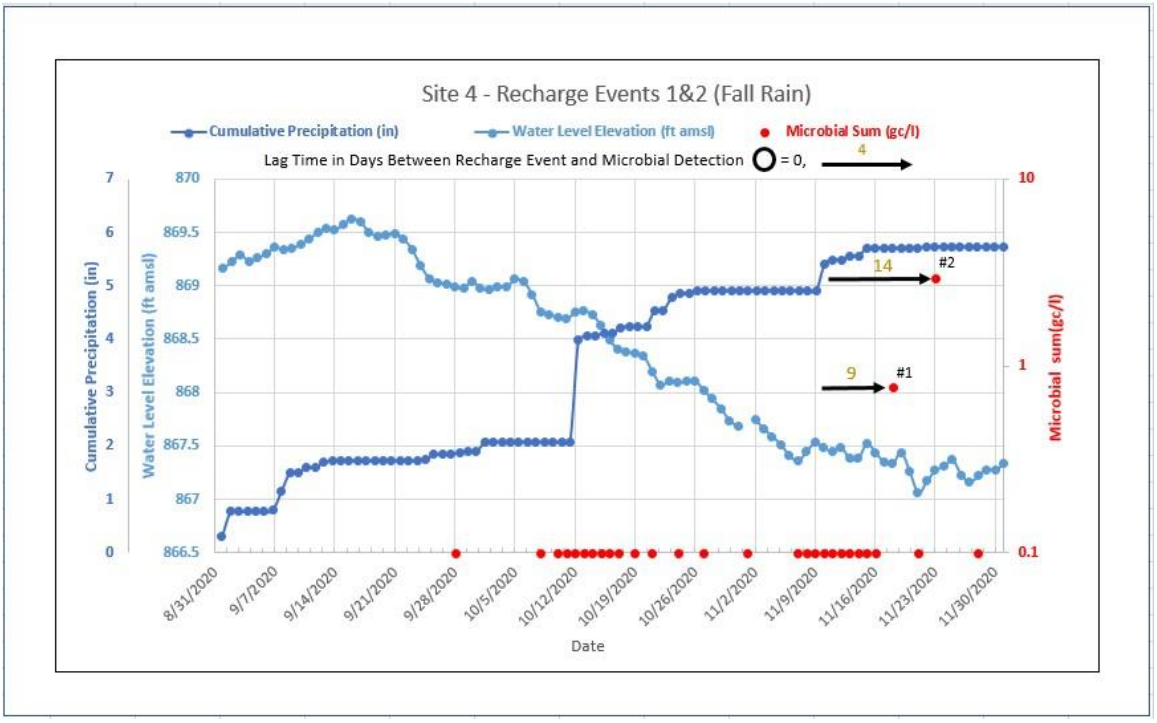

Figure 63. Microbial detections compared to cumulative precipitation and water level changes during Precipitation Events 1 and 2. Microbial non-detections were converted to values of 0.1 for plotting in log space.

In the first spring sampling event, microbial detections were noted shortly after the complete loss of approximately 7-inches of snowpack, which occurred on March 17, and which was preceded by a thaw that began around March 3 (Figure 64). This snowmelt, combined with 2.3 inches of rain, resulted in a water table rise of nearly 1.2 feet. Sampling during this event showed the greatest number of detections during the study (four), although higher percentages were observed during the final three monitoring periods.

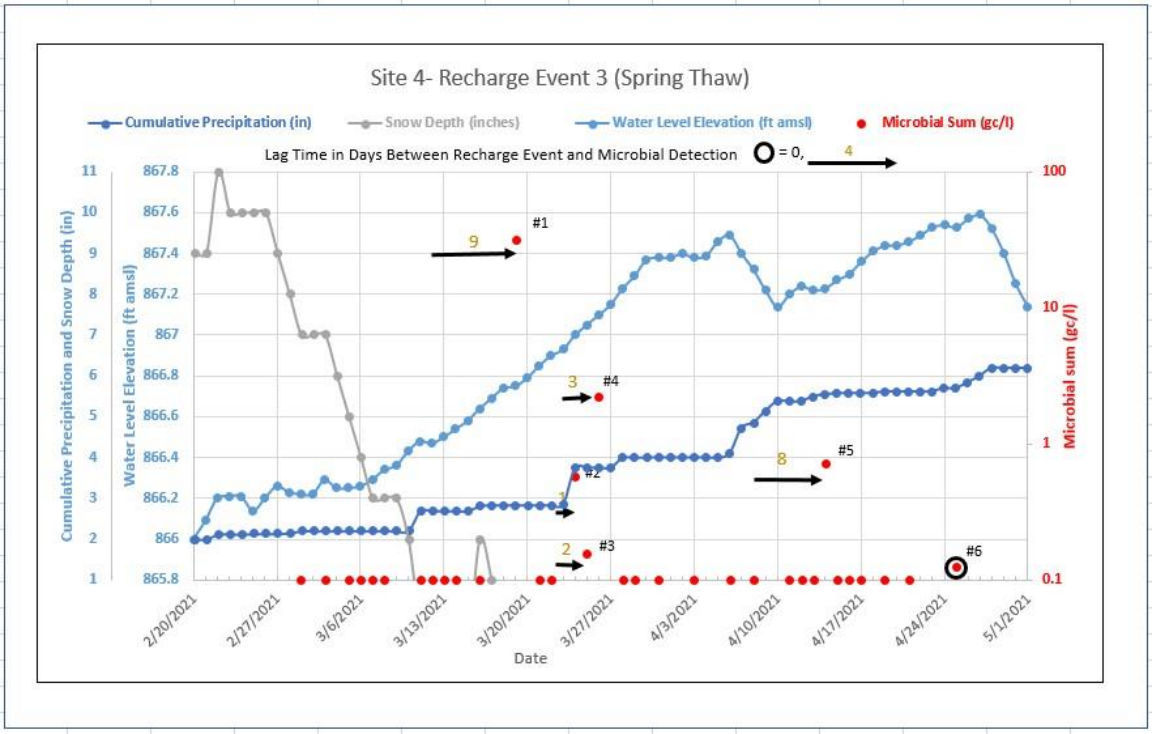

Figure 64. Precipitation monitoring during spring thaw at Site 4.

Water level and chemical responses to precipitation

Water level hydrographs showed rapid responses to precipitation and snowmelt, with rises often noted within a few days of an event, but often these were relatively small on otherwise falling trends (Figure 62). Only the spring thaw and corresponding rainfall resulted in overall rising hydrographs. It is unknown if the trends observed at the water table observation well would have been mimicked within the aquifer tapped by the study well.

Specific conductance values remained relatively constant at this well throughout the study, varying between 418 and 434 µS/cm and averaging 427 µS/cm. Maximum daily coefficients of variance (CV) barely exceeded 1% and the average value was only 0.32%. No obvious correlation was noted with microbial detections (Figure 65), suggesting that recharge water responsible for microbial transport was either of similar conductance to that generally observed in this well water or, if significantly different, likely represented a very small proportion of the overall volume. For example, the addition of only 4% by volume of relatively low conductance recharge water (assuming a specific conductance of 200 µS/cm) could reduce the average well water value of 427 µS/cm to the minimum observed value of 418 µS/cm.

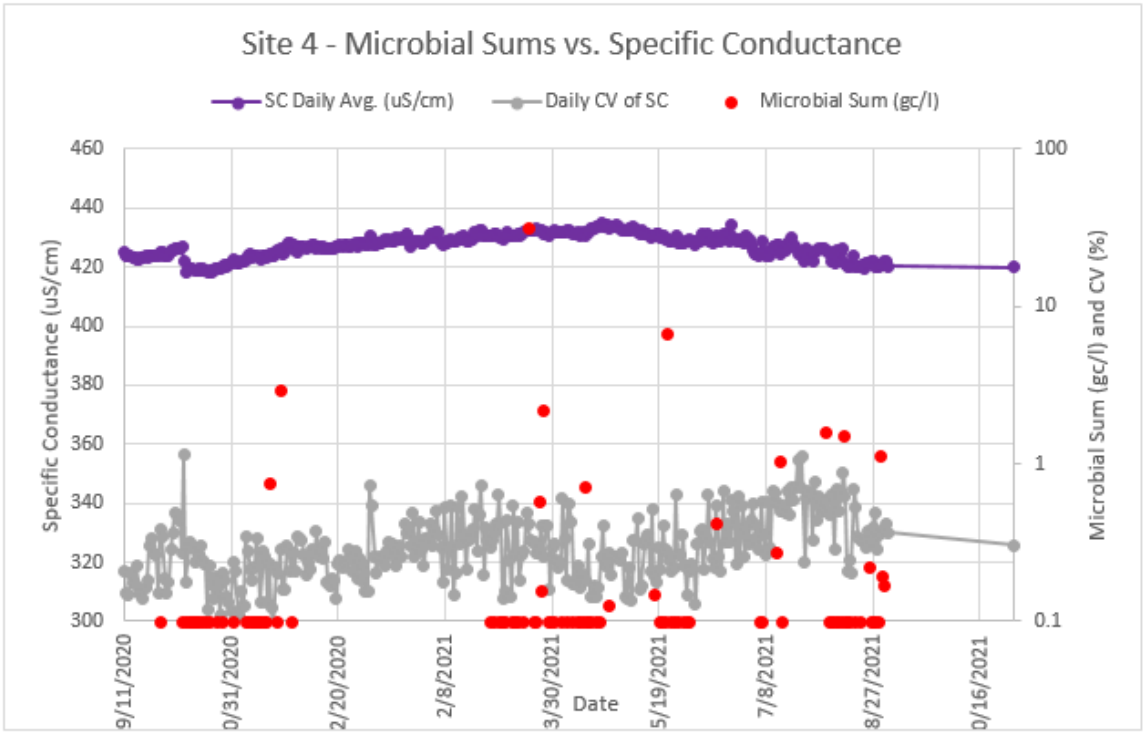

Figure 65. Specific conductance daily average values and variability during the monitoring study compared with microbial detections.

Water temperature was relatively variable compared to specific conductance, with an average CV 0f 7.2% (Figure 66). This variability appeared to reflect warming and cooling cycles within the autosampler rather than response to recharge events, since this variability was seen on a daily basis throughout the monitoring period. Average daily water temperatures were cooler during the early part of the study, with values from September 2020 to June 1, 2021 averaging just over 12°C, compared with an average of 13.5°C from that point onward. This may simply reflect warmer ambient air temperature during that part of the monitoring period. This is further supported by the water temperature data from the observation well completed in the overlying Jordan Sandstone aquifer, the daily average of which never varied from 10.5°C throughout the study. The observation well completed in the water table aquifer that was used for hydrograph comparisons was not equipped for temperature logging so is not available for comparison.

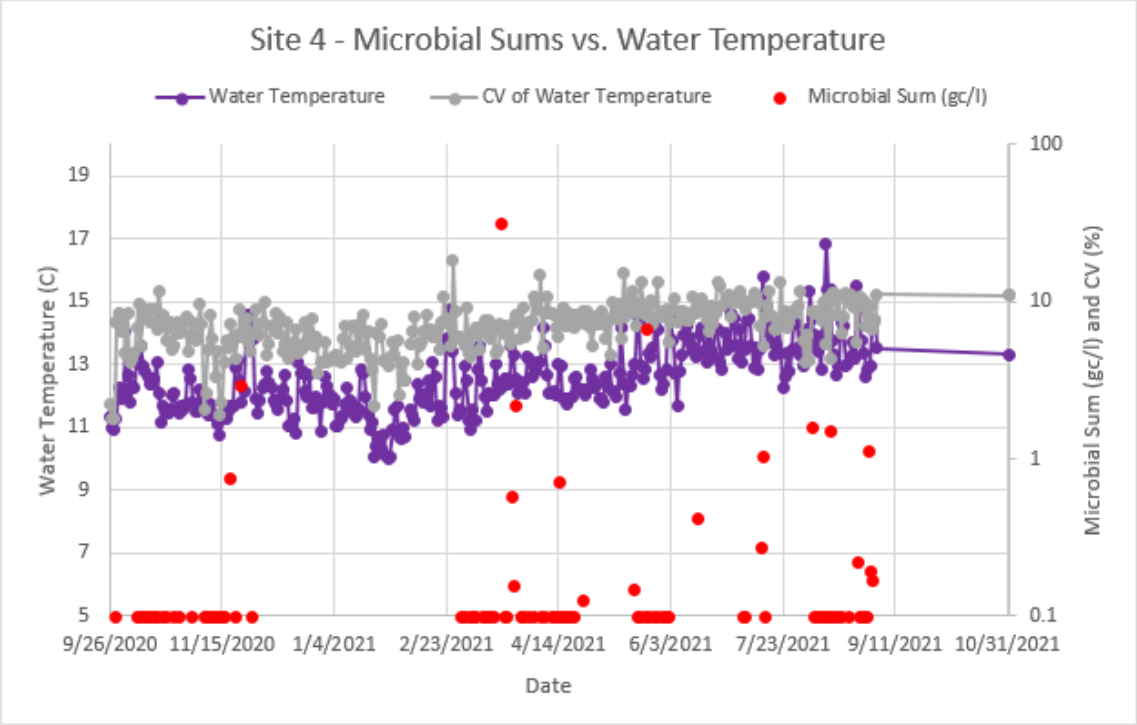

Figure 66. Water temperature variations during the monitoring study at Site 4.

Well water pH varied between approximately 7.3 and 7.8 over the course of the study, with relatively little daily variation (daily CVs averaged 0.37%). There was no clear relationship observed between pH of the well water and microbial occurrence, although several of the higher concentration detections were coincident with local minima (Figure 67).

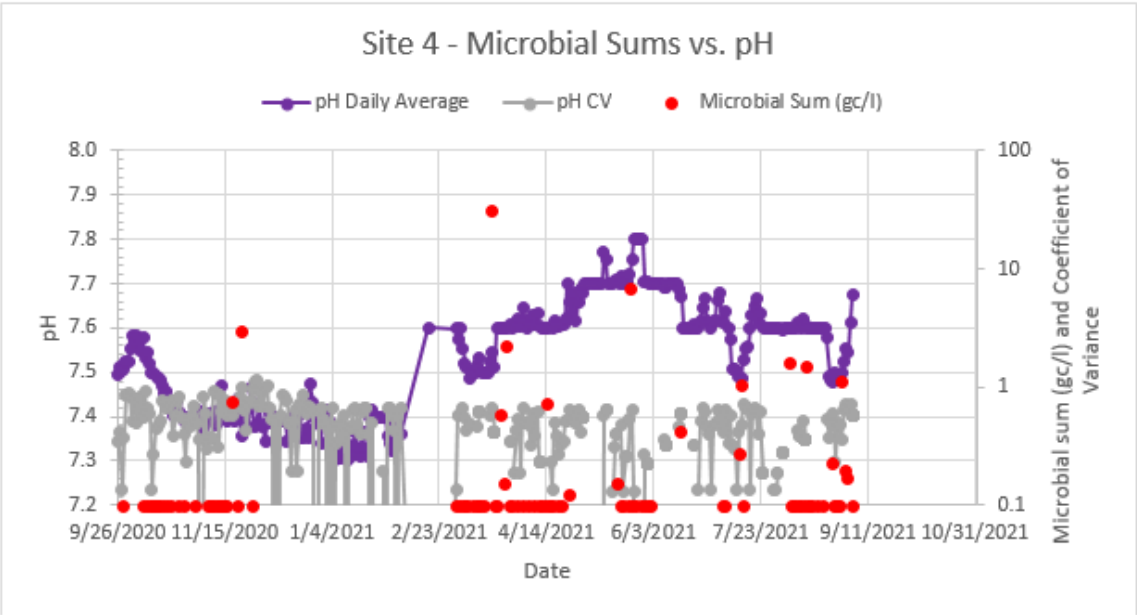

Figure 67. Observations of pH at Site 4.

Aside from the observations about specific conductance, temperature and pH noted above, the other data from the water quality sondes yielded significant noise and lack of sensitivity to the parameters being detected and are not discussed further in this report.

Chemical and isotopic results

The results from the whole water samples showed a relatively tight clustering just outside the boundaries of the field for dilute groundwater when plotting chloride vs. chloride/bromide (Figure 68). Results fall along curve 1, indicating water quality degradation from a halite source. A softener is used at this facility, so the wastewater system likely receives effluent that is impacted by halite from this source, as shown by the wastewater sample results in Figure 68. When compared with results from the 2014-2016 study, the more recent values show that water quality at this well has declined over time, with greater influence from higher Cl/Br sources such as wastewater.

Chloride/bromide ratios generally showed a positively correlated trend with at least the higher microbial detections (Figure 69). Detections, especially those of 1 gc/l, were associated with an increased chloride/bromide ratio when compared with preceding sample results. Chloride/bromide ratios of 370 or greater characterized detections where the microbial sum was at least 1 gc/l. This suggests that microbial detections were associated with volumetrically small and short-lived pulses of relatively elevated chloride/bromide water that was likely impacted by a septic source. The addition of only 1-2% by volume of wastewater with the average chloride/bromide value measured from that source during this study (4,283) would be enough to raise the well water value by 60-80 points, which was a typical increase noted during one of these “spikes” associated with a higher microbial detection.

Chloride values ranged from approximately 6.5 to 9 mg/l, which significantly exceeded the average value from 2014-2016 of 3.5 mg/l, again suggesting water quality degradation over time (Figure 70). Addition of 2.2% by volume of wastewater with the average value observed in this study (250 mg/l) would raise the 2014-2016 average value to the highest values seen in this study phase. Chloride values rose early in the study, nearly peaking towards the end of sampling Event 2 in the fall of 2020. They maintained or slightly exceeded those values through the spring of 2020, before declining to the lowest values observed in the study during the final precipitation events of late summer/fall 2021. These trends seem most correlated with water level observations, with the early rising values relating to the generally falling hydrograph due to antecedent dry conditions resulting in relatively large chloride contributions from wastewater sources. Later declining chloride trends seem related to stabilized or rising hydrographs, suggesting dilution associated with fresh recharge.

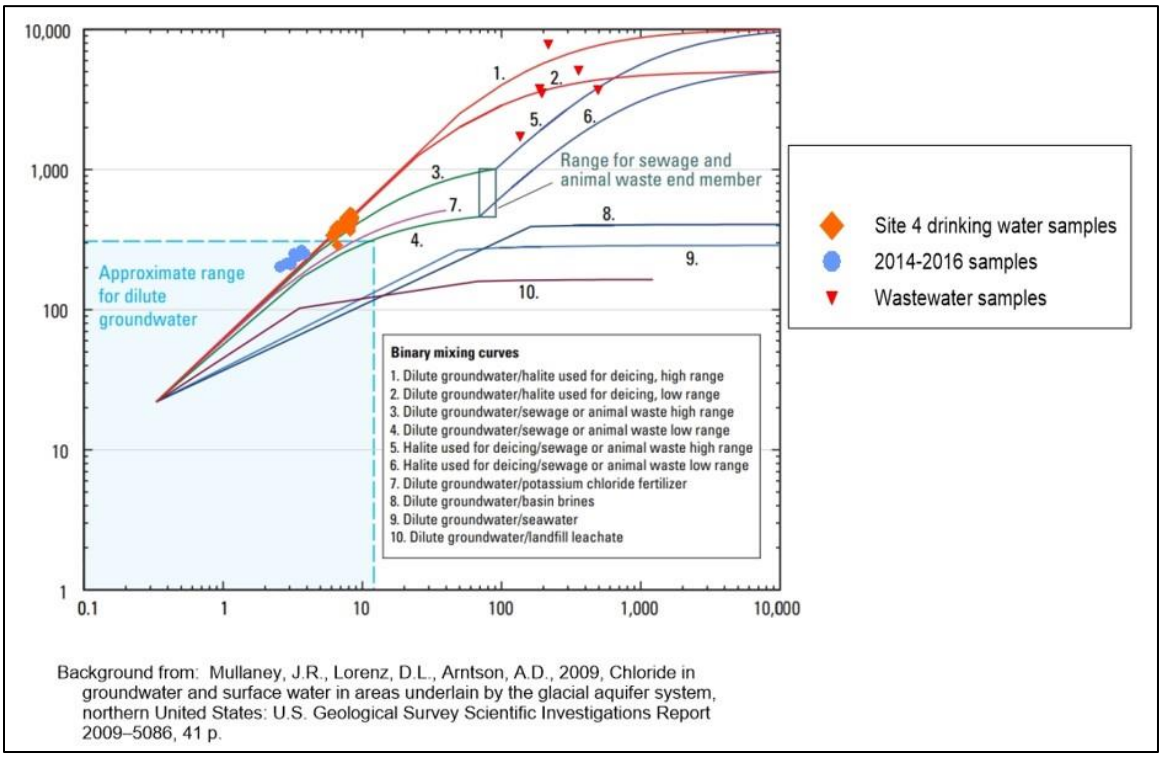

Figure 68. Chloride vs. chloride/bromide results for Site 4 compared to the fields shown in Mullaney et al., 2009.

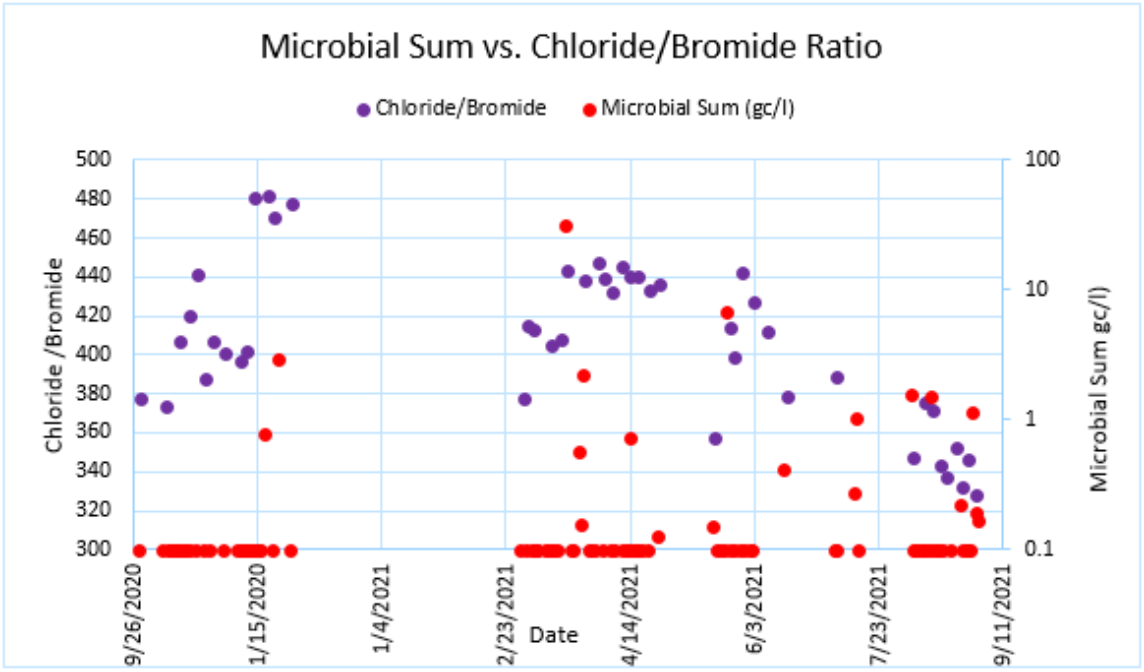

Figure 69. Chloride/bromide ratios from whole water samples compared with microbial detections at Site 4. Non-detect microbial results were changed to 0.1 for plotting in log scale.

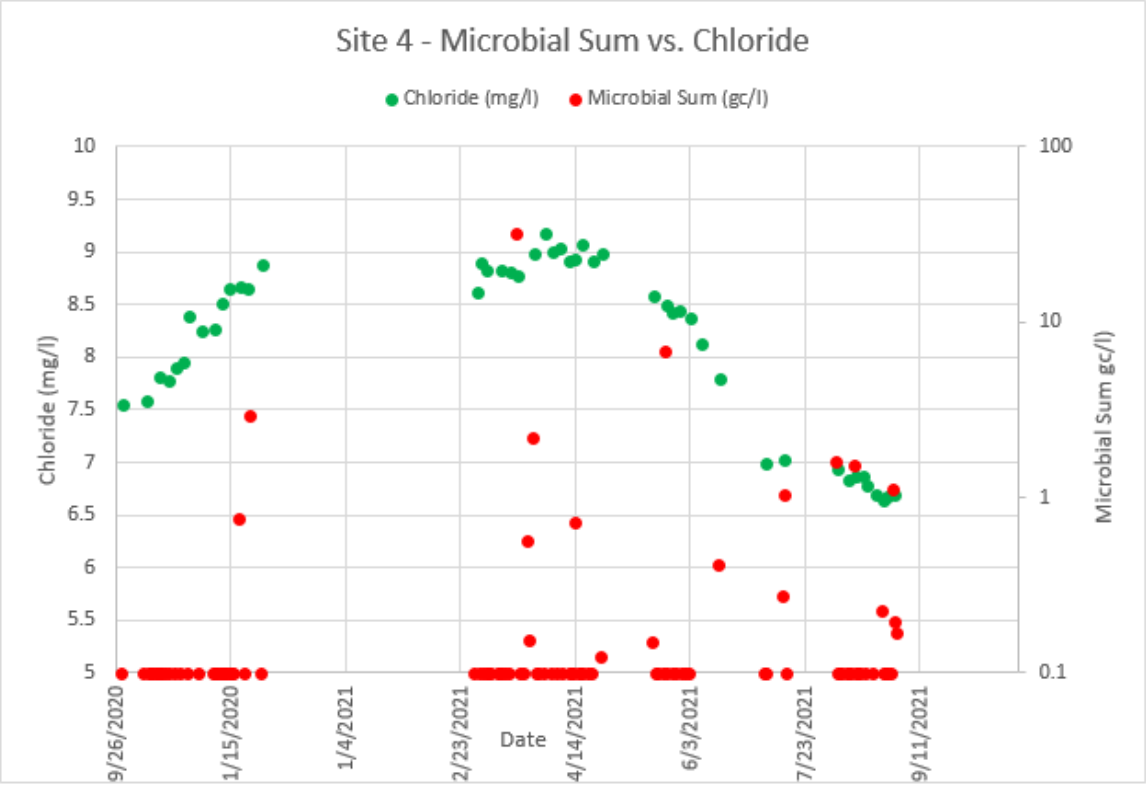

Figure 70. Chloride values versus microbial sums at Site 4. Microbial non-detects converted to values of 0.1 for plotting.

The stable isotopes of water showed no evidence that this well captured any significant quantities of evaporated surface water during the study. All samples cluster near the MWL of Landon et al. (2000), with only one of the fifty samples showing any significant deviation from the line based on a line-conditioned excess value less than -1.0 (Landwehr, J.M. and Coplen, T.B. (2004). This confirms that the nearest surface water body, the Mississippi River, is a discharge feature that was not contributing to the well water.

The variation in oxygen-18 and deuterium observed during the study showed no consistent patterns, other than being isotopically lighter during the March 2021 sampling events, consistent with additional contributions from snowmelt recharging the aquifer (Figure 71).

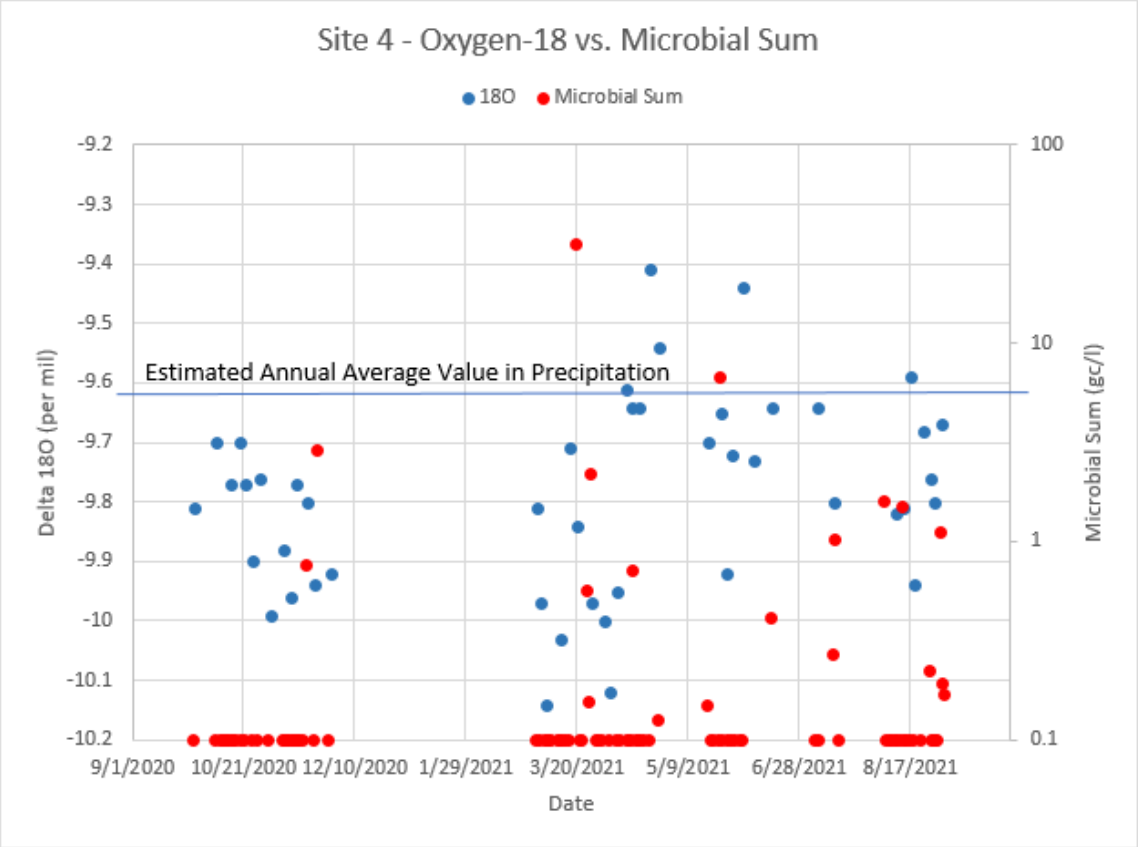

Figure 71. Comparison between oxgen-18 values and microbial detections at Site 4. Microbial non-detections were converted to values of 0.01 for plotting purposes.

Comparison with wastewater samples

Human *Bacteroides* (HF183/R287) was found consistently at high levels in the wastewater and was the most commonly observed organism in the drinking water samples, though at much lower concentrations (Figure 72). Pepper mild mottle virus was also commonly detected in both wastewater and drinking water, though not always during the same sampling event. *Cryptosporidium* was detected only once in both wastewater and drinking water, both during the last sampling event. Some microbes were only detected in one source and not the other. For example, norovirus genogroup 2 was only detected in the drinking water samples. Human adenovirus was detected in both, but widely separated in time (nearly one year apart). Finally, several organisms were only identified in wastewater samples, including rotovirus A, human enterovirus and human polyomavirus, the latter being commonly found in wastewater but never in the drinking water. The chemical comparisons noted previously between the wastewater and drinking water samples reflect that these are likely connected, and that volumetrically small contributions from the wastewater effluent appear to be correlated with recharge events and microbial occurrence at the well.

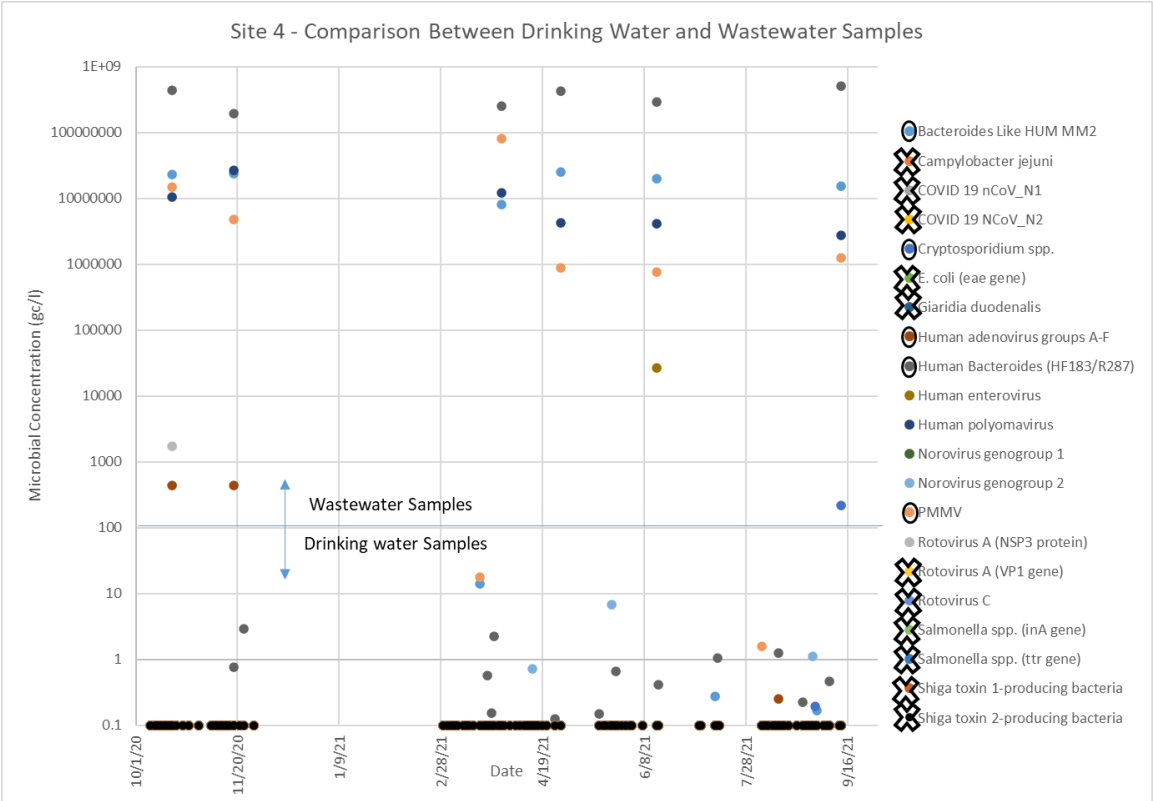

Figure 72. Comparison between drinking water samples and wastewater samples microbial results at Site 4. Results below detection were converted to 0.1 for plotting purposes. Circled organisms were detected in both the drinking water and wastewater. Organisms with an "X" were not detected in either source. The remaining organisms were detected in only drinking water or wastewater, not both.

Site 4 - Groundwater age dating

Samples were collected for SF6 and dissolved gas and tritium analysis on September 28, 2021 and analyzed at the University of Utah Department of Geology and Geophysics Dissolved Gas lab. The results showed recharge age estimates that ranged from 1982-2003, with a best estimate of approximately 1990. This suggests that the bulk age of the well water was approximately 31 years at the time of sampling. However, the microbial, chemical, and isotopic response of the well water to precipitation events suggest that there is a component of very young water mixing with this body of much older groundwater. Lag time analysis suggests that this young water fraction recharges the aquifer on time frames of days. Volumetric estimates indicate that these fast recharge pulses, sometimes accompanied by microbial DNA and wastewater signatures, account for approximately 2% or less of the overall well water volume, but likely result in the microbial detections noted in this study.

Site 4 - Annular Space Test

The competency of the grout seal in the annular space between the well casing and borehole wall was tested using a brine solution deployed at the surface and specific conductance measurements conducted in the well water after methods described in Walsh (2018). Approximately 600 gallons of a 1% NaCl solution with an average specific conductance of

approximately 16,000 µS/cm was allowed to soak into the approximately 2-inch annular space outside the innermost well casing that extends to the land surface. It was calculated that if 10-20% of this solution were to permeate the grout seal and make it to the well bore, it should raise the specific conductance of the well water to at least 500 µS/cm, which would significantly exceed any measurement noted during the study. This solution was deployed continuously from 08:00-17:00 on September 13-14, 2021 and specific conductance was measured at the raw water tap used for the microbial sampling via the water quality sonde deployed in the autosampler. Specific conductance measurements continued for two weeks following the end of brine deployment. No rise in specific conductance beyond the range observed during the study was noted, suggesting that rapid movement of surface water along the annular space of the well was not a likely pathway for the microbial detections observed in this study.

Site 4 - QMRA

Site 4 had only five pathogen detections out of 109 samples. Detections included norovirus, adenovirus, and *Cryptosporidium*. Maximum risk estimates for the three microbes were 0.47, .00017 and .011 respectively. While the detections indicate vulnerability, the overall concern is lower at this site compared to the other three sites because of the infrequent detections.

Site 4 - Conclusions

The well at Site 4 showed microbial detections that significantly lagged precipitation events following the dry fall of 2020, but which became more coincident in time in subsequent events once wetter precipitation regimes were in place, except for the drought summer of 2021 (Figure 60). Average lag times reduced from nearly 26 days to less than 10 days later in the study, with one same-day detection noted. Microbial sum peaked in spring of 2021 and then again that summer, while detection frequency continued to rise until late in the summer of 2021 before declining during the final sampling episode in fall 2021. Accompanying these detections, especially those of higher concentrations, were short-term increases in chloride/bromide that seem related to wastewater from the on-site septic system. Coincident occurrence with microbial detections from wastewater samples further supports this relationship, as does the location of the wastewater system being upgradient of the well and within the 1-year time of travel well capture zone. Mass-balance analysis suggests that these wastewater-impacted contributions likely constitute less than 2% of the well water volume.

These results match a conceptual model of small volumes of fast-moving recharge driven by precipitation events and mixing with a reservoir of older, relatively unimpacted groundwater in the aquifer tapped by this well. The exact pathways traveled by these pulses of young recharge are unknown, but the absence of any obvious problems with well construction or the grout seal at this well suggests they are not specifically well-related and may be naturally occurring within the groundwater system. Examples may include small-scale features such as bedrock fractures or other high-conductivity pathways such as gravel lags in the glacial drift. The lag times noted for maximum microbial sums and detection frequencies are consistent with relatively long transit times through the thick vadose zone at this site.

Reducing the threat to this well might be achieved by relocating the septic system downgradient of the well and outside the well capture zone, if possible, and/or constructing a

new well that is cased and grouted through the entirety of the St. Lawrence Formation. This regional confining unit is currently open to the well, so its function as an aquitard is reduced.

Overall Study Conclusions

The results of this study suggest that wet conditions near the time of sampling promote the detection of microbial genetic material in drinking water supplies, with lag times between precipitation events and microbial occurrence dependent on antecedent moisture conditions as well as depth to water/thickness of the vadose zone. When more than four samples were collected during a precipitation regime, wet months of sampling had highest microbiological sums compared to dry and normal periods (Table 9). No relation was seen between pathogen sums and degree of dryness in months that preceded sampling, however at three of the four sites the highest single pathogen concentration was observed in the second precipitation event following the transition from a dry to wet period. This observation suggests that pathogenic material may accumulate in the subsurface during dry periods and be transported to the water table following the propagation of wetting fronts that accompany the return of wet conditions.

Table 9. Microbial detections for each study site summarized by precipitation regime present during the month of sampling. Source = Minnesota Climatology, 2022.

Site Number	Precipitation Regime During Month of Sampling	Microbial Sum (gc/l)	Count	Average (gc/l)
1	Dry	8.06	24	0.34
1	Normal	0	1	0
1	Wet	49.44	64	0.77
2	Dry	5.10	4	1.27
2	Normal	22.10	26	0.85
2	Wet	77.71	62	1.25
3	Dry	1.87	8	0.23
3	Normal	3.97	28	0.14
3	Wet	65.95	57	1.16
4	Dry	1.73	10	0.17
4	Normal	12.83	44	0.29
4	Wet	39.51	55	0.72

At the fine temporal scale of individual sampling events, the sampling results have a high degree of noise, but at the coarse temporal scale of the year-long study, these results generally match a classic tracer breakthrough curve (Figure 73), with an early flush of relatively concentrated microbial genetic material following the transition from a dry to a wet precipitation regime (Figure 74). After this initial flush, and with continued wetness, concentrations dropped, but a "tail" consisting of persistent low-level detections persisted until the onset of the next dry period and was accompanied by a second, small concentration spike. Lag times were long initially during the wetting phase but decreased with time so that during the tailing period they reach their minima, the duration of which is established by the local hydrogeologic setting (Figure 75).

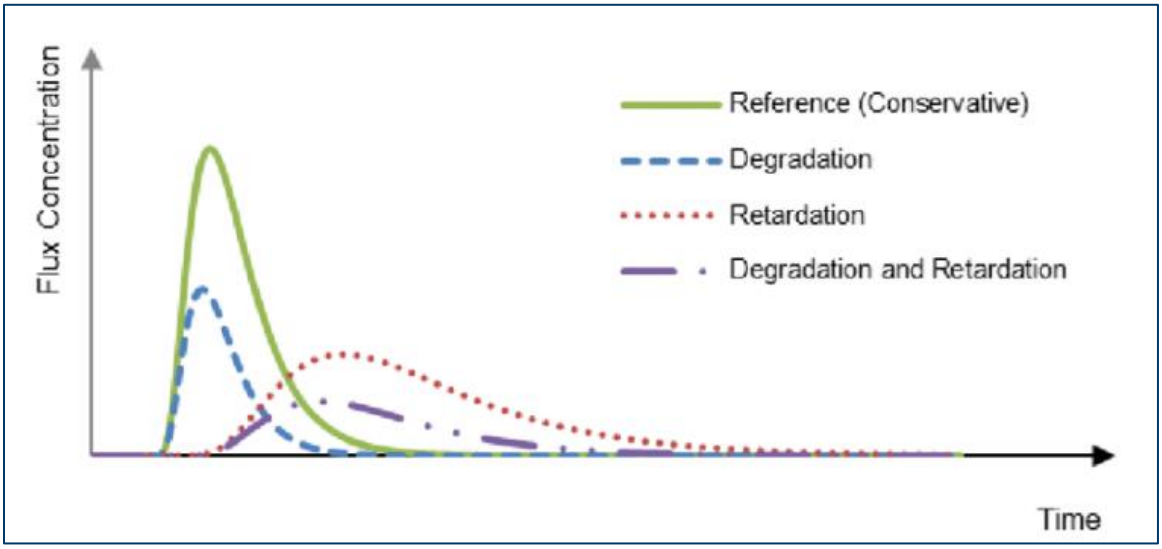

Figure 73. Breakthrough curves for different types of groundwater tracers. From Cao et al., 2020.

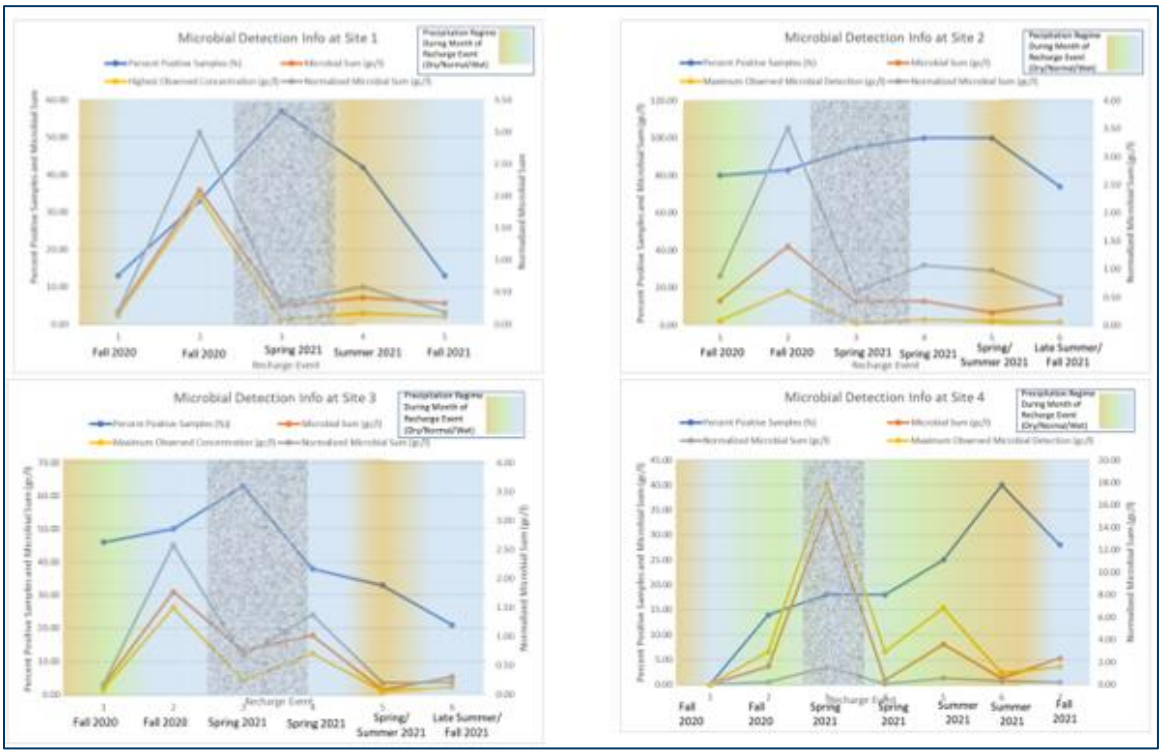

Figure 74. Microbial detection trends at the four study sites. Stippled pattern indicates period of possible frozen ground conditions based on indicators such as lake ice and frost depth beneath area highways. Precipitation regimes from Minnesota Climatology (2022).

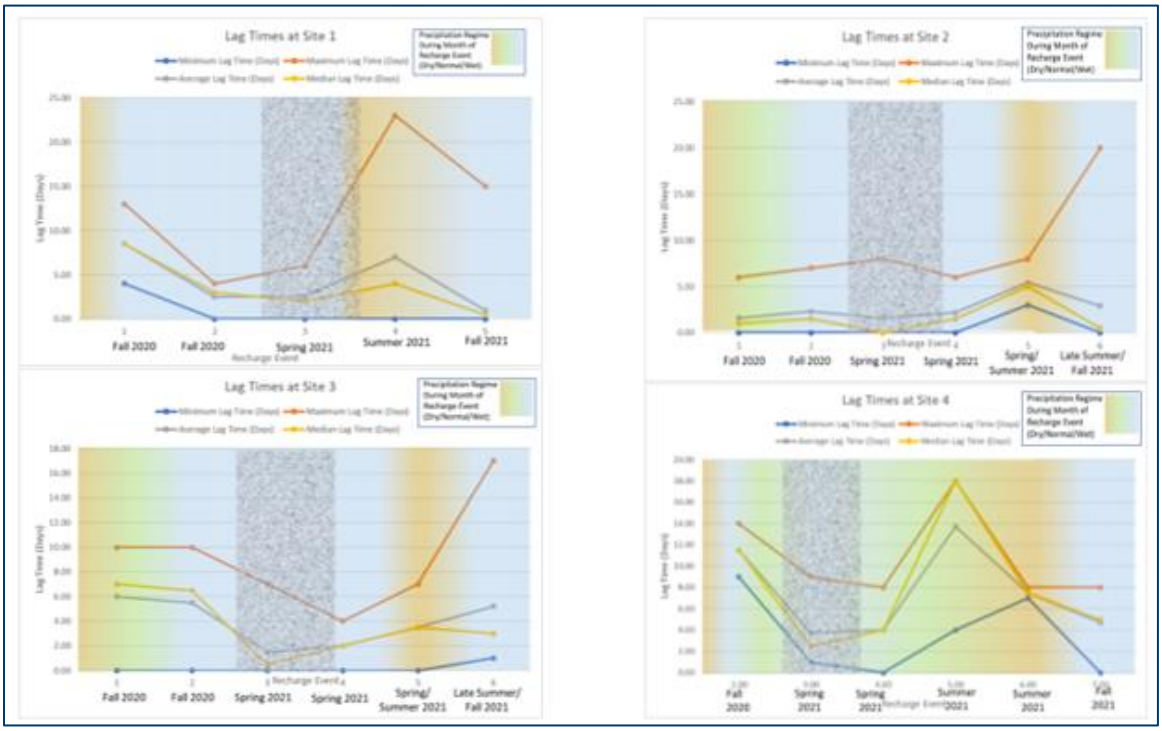

Figure 75. Lag times at the four study sites. Stippled pattern indicates period of period of possible frozen ground conditions based on indicators such as lake ice and frost depth beneath area highways. Precipitation regimes from Minnesota Climatology (2022).

Although microbial concentrations peaked in the late fall of 2020 at three of the four sites, overall detection frequency peaked in the spring of 2021. Only Site 4, with its 180-foot-thick vadose zone, showed a delay in both peak microbial sum and detection frequency, occurring in the spring and summer of 2021 respectively. The spring spike in detection frequency and decrease in lag times, including many same-day detections, corresponded with the onset of above freezing air temperatures and associated snowmelt, with or without additional rainfall. Hydrograph rises were also noted during these periods, confirming that rapid groundwater recharge was occurring, despite the presence of indicators of locally frozen ground such as ice on area lakes and subsurface thermal measurements beneath area highways (Minnesota Climatology, 2022 and Minnesota Department of Transportation, 2022). This reveals the shortcomings of those indicators for assessing the likelihood of groundwater recharge during spring thaw and may reflect the local importance of recharge via macropore flow in partially frozen ground (Mohammed et al., 2019). This finding may have ramifications for future monitoring studies or even required regulatory sampling.

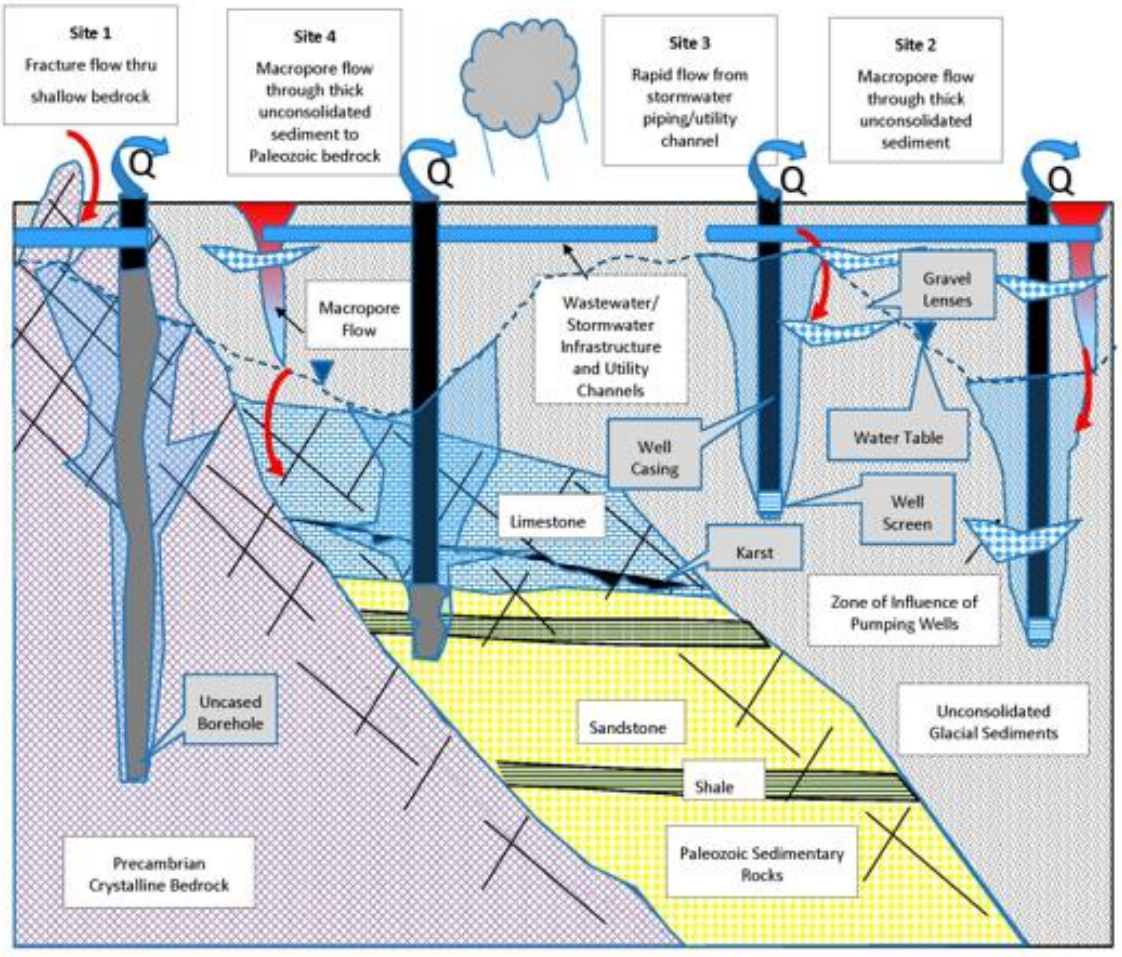

Figure 76. Conceptual model of small-volume, fast-flow pathways to wells in this study.

Overall, these results match a conceptual model of small volumes of fast-moving recharge driven by precipitation events and mixing with a reservoir of older, relatively unimpacted groundwater in the aquifers tapped by these wells (Hunt et al, 2010). Volumetric estimates

suggest that these fast-flow contributions represented no more than 10-20% of the water in these wells, with most estimates being 5% or less and with a volume as small as 0.3% noted at one site based on a brine trace. The exact pathways traveled by these pulses of young recharge are unknown, but the absence of any obvious problems with well construction or the grout seal at these wells suggests they are not specifically well-related and may be naturally occurring within the groundwater system. Examples may include macropores in the soil horizon and small-scale, high conductivity features such as fractures or preferential flowpaths resulting from thin coarse-grained unconsolidated deposits (Figure 76). The observed commonality in microbial detection patterns across these four sites with their varied hydrogeologic settings suggests similarity in transport mechanisms, which may allow for generalization to other well sites if the lag times associated with thick vadose zones are appropriately accounted for.

Temporal lags in the hydrograph responses at Site 2, where a 40-foot difference in vadose zone thickness differentiated the two observation wells, showed coincidence with average lag times based on microbial detection (just under two days). This confirms bulk transit time through the vadose zone for water and contaminants, microbial and otherwise, but the wide variance in individual microbial lags points to varying transport pathways or mechanisms within this overall framework. Such variability may be introduced by the presence of wetting or drying fronts in the vadose zone and small-scale heterogeneity in subsurface geologic materials. Lag times between antecedent moisture conditions and microbial detections in the subsurface may be important where vadose zones are especially thick. For example, Site 4, with a 180-foot depth to water, showed relatively long lag times compared to other sites in the study. Where such conditions are encountered, monitoring studies may need to account for this dynamic.

Some correlation was noted between microbial detections and chemical and isotopic parameters, giving credence to including parameters such as specific conductance and chloride/bromide in future studies as surrogates for microbial risk or groundwater susceptibility to contamination more generally. These parameters, combined with other techniques such as microbial matching, tracer studies and groundwater flow modeling, provided insights into most likely sources of pathogen contamination at study wells, resulting in potential infrastructure changes to address these issues. Similar approaches could be established for other public wells considered prone to microbial contamination.

The use of weather forecasting tools proved invaluable for triggering sampling events during this study, and the use of precipitation histories such as WETS (Minnesota State Climatology Office, 2022) proved similarly crucial for assessing the relationship between microbial detections and both prevailing and antecedent moisture conditions. Future sampling studies involving analytically sensitive chemical or biologic parameters that may exploit similar short time of travel pathways as implied in this study, such as PFAS, may benefit from this approach for both sampling and data analysis.

The SARS-CoV2 virus was analyzed for throughout the study, which overlapped with the COVID-19 pandemic, but it was not detected in drinking water or wastewater. This may simply reflect that the virus was not present in the communities served by the wastewater systems at these four sites during the study, as suggested by the limited wastewater sampling that occurred. Alternatively, we cannot discount the possibility that the virus was shed intermittently into the wastewater systems at the study sites, but at times between sampling events. In the latter case,

the absence of any detections in the drinking water samples would argue for the limited environmental persistence of this virus in groundwater, as suggested by other studies (La Rosa et al., 2020).

The results of this study show that the health risk associated with consuming water from these wells was highly variable in time, with most daily risk estimates being very low. The less frequent but higher concentration pathogen detections indicate increased daily risk but may be hard to predict. If they are generally associated with subsurface wetting fronts that follow abnormally dry periods, as suggested by this study, then those characteristics could be used to guide "worst case" sampling studies. In contrast, the relatively short lag times and high detection frequencies observed during spring thaw indicate that these time periods may be most fruitful for sampling intended to identify the likelihood of microbial occurrence rather than maximum concentration. It should be noted that risk from a well is also dependent on the type of population served by the water system (e.g., transient or residential) and the amount of water consumed.

The results seen here are supported by the broad but irregular level of pathogen occurrence seen in Stokdyk (2020) and other comparable studies in Wisconsin (Borchardt et al., 2003, 2004 and 2007). Although the results obtained in this study were from wells in relatively vulnerable geologic settings, the broad occurrence of microbial genetic material noted in the preceding study (Stokdyk et al., 2020), along with the similarities in occurrence patterns observed between sites with widely varying geologic settings observed here, may reflect that these findings have some general applicability for assessing risk. It seems likely that whatever types of subsurface heterogeneities were exploited by well pumping at the sites in this study, such as fractures or small-scale coarse-grained deposits, may exist even in relatively protected geologic settings. In addition, it should be acknowledged that subsurface infrastructure that is either designed to discharge to the subsurface, such as septic drainfields, or that may do so through leakage, such as sanitary or storm sewer lines, may be a source of year-round contribution of contaminated recharge that may promote relatively rapid transport through the vadose zone, even when overlying soils may be frozen. Similar correlation between precipitation events and chemical contamination of groundwater has been noted in other studies (Yu et al., 2020), further lending credence to accounting for these events when considering sampling studies for determining well vulnerability.

Recommendations

Actions that might be taken to maximize pathogen protection at public wells based on these study results might include:

- Focusing future sampling studies or routine monitoring on either the spring thaw period, to maximize the likelihood of detections, or after the return to wet conditions following abnormally dry ones, to maximize the likelihood of capturing peak concentrations. For spring thaw sampling, it is important to note that recharge may be occurring despite the presence of standard indicators of frozen ground conditions, such as ice on area lakes or subsoil temperature measurements for area roadways. However, pathogen occurrence at a well is likely more robustly identified as compared to pathogen concentration characterization when only a few samples can be collected.

- Factoring in vadose zone thickness when designing future monitoring studies designed to address short-term responses to precipitation events. Sites with thicker vadose zones will likely have appreciable lag times for contaminant breakthrough, based on the findings of this study.
- Factor changing climactic conditions into future monitoring strategies and vulnerability assessments. Although rainfall intensity was not evaluated as a controlling factor in this study, the observations about prevailing moisture conditions may be important when considering microbial risk to public water supply wells as changing climatic conditions anticipate increasingly wide swings in precipitation patterns. In addition, other studies have noted correlations between rainfall intensity or seasonality and chemical contamination in the subsurface (Yu et.al., 2021), providing further rationale for incorporating these considerations.
- More fully considering hydrogeologic conditions when siting wells and potential contaminant sources such as septic systems or sewers. Keeping contaminant sources from the upgradient direction of groundwater flow, and outside the one-year time of travel well capture zone, where known, can provide additional protection beyond that provided by isolation distances alone.
- Incorporating repeated measurement of parameters such as chloride, bromide, and water isotopes in sampling studies to look at trends that may reflect on flashy response to precipitation events and related microbial transport and susceptibility.
- Monitoring for chemical indicators, such as specific conductance and chloride/bromide ratios, will be most meaningful when assessing contributions from sources of different but known values or ranges. This may be especially relevant in settings like northeastern Minnesota where the existence of naturally occurring brines at depth may mix with shallow groundwater flow horizons of differing residence time and chemistry, or where specific sources, such as stormwater runoff or septic waste, are present in the contributing area of a well and are not confounded by multiple sources with identical chemical signatures.
- Incorporating data loggers in public supply wells or paired observation wells for continuous measurement of parameters such as water level or specific conductance to assess variability over time that might be related to recharge pulses and serve as surrogates for microbial risk.
- In low-hydraulic conductivity bedrock aquifer settings where long open-hole intervals are used to maximize yield and provide in-well storage, borehole logging studies may be able to identify different flow regimes at depth. This information may be useful for assessing mixing dynamics during recharge events and reflect on microbial susceptibility.
- Where feasible, consider using water storage to respond to forecast weather events that might promote microbial transport, especially during spring thaw when microbial lag times are relatively short.
- Increasing chlorine residuals or other disinfection treatments during spring thaw and other recharge events identified by monitoring for microbial contaminants or surrogate indicator parameters, as noted above.

- Like the suggestions of Hunt et al. (2010), the volumetrically small contributions of fast-moving recharge attributed to pathogen occurrence in this study argues for either the continued use of high-sensitivity microbial genetic analysis as the most robust indicator of well vulnerability, or for the use of surrogate parameters with similar levels of analytical sensitivity. Examples might include PFAS compounds, especially PFBA. Reliance on less sensitive parameters, such as tritium, may miss detection of the small components of young water noted here, thereby providing a nonconservative estimate of risk.
- If tritium is to be continued as the dominant indicator of groundwater residence time, it would be more predictive if the lowest analytical reporting limits are sought, even if they result in higher cost or turnaround times. The ultra-low level tritium analysis offered by the Environmental Isotope Lab at the University of Waterloo, the current state vendor, offers reporting levels of 0.1 TU. With a reporting limit nearly an order of magnitude lower than the enriched tritium analysis currently used as the standard (reporting limit of 0.8 TU), and assuming annual average atmospheric tritium levels of approximately 7 TU, ultra-low level tritium analysis should be able to detect as little as 2-3% young water in a sample, like the low mixing levels observed in this study that appear to equate to microbial risk. This compares with the approximate 11% of young water that might be masked by the higher reporting limit. Budgets and sampling schedules would need to be adjusted proportionately for the increase in cost (approximately triple) and turnaround times (at least 6 months) for the more sensitive method.
- The results of this study also argue that the ratio of chloride to bromide should be routinely incorporated when assessing well vulnerability and infrastructure mitigation efficacy. Taking a weight-of-evidence approach to assessing the vulnerability of public wells, rather than over-reliance on a single indicator, will provide a stronger basis for assessing risk, as will acknowledging that well vulnerability represents a spectrum rather than a binary outcome.

Acknowledgements

This study would not have been possible without the support and patience of the participating public water suppliers who allowed significant meddling with their water systems for the sampling to occur. In particular, the staff at Site 1 assisted with sample collection and shipment throughout the project, which was a significant burden to them and help to the study. The project also required the dedication of those who kept equipment running and samples collected and shipped regardless of difficult timing or field conditions. Special thanks go to the MDH team of Ernie Jorgensen, Arianna Giorgi, Tom Alvarez, Hannah Wilson, Scott Gullicksrud and Bob Tipping, who unfailingly kept samples collected on time and troubleshot problems as they arose. Thanks also to the sanitarians and engineers at MDH responsible for these water systems and who provided significant assistance with enabling the study. These include Cody Tennant, Jenny Soltys and Ezekiel Etukodo. Field and communications support was provided by John Woodside, Jane de Lambert and Alycia Overbo. Project leadership was divided between MDH (Anita Andersen and Jim Walsh) and USGS (Randy Hunt). Dave Owens of USGS oversaw development, installation, and maintenance of the autosamplers and related equipment and was on-call 24-7 throughout the project for a wide range of troubleshooting issues, and Andrew Berg of USGS provided timely and invaluable field assistance. Paul Felling, formerly of MDH,

supplied great insights into each of the study sites based on detailed inspections and research conducted prior to his retirement. Finally, thanks to the tracer team at DNR, consisting of John Barry, Jeff Green, Randy Bradt and Paul Putzier, who provided great expertise on tracer techniques and insights into each of the study sites, as well as Calvin Alexander, Scott Alexander and David Crisman who also provided invaluable contributions along these lines.

References

Barry, J. (2022a) Riverton, Minnesota Pathogen Project Dye Trace Investigation, Minnesota Department of Natural Resources internal report, 20p.

Barry, J, (2022b) Pequot Lakes, Minnesota Pathogen Project Dye Trace Investigation, Minnesota Department of Natural Resources internal report, 17p.

Barry, J. (2022c) Ely, Minnesota Pathogen Project Dye Trace Investigation, Minnesota Department of Natural Resources internal report, 20p.

Borchardt, M.A., Bertz, P.D., Spencer, S.K., Battigelli, D.A. (2003) Incidence of enteric viruses in groundwater from household wells in Wisconsin. Applied and Environmental Microbiology 2003 Feb;69(2):1172-80. https//doi: 10.1128/AEM.69.2.1172-1180.2003. PMID: 12571044; PMCID: PMC143602.

Borchardt, M.A., Haas, N. L., Hunt, R.J. (2004) Vulnerability of drinking-water wells in La Crosse, Wisconsin, to enteric-virus contamination from surface water contributions. Applied and Environmental Microbiology 2004 Oct;70(10):5937-46. https//doi: 10.1128/AEM.70.10.5937-5946.2004. PMID: 15466536; PMCID: PMC522136.

Borchardt, M.A., Bradbury, K.R., Gotkowitz, M.B., Cherry, J.A., Parker, B.L. (2005). Human enteric viruses in groundwater from a confined bedrock aquifer. Environmental Science &Technology, 2007 Sep 15;41(18):6606-12. https// doi: 10.1021/es071110+. PMID: 17948815.

Bottomley, D.J., (1996). A review of theories on the origins of saline waters and brines in the Canadian Precambrian Shield. A report prepared for the Wastes and Impacts Division, Directorate of Fuel Cycle and Materials Regulation, Atomic Energy Control Board of Canada, 18p.

Bowen, G.J., Revenaugh, J. (2003). Interpolating the isotopic composition of modern meteoric precipitation. Water Resources Research 39, 1299, https//doi:10.129/2003WR002086.

Bradbury, K., Borchardt, M., Gotkowitz, M., Hunt, R. (2008) Assessment of Virus Presence and Potential Virus Pathways In Deep Municipal Wells, Wisconsin Geological and Natural History Survey Open-File Report WOFR2008-08, 49 p., ISSN 1058-1413.

Burch, T., Stokdyk, J., Rice, N., Anderson, A., Walsh, J., Spencer, S., Firnstahl, A., and Borchardt, M. (2022). Statewide Quantitative Microbial Risk Assessment for Waterborne Viruses, Bacteria, and Protozoa in Public Water Supply Wells in Minnesota. Environmental Science & Technology 56 (10), 6315-6324, https//doi: 10.1021/acs.est.1c06472

Cao, Viet, Schaffer, Mario, Taherdangkoo, Reza, Licha, Tobias. (2020). Solute Reactive Tracers for Hydrogeological Applications: A Short Review and Future Prospects. Water. Volume 12. https://doi:10.3390/w12030653.

Gascoyne, M. (1996) The Evolution of Redox Conditions and Groundwater Geochemistry in Recharge-Discharge Environments on the Canadian Shield. Whiteshell Laboratories, Pinawa, Manitoba, ROE 1L0, AECL-11682 COG-96-500.

Gretsch, S., Koskey, A., Smith., K., and Robinson, T. (2018) The Association Between Precipitation, Temperature, and the Detection of Viruses in Six Community Groundwater Supplies in Minnesota International Conference on Emerging Infectious Diseases, program with abstracts, p. 237.

Hunt, R.J., Borchardt, M.A, Richards, K.D., Spencer, S.K. (2010) Assessment of sewer source contamination of drinking water wells using tracers and human enteric viruses. Environmental Science & Technology 44(20):7956–7963. doi:10.1021/es100698m.

Landwehr, J.M. and Coplen, T.B. (2004). Line-conditioned excess: A new method for characterizing stable hydrogen and oxygen isotope ratios in hydrologic systems. In Isotopes in Environmental Studies, Edition: 1, Chapter: IAEA-CN-118/56, Publisher: IAEA, pp.132-135. See pp. 99-100 in:

http://www.iaea.org/inis/collection/NCLCollectionStore/_Public/36/003/36003223.pdf

La Rosa, G., Bonadonna, L., Lucentini, L., Kenmoe, S., Suffredini, E. (2020). Coronavirus in water environments: Occurrence, persistence and concentration methods - A scoping review. Water Research. 2020 Jul 15;179:115899. https//doi:10.1016/j.watres.2020.115899. Epub 2020 Apr 28. PMID: 32361598; PMCID: PMC7187830.

Metropolitan Council (2014). Twin Cities Metropolitan Area Regional Groundwater Flow Model, Version 3.0. Prepared by Barr Engineering. Metropolitan Council: Saint Paul, MN.

Minnesota Department of Transportation (2022). Frost and thaw depths, as found at: https://www.dot.state.mn.us/materials/pvmtdesign/sll/frost-thaw.html

Minnesota State Climatology Office (2022). Ice in/out dates for area lakes, as found at: https://www.dnr.state.mn.us/ice_out/index.html?year=2021

Minnesota State Climatology Office (2022). Precipitation worksheet using gridded database, as found at:
https://climateapps.dnr.state.mn.us/gridded_data/precip/monthly/monthly_gridded_precip.asp

Mohammed, A., Pavlovskii, I., Cey, E. E., and Hayashi, M. (2019) Effects of preferential flow on snowmelt partitioning and groundwater recharge in frozen soils, Hydrology and Earth System Science, 23, 5017–5031, https://doi.org/10.5194/hess-23-5017-2019, 2019.

National Atmospheric Deposition Program (NRSP-3). (2022). NADP Program Office, Wisconsin State Laboratory of Hygiene, 465 Henry Mall, Madison, WI 53706.

Setterholm, D.R. (2004). C-16 Geologic atlas of Crow Wing County, Minnesota [Part A]. Minnesota Geological Survey. Retrieved from the University of Minnesota Digital Conservancy, https://hdl.handle.net/11299/58716.

Strack, O.D.L. (1999). Multi-layer analytic element model, Version 5.1.08.

Stokdyk, J., Firnstahl, A., Walsh, J, Spencer, S., de Lambert, J., Anderson, A., Rezania, L., Kieke, B. and Borchardt, M. (2020). Viral, bacterial, and protozoan pathogens fecal markers in wells supplying groundwater to public water systems in Minnesota, USA. Water Research 178, 115814.

Walsh, J. (2018). 2018 Annular Space Test at McCarthy Beach State Park. Minnesota Groundwater Association Newsletter, December 2018.

Yu, Xia. Sui, Qian, , Lyu, Shuguang, Zhao, Wentao. Wu, Dongquan, Yu, Gang, Barcelo, Damia. (2021). Rainfall Influences Occurrence of Pharmaceutical and Personal Care Products in Landfill Leachates: Evidence from Seasonal Variations and Extreme Rainfall Episodes. Environmental Science & Technology. 55. 10.1021/acs.est.0c07588.

Appendix A - Quantitative Microbial Risk Assessment

Introduction

Quantitative microbial risk assessment (QMRA) is a relatively new discipline. QMRA was developed to fill the need for assessing potential threats to human health from pathogens. To date, comparisons of the predictive ability of QMRA to epidemiology data (i.e., data from past human disease outbreaks), have shown that QMRA is a reasonably accurate and useful tool (Burch, 2019; Soller et al., 2016).

QMRA often predicts *infection* with a pathogen, but not necessarily an *illness*. In an infection, a part of a person's body, such as the gastrointestinal tract, has been invaded by the pathogen and the pathogen might be reproducing. However, the infection might not cause noticeable symptoms. Sometimes a person's body can stop the infection and remove the pathogen before a person feels sick. If the body cannot fight off the infection, symptoms may occur (e.g., diarrhea or vomiting). The infection is now called an illness. There are many factors involved in developing symptoms. More research is needed to understand when an infection will progress to an illness.

We will now describe how QMRA can help us interpret the precipitation monitoring pathogen results.

Components of QMRA

QMRA includes many of the classic risk assessment components (Haas, Rose, & Gerba, 1999; U.S. EPA, 2012b). These include:

Hazard identification (Which pathogens pose a potential hazard?)

Dose response models (How many pathogens will cause an infection or illness?)

Exposure assessment (What types of pathogens and how many are present in the scenario studied and what is the pathway or route of exposure, if any?)

Risk characterization (Using the data from the first three steps, what is the health risk?)

Each of these four risk assessment components require data and analysis of the data. Each component is broken down into more detail in the following four sections. In each section we will first discuss the QMRA component generally, then describe the analysis used for the precipitation monitoring data.

1. Hazard identification

Hazard identification answers such questions as:

- What types of pathogens might be found in a groundwater well?
- How do they infect people?
- What types of illnesses are possible (Haas, et al., 1999; Medema & Ashbolt, 2006)?

To answer these questions, we used data from our previous studies, and also turned to other researchers and scientists. We focused on pathogens in the groundwater that make people sick

when ingested (swallowed). They affect the gastrointestinal tract (enteric pathogens); symptoms of illnesses may include diarrhea or vomiting.

The precipitation monitoring analyzed for microbes that represent the three major categories of pathogenic microbes in water: virus, protozoa, and bacteria. Not only do these groups vary in frequency of occurrence, but they differ in size, survivability, infectivity, and resistance to treatment. Therefore, it is necessary to look at them as separate groups.

Pathogens whose genetic material was detected during the study were used for the precipitation monitoring QMRA and included:

- Virus: norovirus, adenovirus
- Protozoa: *Giardia*, *Cryptosporidium*
- Bacteria: *Salmonella*

All of these pathogens commonly cause gastrointestinal illness.

Precipitation monitoring looked for pathogens using a laboratory method called quantitative polymerase chain reaction (qPCR), that allows detection of genetic material for specific pathogens. The method does not tell if the microbes are infectious or not. We assumed for the QMRA that detected pathogens were infectious, resulting in a conservative estimate of risk.

2. Dose response models

Dose-response models are equations that provide information about the amount of pathogen that usually causes an infection in a person. Dose-response models are often based on controlled laboratory experiments, but sometimes they are developed or validated using data from disease outbreaks (Burch, 2018; Haas et al., 1999; Haas, 2015; Soller et al., 2016). Selecting an appropriate dose-response model is important in estimating the potential for an unwanted effect to occur.

Several variables are involved in dose-response, such as:

- A person's susceptibility to infection from a particular pathogen.
- The pathogen's infection-causing ability.
- How a person can come in contact with the pathogens.
- The general health status of the person.

Unfortunately, getting health data that can be applied across the entire human population is difficult. Scientists have created statistical models that can be broadly applied, but there are known shortcomings in the models. In addition, the number of dose-response models available for pathogens is limited. Risk assessors sometimes cannot make a risk prediction, or they must make their best estimates using the models available.

In recent years, numerous researchers have been working to find the most accurate dose-response model for various microbes. The task is difficult because there are many unknown factors that could contribute to the accuracy of the dose-response model, such as the infectiousness of the microbe strain or the immunity or resistance of the host. As researchers learn more about microbes, their ability to infect a host, environmental and immune factors

that allow or prevent infections, and other factors, the dose-response models continue to be refined.

Currently several dose-response models are available for some microbes, and no dose-response models exist for others. For example, norovirus has numerous dose-response models, and we considered four of the models for this QMRA (Messner et al., 2014; Teunis et al., 2008; Teunis et al., 2020, Schmidt, 2015). Some of the population is believed to be immune to certain strains of norovirus. The four models account for the potential for immunity through different approaches. A full discussion of the differences is beyond the scope of this paper.

A similar case of differing dose-response models also exists for other pathogens. We ran some of the more widely used models to compare the risk. Primary model forms included the exact Beta-Poisson (also known as the hypergeometric model), the approximate beta-Poisson, and the exponential model. The models implemented and references are listed in Table 1.

Table 1: Dose-response models used in this QMRA.

Microbe	Genes/Species	Dose-response model (for infection) P(inf)=	Author, Year	Parameters
Bacteria	*Salmonella* (Mixed species)	Exact Beta Poisson $1\text{-}1F1(\alpha, \alpha + \beta, -cV)$	Food and Agriculture Organization, 2002	$\alpha = 0.13$ $\beta = 51$ DH = 5.6 (Burch et al., 2022)
Bacteria	*Salmonella* (Mixed species)	Approximate Beta Poisson $1 - [1\text{-dose}/\beta]^{-\alpha}$	Haas, Rose and Gerba, 1999	$\alpha = 0.3126$ $\beta = 2884$ DH = 5.6 (Burch et al., 2022
Bacteria	*Salmonella*	Approximate Beta Poisson $1 - [1\text{-dose}/\beta]^{-\alpha}$	Rose & Gerba, 1991	$\alpha = 0.33$ $\beta = 139.9$ DH = 5.6 (Burch et al., 2022
Bacteria	*Salmonella Typhimurium*	Approximate Beta Poisson $1 - [1\text{-dose}/\beta]^{-\alpha}$	Maynell, 1958 aci QMRAwiki	$\alpha = 0.21$ $\beta = 1.906$ DH = 5.6 (Burch et al., 2022
Protozoa	*Cryptosporidium* (pan)	Fractional Poisson $P * (1\text{-}e^{-d})$	Messner and Berger, 2016	P = 0.737 DH = 14 (Burch et al., 2022)
Protozoa	*Cryptosporidium* (pan)	Exponential $1\text{-}e^{(-d * 0.009)}$	EPA, 2005	r = 0.09 DH = 14 (Burch et al., 2022)

Microbe	Genes/Species	Dose-response model (for infection) P(inf)=	Author, Year	Parameters
Protozoa	*Giardia duodenalis*	Exponential $1-e^{(-d * 0.0199)}$	Rose, 1991	r = 0.0199 DH = 4.5 (Burch et al., 2022)
Virus	Human adenovirus A-F	Exponential $1-e^{(-d * 0.4172)}$	Crabtree, 1997	R=0.4172 DH = 700 (McBride et al., 2013)
Virus	Norovirus	Exact beta-Poisson $1-1F1(\alpha, \alpha + \beta, -cV)$	Teunis, 2008	α = 0.04 β = 0.055
Virus	Norovirus, GII	Exact beta-Poisson $1-1F1(\alpha, \alpha + \beta, -cV)$	Teunis, 2020	α = 0.23 β = 5.04 DH = 1 (Teunis et al., 2020)
Virus	Norovirus	Fractional Poisson $P * (1-e^{(-d * u)}$	Messner, 2014	P = 0.7228 u = 1106 DH = 1 (Teunis et al., 2020)
Virus	Norovirus	Exact beta-Poisson, with immunity (ϕ) $(1-\phi) * (1-1F1(\alpha, \alpha + \beta, -d))$	Schmidt, 2015	α = 2.91 β = 2734 ϕ = 0.2775 DH = 1 (Teunis et al., 2020)

d = dose (concentration in water * volume ingested); DH = dose harmonization; u = parameter for dispersion.

Figure 1 compares the models graphically for the more commonly detected pathogens. You can see in the figure that the same dose of 10 gc/L can result in a wide range of infection risk as a response for different pathogens and models. We expect that more research will continue on this topic and the models will continue to be refined over time.

These models illustrate the range of potential infection risk that example models for norovirus and cryptosporidium predict. For example, a dose of 10 gc/L has a predicted risk of infection that ranges from 0.06 (6%) to 0.74 (74%), depending on the model used.

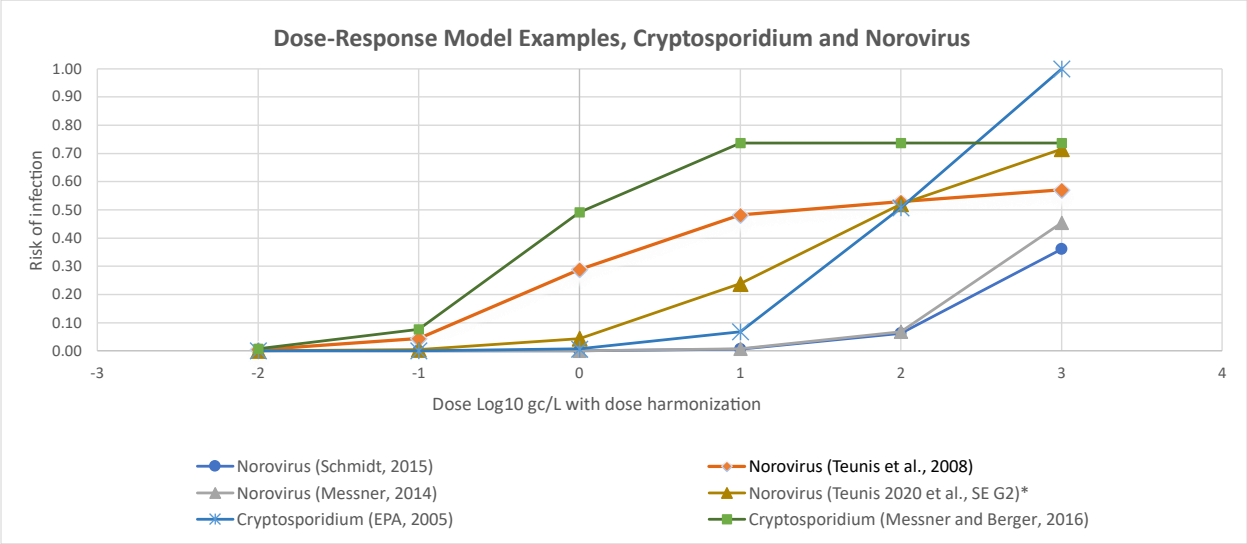

*SE G2 means the dose response is for people who secrete an antigen for norovirus and norovirus genotype G2 is present.

Figure 1: Graphical representation of dose-response models for pathogens commonly detected in this study.

3. Exposure assessment

Exposure assessment involves first determining the type and concentration of microbes present. The Methods section of the main report describes how and when microbial sampling occurred for the precipitation monitoring study, and results for each site are summarized in Figures 2 through 5.

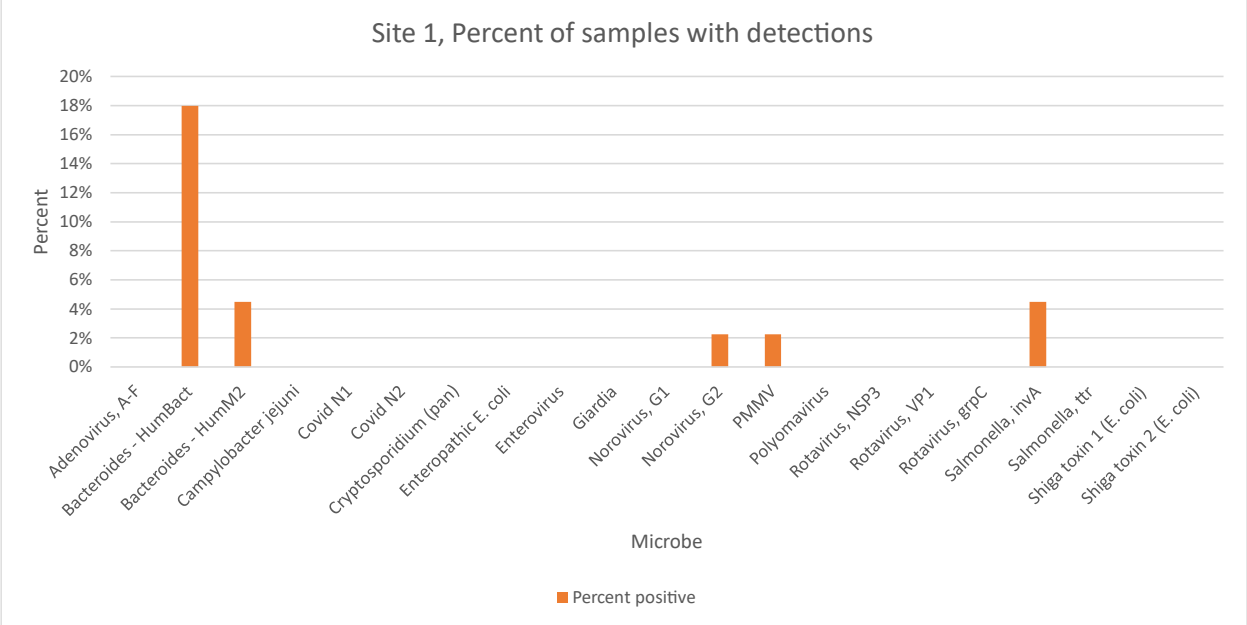

Five microbial targets were detected at Site 1. The highest detection rate was for human bacteriodes at 18 percent.

Figure 2: Percent of Site 1 samples with detections for various microbes.

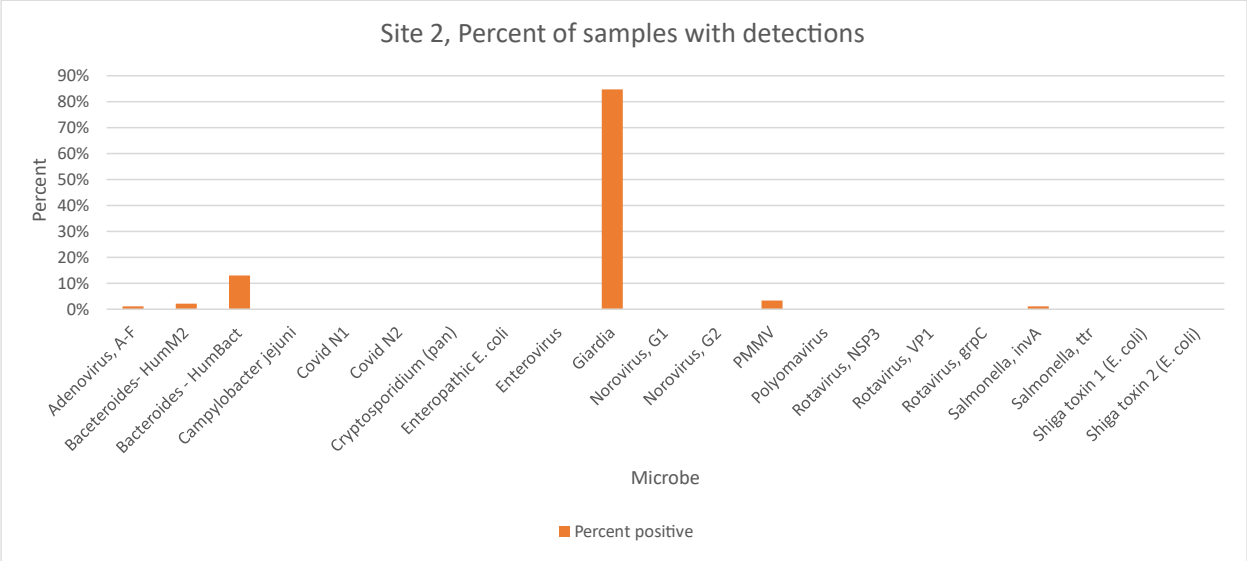

Six microbial targets were detected at Site 2. The highest detection rate was for Giardia at 85 percent.

Figure 3: Percent of Site 2 samples with detections for various microbes.

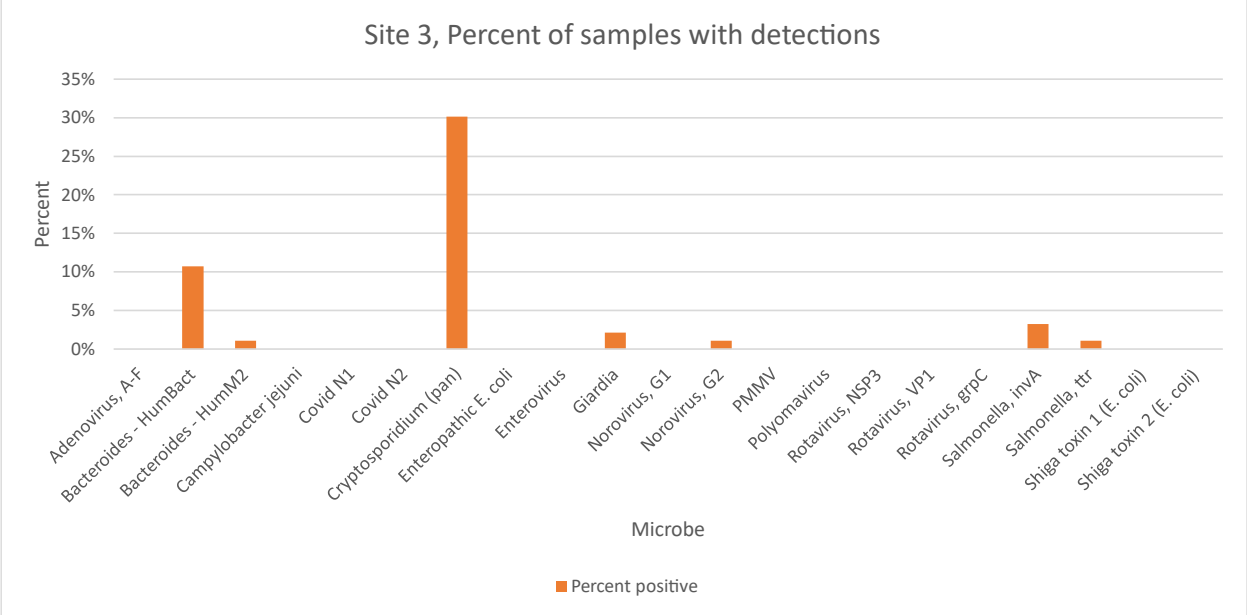

Seven microbial targets were detected at Site 3. The highest detection rate was for Cryptosporidium at 30 percent.

Figure 4: Percent of Site 3 samples with detections for various microbes.

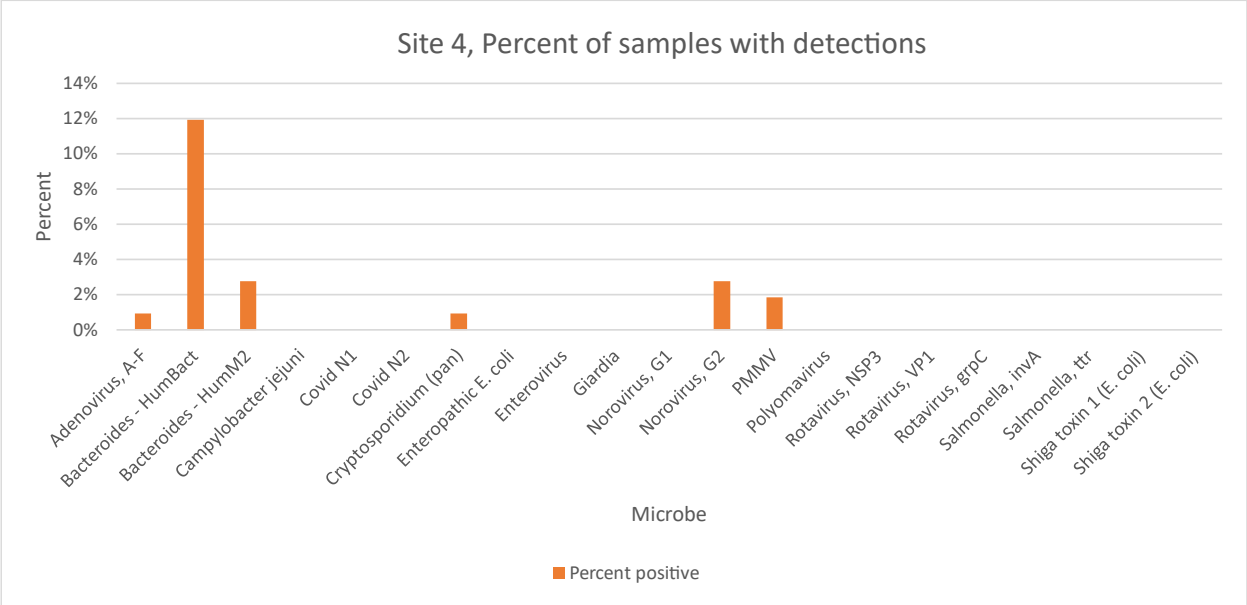

Six microbial targets were detected at Site 4. The highest detection rate was for human bacteroides at 12 percent.

Figure 5: Percent of Site 4 samples with detections for various microbes.

Next, we consider the ways people could be exposed to the microbe. For this QMRA, we assumed the primary exposure is through drinking the water. For drinking water, data from the U.S. EPA Exposure Factors Handbook estimates an average intake of 1.1 liters per day (L/day) in the U.S. for all ages (U.S. EPA, 2019). Because many of the original dose-response models were created before molecular laboratory methods were available, there is a need to estimate the number of genetic copies per units of microbe used in the original model. Dose harmonization is an equation that helps to account for this difference. The dose estimation can then be calculated by multiplying the 1.1 liters ingested per day by the concentration of the microbes detected (in genetic copies (gc) per liter), divided by the dose harmonization published in the literature as noted. For example, for adenovirus, a dose might be shown as:

Dose = 1.1 L water ingested * 0.34 gc/L in sample / 703 gc per infectious dose where gc is genetic copies.

4. Risk characterization

Using all of the information collected in the hazard identification, dose response, and exposure assessment steps, the potential risk can be calculated. Major decision points in risk characterization include whether to calculate a point estimate (single value) for risk or use a risk range to try to account for variability in exposure, and what timeframe of risk to consider.

Since the precipitation monitoring study was designed to sample more frequently after precipitation events, the results may not be representative of what consumers would be drinking over the course of a year. We therefore decided to calculate point estimates for risk for each sample rather than an annual risk estimate to evaluate the potential for public health concern indicated by the results.

An example of a risk calculation for adenovirus, which uses an exponential dose-response model with a constant of 0.4172, is as follows:

$$P_{Inf} = 1 - e^{(-r*dose)}$$

Where P_{inf} is the probability of infection, and r is a constant parameter as described in Crabtree et al., 1997.

Uses data from the study where there were 0.34 genetic copies (gc) per liter, the probability of infection can be calculated as:

$$P_{Inf} = 1 - e^{(-(0.34\ \text{gc/L} * 1.1\ \text{L}/700\ \text{gc per infectious dose}) * 0.4172)}$$

$$= 0.000022 \text{ or } 2.2 \times 10^{-4}$$

For this QMRA, risk is calculated as the estimated risk of infection from one day drinking water with the pathogens found in a given sample. A risk estimate, such as .001, could be viewed as 1/1,000 people who drink the water will get an infection, or an individual has a 1/1,000 chance of getting infected on the given day. The systems studied serve a range of populations from restaurant patrons who may only drink the water once a year to residents who would be expected to drink the water frequently, and a different view of risk can be applied to each site.

Risk Management

Once the microbial risk has been characterized, we can determine the amount (if any) of safeguards to consider to meet the target acceptable risk level. That is, if the amount of pathogens in the source water and the amount of potential exposure is enough to possibly make someone sick, then the amount must be reduced to make the water safe for drinking. Possible safeguards include improving well construction, managing contaminant sources, adjusting system operations in response to precipitation events, or providing treatment of the source water prior to consumption.

The often-applied acceptable risk benchmark for drinking water is .0001 (10^{-4}), typically described as one infection per 10,000 people per year. This level of risk could be predicted under various scenarios, for example: one or more days of people drinking the water containing higher levels of microbials contaminants, or several days within a year of people drinking water with a lower level of microbials contaminants. Our assessment estimated that any day there was a detection of a pathogen, the estimated risk of infection for that day would be over the benchmark, indicating unacceptable risk. Most of the time the risk was below 1/1,000 (10^{-3}). The highest predicted risk was .64 for a *Cryptosporidium* concentration of 26 gc/L. The next highest level of predicted risk was 0.51 for a concentration of 34 gc/L of norovirus using the Teunis 2008 hypergeometric dose response model.

Looking at annual risk, the risk from one exposure drives the risk for the entire year, based on the formula:

Probability of infection = 1- (1-risk)^number of exposures.

If the risk is zero on a given day, the multiple is 1 for that day. If the risk is higher for one day, the risk will be high for the full time period. For example, a risk over a week could be:

P(inf) = 1- ((1-0.6) * (1-0) * (1-0) * (1-0) * (1-0) * (1-0) * (1-0)) = 0.6

This is the same as the risk for one day:

P(inf) = 1 - (1-0.6) = 0.6

Overall, the risk of infection or illness is related to the concentration of microbes in the water, as would be expected. The dose response models vary, which will influence the risk estimate. Optimal dose-response models have not been universally agreed upon at this point, especially for norovirus. There are also many other variables to consider, such as inherent susceptibility of the potential hosts (i.e., some people might not be susceptible to certain microbes based on their genetic makeup and gene expression.) Further, immunity has a strong influence on susceptibility as well, and can vary over time and with various exposures.

People are more convinced of the need to act on a potential risk when they can see illness or infection. However, we need to consider potential reasons why illnesses or infections are not always reported. Some of these reasons are:

- People have been infected, but the infection is subclinical (i.e., there are no symptoms).
- People have been infected and show symptoms (i.e., become ill), but the affected person or family does not seek treatment.
- A few people have been infected and show symptoms, but the public health surveillance system is not robust enough to detect these illnesses as being related.

Site Specific observations

Site 1

The most concerning detections at Site 1 were the two norovirus detections, one on 11/13/2020 with a concentration of 34.04 gc/L, and one on 9/21/2021 with a concentration of 1.37 gc/L. The maximum estimated daily risk was 0.51 for the 11/13/2020 norovirus detection (Figure 6).

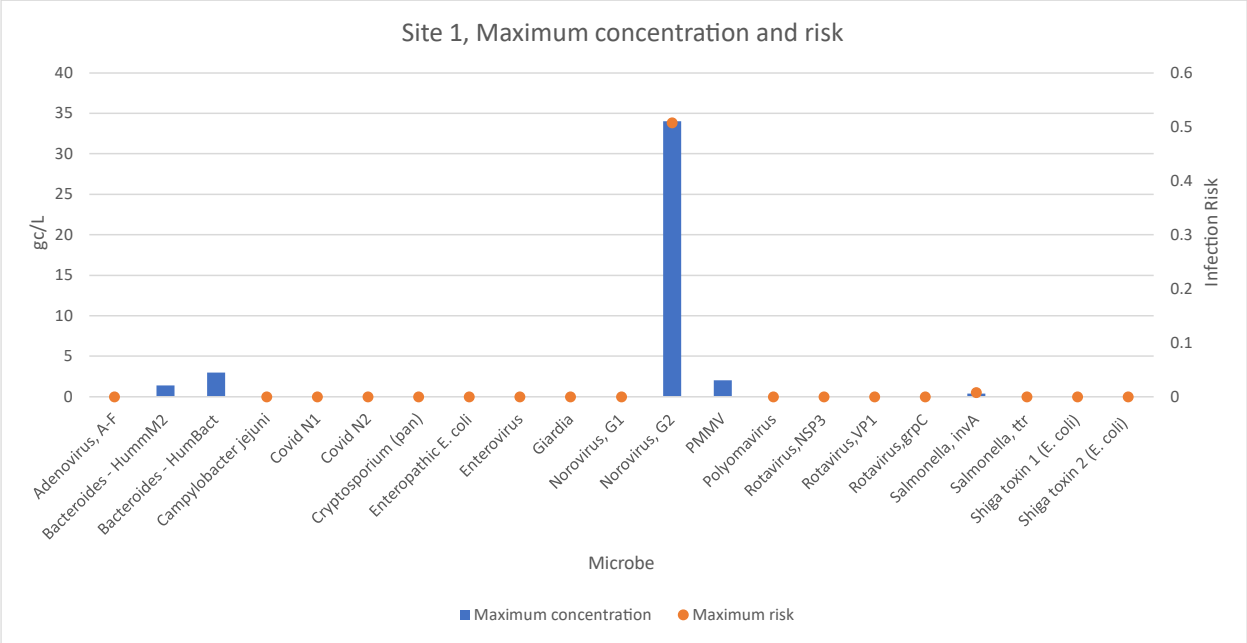

The maximum concentrations for microbes detected at Site 1 ranged from 0.36 to 34 gc/L and the maximum risk ranged from .0075 to .51.

Figure 6: Maximum microbe concentration detected and maximum daily risk predicted per microbe for Site 1.

There were pathogen detections in six out of the 89 samples at Site 1. Given that the public population served by Site 1 is transient (e.g., they are at the facility for approximately one week per year), most people are likely to be served water that is free of pathogens, but treatment or a source free of pathogens would be necessary to ensure full public health protection.

Detections of human fecal indicator bacteria were more frequent than pathogens, and were at very low levels, supportive of small volumes of contaminated water entering the well.

For a norovirus detection to occur in a well at this site, there presumably needs to be someone at the site that is shedding the virus into the wastewater (or possibly onto the ground), making it hard to predict when norovirus risk will occur. Norovirus is easily spread person-to-person and from surfaces, and those transmission pathways are likely to impact risk in addition to any risk from drinking water.

Site 2

Site 2 pathogen detections are characterized by frequent (78 out of 92 samples), low-level detections of *Giardia*. The highest detections of 18.2 and 9.62 gc/L were found on 11/9/2020 and 11/11/2020 respectively. The estimated risk for these detections were .33 and .19 respectively.

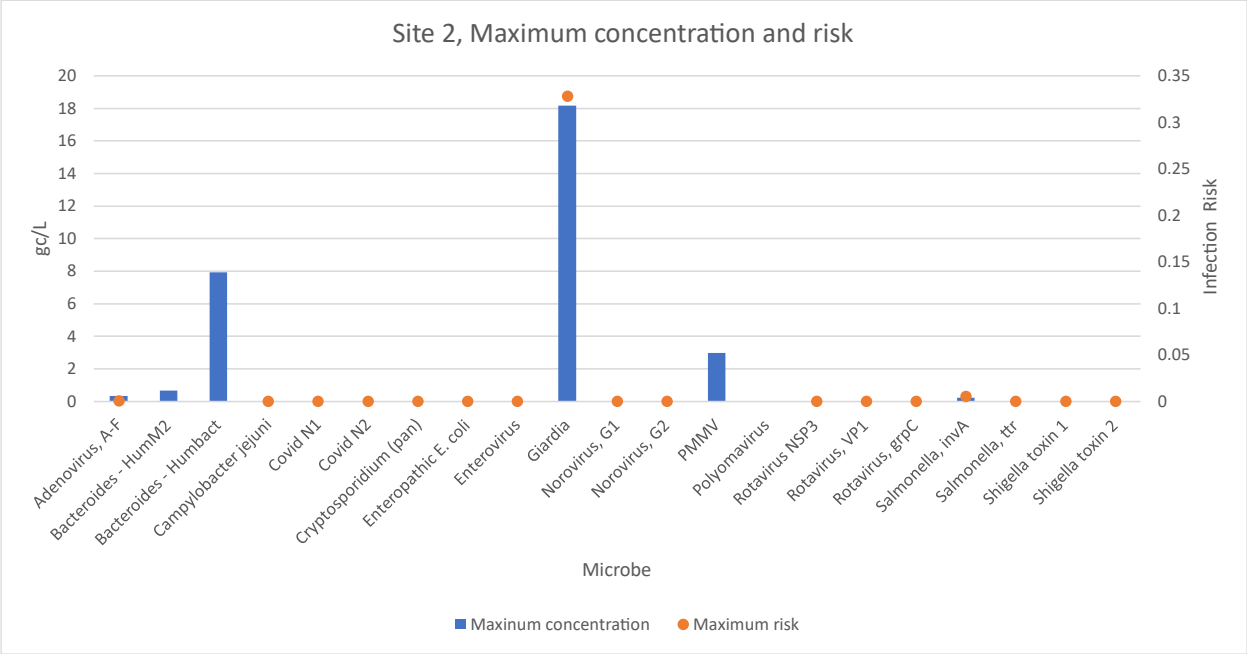

The maximum concentrations for microbes detected at Site 2 ranged from 0.23 to 18 gc/L and the maximum risk ranged from .00022 to .33.

Figure 7: Maximum microbe concentration detected and maximum daily risk predicted per microbe for Site 2.

The population currently served by Site 2 is transient in nature, and on average likely drinks less than the 1.1 L used for calculating risk during each visit to the Site. That said, the frequency of detections means that there is a good chance for infection during any visit, and that only continuous treatment of the water supply or switching to a new source will be effective tools at reducing risk.

Site 3

The most concerning pathogen detections at Site 3 were the frequent (28 out of 93 samples) detections of *Cryptosporidium*, resulting in daily risk estimates consistently above .001 for most detections, and as high as 0.64 on 11/10/2020 when the concentration was 26.2 gc/L. Since this system serves a residential population, it is likely that a resident will be exposed to risk from *Cryptosporidium* multiple times during the year. Given that the risk is still relatively low (the risk estimate of .001 could be viewed as 1 infection per 1,000 people), and that not every infection leads to illness, any health impacts may still not be visible in the community. As for Site 2, given the frequency of detections, treatment of the water supply or use of an alternate source will be the best ways to reduce risk.

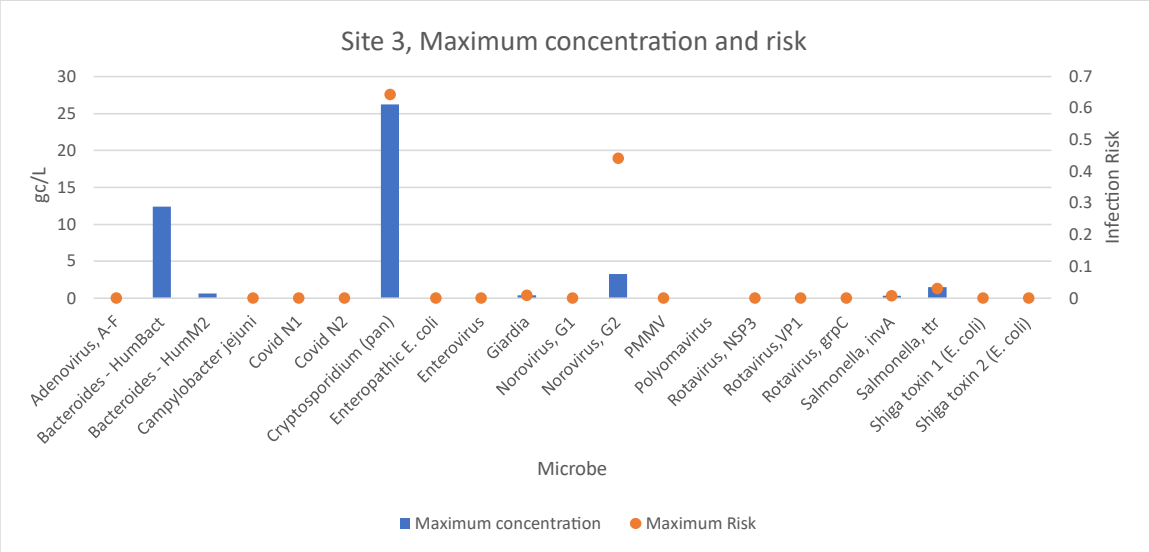

The maximum concentrations for microbes detected at Site 3 ranged from 0.32 to 26 gc/L and the maximum risk ranged from .0069 to .64.

Figure 8: Maximum microbe concentration detected and maximum daily risk predicted per microbe for Site 3.

Site 4

Site 4 had only five pathogen detections out of 109 samples. Detections included norovirus, adenovirus and *Cryptosporidium*. Maximum risk estimates for the three microbes were 0.47, .00017 and .011 respectively. While the detections indicate vulnerability, the overall concern is lower at this site compared to the other three sites because of the infrequent detections.

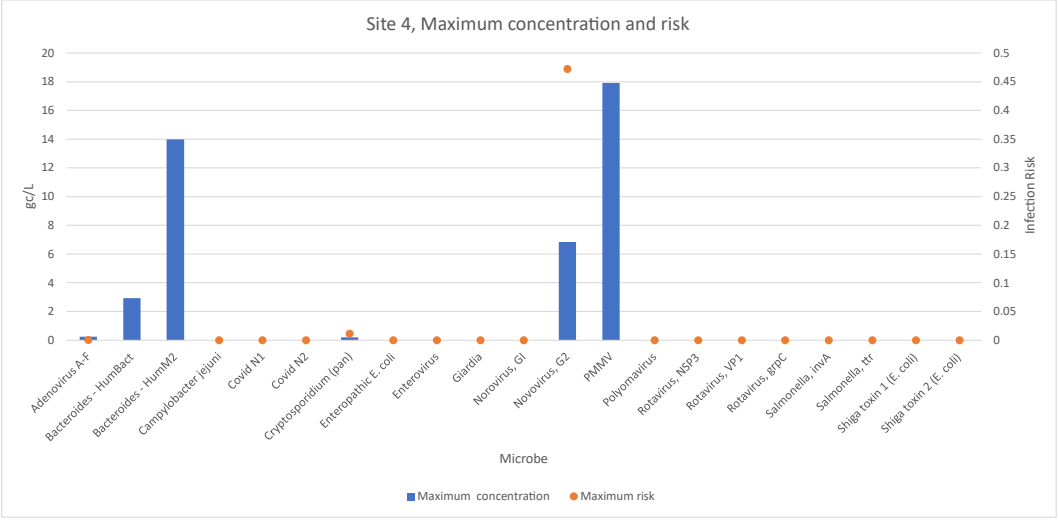

The maximum concentrations for microbes detected at Site 4 ranged from 0.25 to 18 gc/L and the maximum risk ranged from .00017 to .47.

Figure 9: Maximum microbe concentration detected and maximum daily risk predicted per microbe for Site 4.

References

Burch, T. (2019). Validation of quantitative microbial risk assessment using epidemiological data from outbreaks of waterborne gastrointestinal disease. Risk Analysis, *39*(3), 599-615.

Burch, T. R., Stokdyk, J. P., Rice, N., Anderson, A. C., Walsh, J. F., Spencer, S. K., Borchardt, M. A. (2022). Statewide Quantitative Microbial Risk Assessment for Waterborne Viruses, Bacteria, and Protozoa in Public Water Supply Wells in Minnesota. Environmental Science & Technology.

Centers for Disease Control and Prevention. (2022) Nordashboard. https://wwwn.cdc.gov/norsdashboard/

Crabtree, K. D., Gerba, C. P., Rose, J. B., Haas, C. N. (1997). Waterborne adenovirus: a risk assessment. Water Science and Technology, 35(11-12), 1-6.

FAO., World Health Organization. (2002). Risk assessments of Salmonella in eggs and broiler chickens (Vol. 2).

Kundu, A., McBride, G., and Wuertz, S. (2013). Adenovirus-associated health risks for recreational activities in a multi-use coastal watershed based on site-specific quantitative microbial risk assessment. Water Research, *47*(16), 6309-6325.

Messner, M. J., and Berger, P. (2016). Cryptosporidium infection risk: results of new dose-response modeling. Risk Analysis, 36(10), 1969-1982.

Meynell, G. G., & Meynell, E. W. (1958). The growth of micro-organisms in vivo with particular reference to the relation between dose and latent period. Epidemiology & Infection, 5*6*(3), 323-346, as cited in QMRA Wiki. 2022. Salmonella typhimurium does response. https://qmrawiki.org/experiments/salmonella-nontyphoid

Minnesota Department of Health. (2022). Diseases and Conditions. https://www.health.state.mn.us/diseases/index.html

Rose, J. B., and Gerba, C. P. (1991). Use of risk assessment for development of microbial standards. Water Science and Technology, *24*(2), 29-34.

Rose, J. B., Haas, C. N., and Regli, S. (1991). Risk assessment and control of waterborne giardiasis. American Journal of Public Health, 81(6), 709-713.

Teunis, P. F., Le Guyader, F. S., Liu, P., Ollivier, J., and Moe, C. L. (2020). Noroviruses are highly infectious but there is strong variation in host susceptibility and virus pathogenicity. Epidemics, *32*, 100401.

Teunis, P. F., Moe, C. L., Liu, P., Miller, S.E., Lindesmith, L., Baric, R. S., Le Pendu, J. and Calderon, R. L. (2008). Norwalk virus: how infectious is it?. Journal of Medical Virology, *80*(8), 1468-1476.

USEPA (2005) Economic Analysis for the Final Long Term 2 Enhanced Surface Water Treatment Rule.

USEPA. (2010). Quantitative microbial risk assessment to estimate illness in freshwater impacted by agricultural animal sources of fecal contamination.

https://www.epa.gov/sites/default/files/2015-11/documents/quantitiave-microbial-risk-fecal.pdf.

Van Abel, N., Schoen, M. E., Kissel, J. C., and Meschke, J. S. (2017). Comparison of risk predicted by multiple norovirus dose–response models and implications for quantitative microbial risk assessment. Risk Analysis, *37*(2), 245-264.

Vos, T., Lim, S. S., Abbafati, C., Abbas, K. M., Abbasi, M., Abbasifard, M., ... and Bhutta, Z. A. (2020). Global burden of 369 diseases and injuries in 204 countries and territories, 1990–2019: a systematic analysis for the Global Burden of Disease Study 2019. The Lancet, 39*6*(10258), 1204-1222. (Supplementary Appendix 1)